PNNL-14744

Pacific Northwest
National Laboratory
Operated by Battelle for the
U.S. Department of Energy

Recharge Data Package for the 2005 Integrated Disposal Facility Performance Assessment

M. J. Fayer
J. E. Szecsody

June 2004

Prepared for the U.S. Department of Energy
under Contract DE-AC06-76RL01830

DISCLAIMER

PACIFIC NORTHWEST NATIONAL LABORATORY
operated by
BATTELLE
for the
UNITED STATES DEPARTMENT OF ENERGY
under Contract DE-AC06-76RL01830

Printed in the United States of America

Available to DOE and DOE contractors from the
Office of Scientific and Technical Information,
P.O. Box 62, Oak Ridge, TN 37831-0062;
ph: (865) 576-8401
fax: (865) 576-5728
email: reports@adonis.osti.gov

Available to the public from the National Technical Information Service,
U.S. Department of Commerce, 5285 Port Royal Rd., Springfield, VA 22161
ph: (800) 553-6847
fax: (703) 605-6900
email: orders@ntis.fedworld.gov
online ordering: http://www.ntis.gov/ordering.htm


This document was printed on recycled paper.

(8/00)

PNNL-14744

Recharge Data Package for the 2005 Integrated Disposal Facility Performance Assessment

M. J. Fayer
J. E. Szecsody

June 2004

Prepared for
the U.S. Department of Energy
under Contract DE-AC06-76RL01830

Pacific Northwest National Laboratory
Richland, Washington 99352

Summary

CH2M HILL Hanford Group, Inc., (CH2M HILL) is designing and assessing the performance of a near-surface disposal facility at Hanford for radioactive and hazardous waste. The waste includes immobilized low-activity waste (ILAW), which consists of vitrified low-level radioactive waste that will be retrieved from Hanford's single- and double-shell tanks, unvitrified low-level radioactive waste, mixed low-level waste, and vitrification melters.

The CH2M HILL effort to assess the performance of this disposal facility is known as the Integrated Disposal Facility (IDF) Performance Assessment (PA) activity. The goal of this activity is to provide a reasonable expectation that the disposal of waste will be protective of the general public, groundwater resources, air resources, surface-water resources, and inadvertent intruders. Achieving this goal will require predictions of contaminant migration from the facility. To make such predictions will require estimates of the fluxes of water moving through the sediment within the vadose zone around and beneath the disposal facility. These fluxes, loosely called recharge rates, are the primary mechanism for transporting contaminants to the groundwater.

Pacific Northwest National Laboratory (PNNL) assists CH2M HILL in their performance assessment activities by providing estimates of recharge rates for current conditions and long-term scenarios involving disposal in the IDF. The recharge estimates for each scenario were derived from modeling studies and lysimeter and tracer data collected by the IDF PA activity. CH2M HILL plans to conduct a performance assessment of the latest IDF design and call it the 2005 IDF PA. This recharge data package is being prepared to support the upcoming 2005 IDF PA.

The elements of this report compose the Recharge Data Package, which provides estimates of recharge rates for the scenarios being considered in the 2005 IDF PA. Table S.1 identifies the surface features and time periods evaluated. The most important feature, the surface barrier, is expected to be the modified RCRA Subtitle C design. This design uses a 1-m-thick silt loam layer above sand and gravel filter layers to create a capillary break. A 0.15-m-thick asphalt layer underlies the filter layers to function as a backup barrier and to promote lateral drainage. However, the recharge-limiting benefits of the asphalt layer were not included in the analyses or recommendations of this report. Although barrier side slopes are not expected to be part of the design, rates are provided as a contingency.

Table S.1 shows that for the best estimate case, a recharge rate of 0.1 mm/yr is proposed for the surface barrier with a shrub-steppe plant community. This rate is the same one used in the 2001 ILAW PA and the data collected since then support its continued use. If side slopes are part of the surface barrier design, a two-step recharge rate is proposed: 22.3 mm/yr for the first 16 years while plants get established and 4.2 mm/yr thereafter. These rates are lower than the 50 mm/yr used in the 2001 ILAW PA because they better reflect the data collected from the prototype barrier. The case is made in this data package that the soils at the IDF should be considered a single soil type. Therefore, a single recharge rate of 0.9 mm/yr is proposed for the soil at the IDF site. This rate is identical to that used for Rupert sand in the 2001 ILAW PA. This rate is much lower than the rate of 4.2 mm/yr used for Burbank loamy sand in the 2001 ILAW PA. The lower rate is the result of using site-specific chloride data rather than chloride

data from a site 1.5 km to the northeast. For Hanford formation sediment during construction, a recharge rate of 55.4 mm/yr is proposed (same as for the 2001 ILAW PA). Using the available recharge estimates, a set of reasonable bounding rates is also identified.

Table S.1. Recharge Estimates for the Best Estimate Case and Reasonable Bounding Cases During Each Period of Interest to the 2005 Integrated Disposal Facility Performance Assessment

Surface Feature	Estimated Recharge Rates (mm/yr)			
	Time Period of Recharge Evaluation			
	Pre-Hanford	During Disposal Operations	During Surface Barrier Design Life	After Surface Barrier Design Life
Modified RCRA Subtitle C Barrier	NA	NA	Best: 0.1 Lower: 0.008 Upper: 0.2	Best: 0.1 Lower: 0.008 Upper: 0.9
Barrier Side Slope	NA	NA	Best: 22.3 for 0 to 16 yrs, 4.2 for >16 yrs Lower: 2.8 Upper: 47.5 for 0 to 16 yrs, 21.8 for >16 yrs	Best: 4.2 Lower: 2.8 Upper: 21.8
Rupert Sand[(a)]	Best: 0.9 Lower: 0.16 Upper: 2.1	Best: 0.9 Lower: 0.16 Upper: 2.1	Best: 0.9 Lower: 0.16 Upper: 2.1	Best: 0.9 Lower: 0.16 Upper: 4.0
Burbank Loamy Sand[(a)]	Best: 0.9 Lower: 0.16 Upper: 2.1	Best: 0.9 Lower: 0.16 Upper: 2.1	Best: 0.9 Lower: 0.16 Upper: 2.1	Best: 0.9 Lower: 0.16 Upper: 4.0
Hanford Formation Sediments	NA	Best: 55.4 Lower: 47.5 Upper: 99.8	NA	NA

NA = Not applicable.
(a) The soil at the IDF does not exactly fit the description of either official soil type, so it was treated as a single unique soil. Recharge rates were determined for the IDF soil and assigned to both soil types.

The sensitivity tests conducted for the 2001 ILAW PA are still applicable. The results showed that the surface barrier limited recharge to less than 0.1 mm/yr regardless of the plant type, the presence of plants, or any of the climate change conditions. In contrast, recharge in the Rupert sand showed a significant sensitivity to vegetation type and climate change conditions, but less sensitivity to small variations in hydraulic properties.

The conceptual model evaluations for the 2001 ILAW PA are still applicable. Replacement of the shrub cover with cheatgrass had no impact on recharge through the surface barrier, but it increased recharge in Rupert sand from 2.2 to 33.2 mm/yr. Deposition of dune sand on the barrier reduced

evaporation. The barrier still performed as expected, but only if the shrub-steppe plant community remained. In essence, the dune sand makes the barrier performance sensitive to vegetation conditions such as fire removal and species replacement. Under the climate change condition most likely to promote recharge (i.e., increased precipitation and decreased temperature), recharge through the barrier remained <0.1 mm/yr in contrast to recharge in Rupert sand, which increased from 2.2 to 27 mm/yr. Land use restrictions are expected to preclude farming at the IDF. To understand the consequences of farming, a simulation was conducted of irrigated potatoes. The results showed that irrigation on the surface barrier significantly increased recharge.

Remaining issues concern assumptions about climate change, bioturbation, dune sand deposition, unstable and preferential flow, variability of the properties of the barrier materials and surrounding soil, longevity of the barrier, flaws in the barrier, possible facility deposition of chloride, and the importance of temperature and water vapor flow when recharge rates are lower than 1 mm/yr.

The recharge estimates provided in this report were based on a pre-conceptual design of the surface barrier. The final barrier design and the materials that will be used to construct it have not yet been identified. When they are, the final design should be re-evaluated to confirm that its performance is acceptable. In the same vein, the properties of the soil that will surround the final barrier will depend on the plan for reclamation following construction. Once identified, the proposed reclaimed soil should be re-evaluated to confirm that its performance is acceptable. Lastly, the recharge estimates provided in this report were based on a set of assumptions regarding future climate, vegetation, and land use. As new information and understanding (e.g., improved climate predictions) are developed, the assumptions should be re-evaluated and, if needed, the recharge estimates should be revised accordingly.

Acknowledgments

The authors express their gratitude for the helpful comments provided by the reviewers, Dr. Bridgit Scanlon of the Bureau of Economic Geology at the University of Texas at Austin and Dr. Glendon Gee at Pacific Northwest National Laboratory. The authors thank Dr. Fred Mann (CH2M HILL, Inc.) for providing guidance and support through this multiyear effort as well as for being a sounding board for new ideas. The authors are grateful for the FY 2004 support provided by Mark Freshley and the Remediation and Closure Science Project to ensure that the long-term recharge testing that Hanford needs continues uninterrupted at the Field Lysimeter Test Facility. The authors thank Mike Singleton of Lawrence Berkeley National Laboratory for performing isotope measurements and discussing results. The authors extend their appreciation to Launa Morasch, Lila Andor, and Kathy Neiderhiser for their editing and text processing support. Finally, the authors are grateful to the many DOE, Laboratory, and contractor staff whose pursuit of understanding of the environment provided us with some of the data and knowledge that was needed to make this data package possible.

Contents

Figures

Tables

1.0 Introduction

CH2M HILL Hanford Group, Inc. (CH2M HILL) is designing and assessing the performance of a near-surface disposal facility at Hanford for radioactive and hazardous waste. Preliminary designs prepared several years ago focused solely on immobilized low-activity waste (ILAW), which will consist of vitrified low-level radioactive waste that will be retrieved from Hanford's single- and double-shell tanks (Mann et al. 2001). According to DOE (2003), the latest disposal facility design includes ILAW as well as unvitrified low-level radioactive waste, mixed low-level waste, and vitrification melters.

The CH2M HILL effort to assess the performance of this disposal facility is known as the Integrated Disposal Facility (IDF) Performance Assessment (PA) activity, hereafter called the IDF PA activity. The goal of this activity is to provide a reasonable expectation that the disposal of waste will be protective of the general public, groundwater resources, air resources, surface-water resources, and inadvertent intruders. Achieving this goal will require predictions of contaminant migration from the facility. To make such predictions will require estimates of the fluxes of water moving through the sediment within the vadose zone around and beneath the disposal facility. These fluxes, loosely called recharge rates, are the primary mechanism for transporting contaminants to the groundwater.

Pacific Northwest National Laboratory (PNNL) assists CH2M HILL in their performance assessment activities. One of the PNNL tasks is to provide estimates of recharge rates for current conditions and long-term scenarios involving disposal at the IDF location (Puigh and Mann 2002). Previous efforts were summarized by Rockhold et al. (1995) for the 1998 ILAW PA (Mann et al. 1998) and Fayer et al. (1999) for the 2001 ILAW PA (Mann et al. 2001). Since 1999, the IDF PA activity (formerly the ILAW Project) has collected additional site-specific data. In addition to these IDF activities, other projects have collected data that are relevant to the IDF facility. CH2M HILL plans to conduct a performance assessment of the latest IDF design and call it the 2005 IDF PA. This recharge data package is being prepared to support the upcoming 2005 IDF PA.

The IDF will be located in the 200 East Area of the Hanford Site. Figure 1.1 shows that the 200 East Area is in the central part of the Hanford Site on what is known as the Central Plateau. Figure 1.2 shows a more detailed view of the southeast quadrant of the 200 East Area and the exact location of the IDF. The temporal scope of the 2005 IDF PA is 10,000 years and could be longer if, as expected, some contaminant peaks occur after 10,000 years (DOE 2003).

The objective of this data package is to provide recharge estimates for the scenarios being considered in the 2005 IDF PA. Recharge estimates are needed for a fully functional surface barrier, a barrier side slope (if present), and the immediately surrounding terrain. In addition, recharge estimates are needed for surface barrier conditions after the design life. Multiple recharge estimation techniques were used to satisfy the objective, including lysimetry, tracer studies, and modeling studies. The report identifies how the data were used to generate recharge rate estimates for the best estimate case and reasonable bounding cases, as well as indicate the uncertainties in these estimates. The report updates the recharge estimates

provided in the earlier data package (Fayer et al. 1999) with data collected since 1999. The report uses the structure of the earlier recharge data package and retains some of the written material that is pertinent to the 2005 IDF PA.

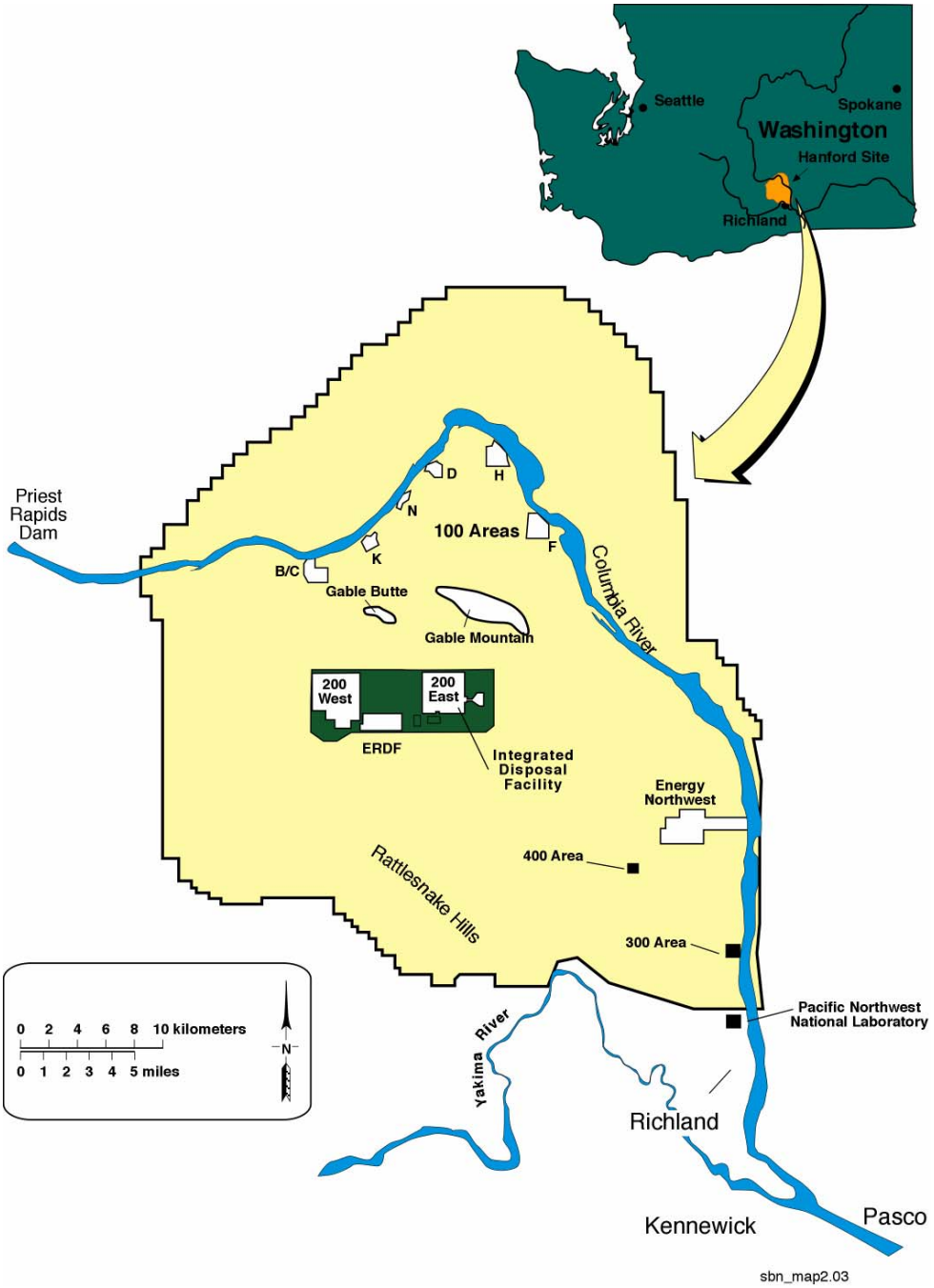

Figure 1.1. Map of the Hanford Site and its Location within Washington. The Integrated Disposal Facility is located in the southeast quadrant of the 200 East Area. (ERDF is the Environmental Restoration Disposal Facility)

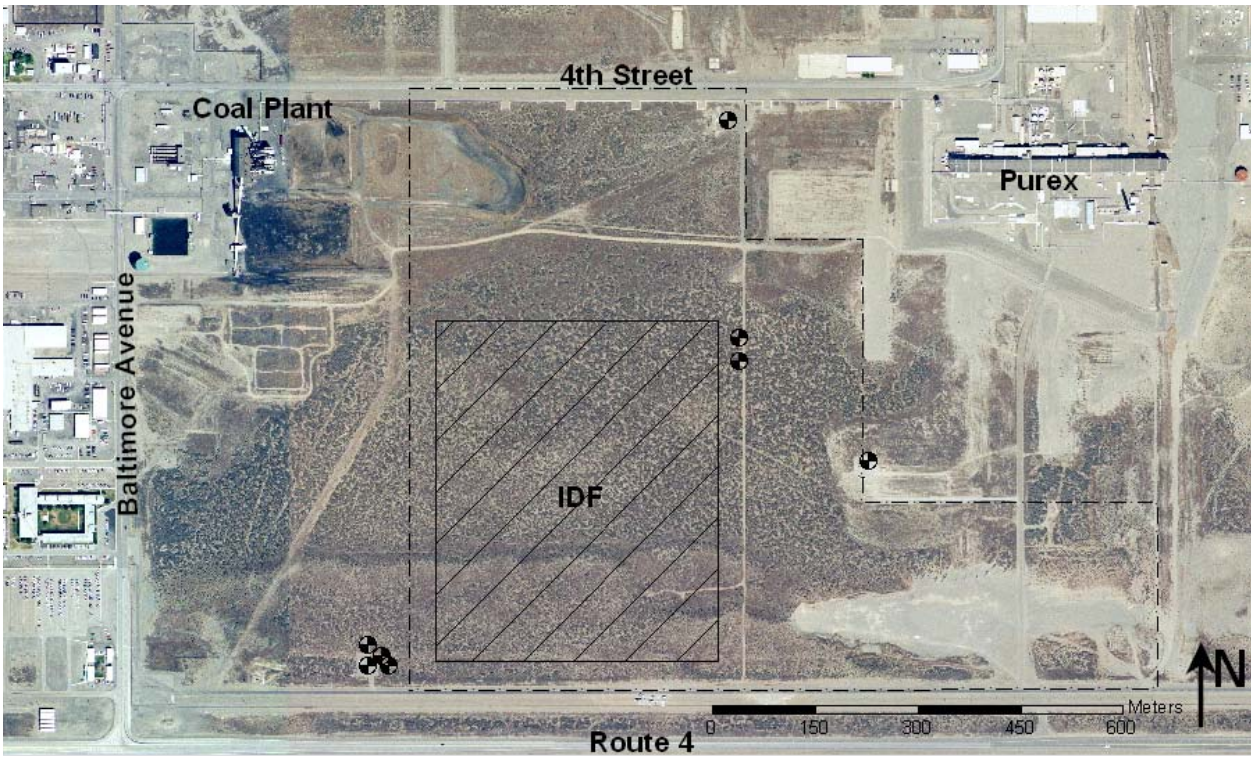

Figure 1.2. Location of the Integrated Disposal Facility within the Southeast Corner of the 200 East Area at Hanford (image courtesy of Fluor Hanford, Inc. Central Mapping, 2002)

2.0 Background

The Hanford Site was established in 1944 as a U.S. government nuclear materials production facility. During its history, the site mission included nuclear reactor operation, storage and reprocessing of spent nuclear fuel, and management of radioactive and hazardous waste. The years of operations resulted in the accumulation of significant quantities of radioactive and hazardous waste as well as their intentional and unintentional release to the environment. Today, activities on the Hanford Site involve environmental restoration, energy-related research, and technology development. One of the restoration activities is to design and construct the IDF. This activity will need evaluations of IDF performance that require estimates of recharge rates. This section defines recharge as it is used for this data package, illustrates why the recharge rate is so important, and briefly summarizes the recharge studies conducted for this and other projects.

2.1 Definition of Recharge

The precise definition of recharge is that flux of water reaching (i.e., recharging) the water table. There is no effective way to measure recharge at the water table beneath the IDF given the inaccessibility (depth >80 m); influence of operations (e.g., discharges, remediation pumping); and multiple contaminant plumes. Instead, shallow unsaturated measurements and analyses are used to estimate the deep drainage flux, i.e., that flux leaving the evapotranspiration zone and ostensibly traveling to the water table. Given sufficient time, the deep drainage flux will eventually manifest itself as the recharge flux. However, when deep drainage fluxes change, the change may not be manifested at the water table for hundreds to thousands of years. The length of time will depend on the thickness and hydraulic properties of the vadose zone and the initial and final deep drainage rates. Sediment stratification can lengthen that time further.

For the 2005 IDF PA, scenarios involving changes in recharge rates should address the time delay between deep drainage rate changes and changes in the flux reaching the water table.

2.2 Importance of Recharge

As noted in Section 1.0, the deep drainage flux (i.e., recharge) is the primary mechanism for transporting contaminants to the groundwater. Bacon and McGrail (2002) demonstrated the importance of recharge by showing how it affected the performance of buried ILAW glass. They evaluated the release of technetium-99 from the ILAW glass when subjected to five different recharge rates. Figure 2.1 shows that the technetium-99 flux beneath the ILAW disposal zone is most sensitive to the recharge rate when ratios are less than 10 mm/yr. For example, lowering the recharge rate from 4.2 mm/yr to 0.9 mm/yr reduced the technetium-99 flux from 0.6 to 0.008 mm/yr, a 16-fold reduction. Such high sensitivity demonstrates the importance of estimating the recharge rate as accurately as possible.

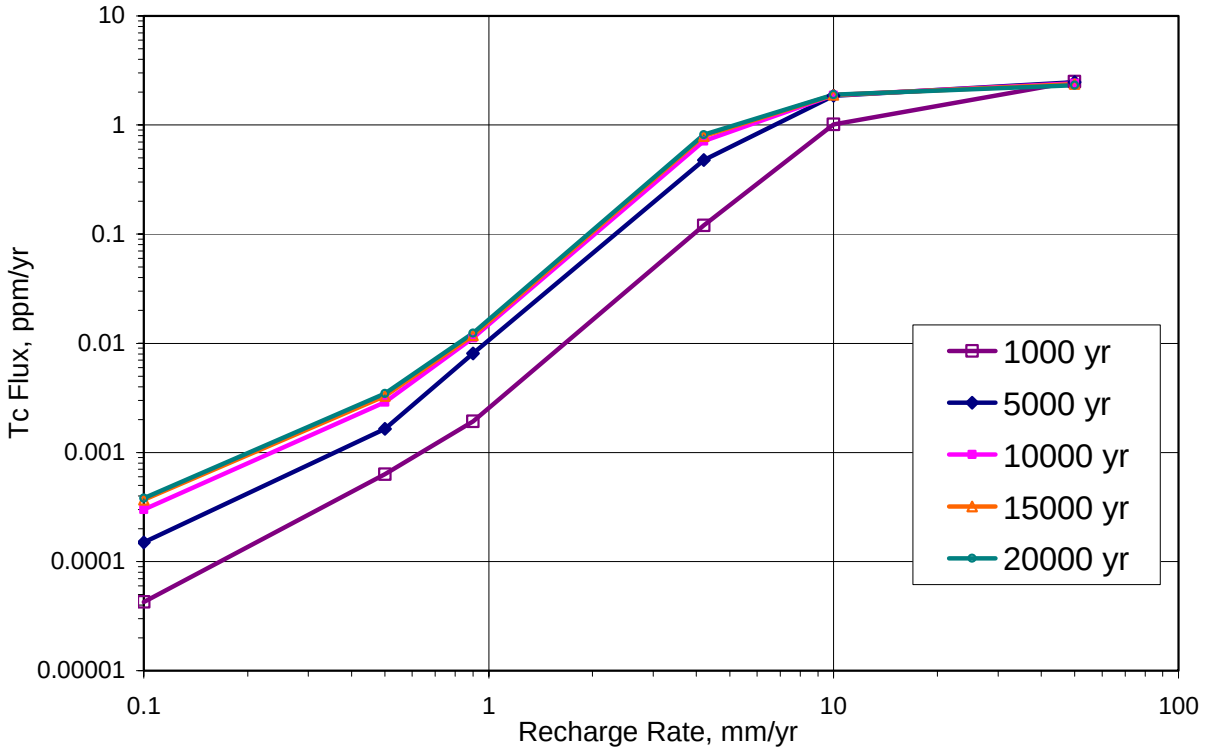

Figure 2.1. Technetium-99 Flux Beneath the Immobilized Low-Activity Waste Disposal Zone at Selected Times as a Function of Recharge Rate (adapted from Figure 5 of Bacon and McGrail 2002)

2.3 Prior Estimates of Recharge

In the early years of the Hanford Site, the perception was that recharge occurred only along the upper elevations of Rattlesnake Mountain and the valleys to the north, and it did not occur across the remainder of the site. The Hanford Defense Waste Environmental Impact Statement assumed that natural recharge was essentially zero in and around the storage and disposal areas (DOE 1987). A panel of nationally recognized scientists was convened in 1985 to discuss the recharge issue (Gee 1987). The reviewers disputed the notion of zero recharge. Data collected before and after the 1985 review showed clearly that recharge can and does occur under certain soil and plant conditions. Gee et al. (1992) presented evidence that recharge rates can vary from nearly zero in silt loam soil covered by sagebrush to more than 100 mm/yr in gravel-covered soil without vegetation.

Rockhold et al. (1995) presented a review of past work related to recharge. Appendix B of their report describes the numerous studies conducted since 1969 using field measurements of soil water, matric potential, and temperature; tracer measurements; lysimeter measurements; and numerical

modeling. All of these studies showed the potential for recharge to occur if conditions are right (i.e., coarse-textured rather than fine-textured soil, sparse plant community, and shallow-rooted rather than deep-rooted plants).

2.4 Prior Assessments

Since 1995, two performance assessments have been conducted for waste to be disposed at the IDF site: the 1998 PA and 2001 PA. Although each addressed slightly different conditions (e.g., waste loading; waste formulations; facility designs), both assessments provided data and recharge estimates relevant to the 2005 IDF PA.

1998 ILAW PA. Mann et al. (1998) is commonly referred to as the 1998 PA. It was the initial effort to demonstrate the feasibility of safely disposing of ILAW at the Hanford Site. Because the ILAW Project was only just beginning, the analyses were conducted using reasonable estimates of the parameters without having site-specific information. The intention was to initiate a program to collect data relevant to the actual disposal sites and glass product.

In lieu of site-specific data, Rockhold et al. (1995) assembled their best estimate of recharge rates to use in the 1998 PA (called the preliminary PA by Mann et al. 1995). Their recommendations were

> "The existing recharge data were used to provide recharge estimates that can be used in preliminary performance assessment calculations. Estimates are provided for the barrier, the barrier edge, the surrounding natural ecosystem, and the entire Hanford Site. We recommend assuming a recharge rate of 0.5 mm/yr through the Hanford protective barrier. This assumption is supported by an 8-year record of lysimeter data (Table 3.1) and is consistent with engineering design specifications over the 1000-year design life of the barrier (Wing 1994). At the barrier edge, a higher recharge rate of 75 mm/yr should be assumed. This assumption is based on four years of data for a lysimeter with a graveled surface (Table 3.1) that is similar to the riprap side slope of the protective barrier. This estimate does not include possible overland flow or lateral drainage from the barrier. Beyond the barrier, the recharge rate of the natural ecosystem can be represented with one of two rates. If the plant community is assumed to be sagebrush, an estimate of 5.0 mm/yr should be used. This is a conservative value chosen to be slightly greater than all the rates reported by Prych (1995) using tracer measurements. If the plant community is assumed to be cheatgrass, an estimate of 25.4 mm/yr should be used. This value is based on an 8-year record of water content observations at the Grass Site in the 300 Area (Fayer and Walters 1995). For the entire Hanford Site, we recommend using the recharge distribution map reported by Fayer and Walters (1995)."

2001 ILAW PA. Mann et al. (2001) is commonly referred to as the 2001 PA. In contrast to the 1998 PA, the 2001 PA was based on a significant quantity of site-specific data. The data collection effort was supported by a panel of nationally recognized scientists that was convened to review the ILAW Project needs for recharge information. The panel concluded that enough information existed to proceed with the

1998 PA, but that site-specific data would be needed to provide technically defensible estimates.[a] They supported efforts to use lysimetry, tracers, and modeling. The panel noted that the results might not change the recharge estimates significantly but would strengthen the technical credibility of the final recharge estimates used in the performance assessment. The panel also cautioned that uncertainty in conceptual models and supporting data should not be ignored.

During and after preparation of the 1998 ILAW PA, the ILAW Project continued to conduct studies to improve the estimates of natural recharge. These studies included direct measurements of recharge using lysimetry, tracer evaluations of recharge, and numerical simulations of recharge. In addition to these studies, the project analyzed the origin of sand dunes at Hanford, examined the possibility of deposition of facility emissions (and their possible impact on tracer analyses), and characterized the current plant community at the disposal sites to provide better parameters for numerical simulations of recharge. The full body of work was known as the Recharge Data Package for the 2001 ILAW PA (Fayer et al. 1999).

2.5 Recent Performance Assessment Activities

Following the publication of Fayer et al. (1999), the IDF activity and its precursor ILAW Project conducted several studies to improve the estimates of natural recharge. The results of these studies are contained within this report and include direct measurements of recharge using lysimetry (Appendix A), tracer evaluations of recharge (Appendix B), and numerical simulations of recharge (Appendix C).

(a) Honeyman, JO. 1995. Letter to L Erickson transmitting the results of the 1995 workshop titled *Summary of peer review comments resulting from the second Hanford groundwater recharge workshop*. May 22-23, 1995, Richland, Washington.

3.0 Affected Environment

An adequate evaluation of the impact of the IDF requires an understanding of the local environment. This section summarizes information on the climate and meteorology, geology and soil, hydrology, and ecology. Portions of this section were extracted from existing reports, including Neitzel et al. (2003) Hoitink et al. (2003), Reidel and Reynolds (1998), Fayer et al. (1999), and Reidel (2004). For brevity, references in the original texts are not included here.

The Hanford Site lies within the semiarid Pasco Basin of the Columbia Plateau in southeastern Washington State (Figure 1.1). The Hanford Site occupies an area of about 1,517 km^2; only about 6% of the land area has been disturbed and is actively used for the storage of nuclear materials and waste and waste disposal. The Columbia River flows through the northern part of the Hanford Site and forms part of the site's eastern boundary. The Yakima River runs near the southern boundary of the Hanford Site and joins the Columbia River at the city of Richland, which bounds the Hanford Site on the southeast. Rattlesnake Mountain, Yakima Ridge, and Umtanum Ridge form the southwestern and western boundaries. The Saddle Mountains form the northern boundary of the Hanford Site. Two small east-west ridges, Gable Butte and Gable Mountain, rise above the plateau of the central part of the Hanford Site. Adjoining lands to the west, north, and east are principally range and agricultural land. The cities of Kennewick, Pasco, and Richland (Tri-Cities) constitute the nearest population centers and are located southeast of the Hanford Site.

3.1 Climate and Meteorology

The Cascade Mountains, 100 km to the west, greatly influence the climate of the Hanford area by means of their "rain shadow" effect. This mountain range also serves as a source of cold air drainage, which has a considerable effect on the wind regime on the Hanford Site. Climatological data have been collected at the Hanford Meteorological Station (HMS) since 1945 (Hoitink et al. 2003). The HMS is located between the 200 East and 200 West Areas at an elevation of 223 m. The data are representative of the general climatic conditions for the region and describe the specific climate of the Central Plateau. The IDF site is close to the HMS and at nearly the same elevation.

Precipitation. Between 1946 and 2002, annual precipitation at the HMS averaged 172 mm and varied between 76 and 313 mm. Table 3.1 shows how monthly averages have varied in that time. The wettest season on record was the winter of 1996-1997 with 141 mm of precipitation; the driest season was the summer of 1973 when only 1 mm of precipitation was measured. Most precipitation occurs during the winter, with half of the annual amount occurring from November through February. A rainfall intensity of 20 mm/h persisting for 1 hour is expected only once every 1,000 years. A day with more than 13 mm precipitation is expected to occur about once a year, while a day with 51.6 mm precipitation is expected only once every 1,000 years. Hanford nearly experienced such a 1,000-yr event when it received 48.5 mm in a 24-hr period in October 1957.

Table 3.1. Monthly Precipitation Variations Between 1946 and 2002 at the Hanford Meteorological Station

Month	Monthly Precipitation (mm)		
	Maximum	Mean	Minimum
January	62.7	23.1	2.0
February	53.3	16.3	0.0
March	47.2	13.0	0.5
April	39.1	11.4	0.0
May	51.6	13.0	0.0
June	74.2	13.5	0.0
July	44.7	5.6	0.0
August	34.5	5.8	0.0
September	34.0	7.6	0.0
October	69.1	13.5	0.0
November	67.8	23.1	0.0
December	93.7	25.9	2.8
Annual	313	171.7	76

Snowfall accounts for about 38% of all precipitation from December through February. Monthly average snowfall is greatest in December (132 mm) and January (124 mm). The record monthly snowfall of 594 mm occurred in January 1950. The seasonal record snowfall of 1,425 mm occurred during the winter of 1992–1993. This amount has a return period of 500 years. On average, snow first appears by November 30 and is last seen on February 13. Since 1946, snow has been measured as early as October 26 and as late as April 30.

Air Temperature. Table 3.2 shows the range of monthly temperatures since 1946. The highest winter monthly average temperature was 6.9°C in February 1958, while the lowest average temperature was -11.1°C in January 1950. The highest summer monthly average temperature was 27.9°C in July 1985, while the lowest average temperature was 17.2°C in June 1953. There were, on the average, 52 days during the summer months with maximum temperatures ≥32°C and 12 days with maxima ≥38°C. During winter seasons, an average of 106 days had temperature minimums below 0°C; an average of 3 days had minimum temperatures that were ≤-18°C, but only one winter in two experienced such temperatures. The record maximum temperature is 45°C, and the record minimum temperature is -31°C. The potential for plant activity can be represented by the number of growing days, which is the number of days between the last freezing temperature in spring and the first freezing temperature in autumn. Since 1945, the number of growing days has averaged 181 days per year, with annual values ranging from 142 (in 1974) and 216 days (in 1994).

Table 3.2. Monthly Air Temperature Variations Between 1946 and 2002 at the Hanford Meteorological Station

Month	Monthly Air Temperature (°C)		
	Maximum	Mean	Minimum
January	5.8	-0.6	-11.1
February	6.9	3.2	-3.6
March	10.8	7.3	4.1
April	14.6	11.6	8.6
May	20.4	16.6	13.3
June	24.9	20.7	17.2
July	27.9	24.7	21.4
August	27.5	23.9	21.0
September	22.4	19.0	14.9
October	15.3	11.6	8.8
November	8.1	4.5	-4.0
December	3.6	0.3	-6.1
Annual		11.9	

Humidity. Since 1950, the average annual relative humidity at the HMS has been 55%; annual values ranged from 49 to 59%. December had the highest monthly average humidity (80%), with values that ranged from 69 to 91%. July had the lowest monthly average humidity (33%), with values that ranged from 22 to 46%.

Solar Radiation. Since 1953, the average annual daily solar radiation at the HMS has been 172 W/m^2 (353 ly). Average daily values were lowest in December (85 W/m^2) and highest in July (304 W/m^2). The lowest observed daily value was 4.4 W/m^2 in December 2002; the highest observed daily value was 406 W/m^2 in May 1977.

Wind. Prevailing wind directions on the Central Plateau were from the west-northwest and northwest in all months of the year. Summaries of wind direction indicate that winds from the northwest quadrant occur most often during the winter and summer. During the spring and fall, the frequency of southwesterly winds increases with a corresponding decrease in northwest flow. Winds blowing from other directions (e.g., northeast) display minimal variation from month to month. Monthly average wind speeds are lowest during the winter months, averaging 10 to 11 km/h, and highest during the summer, averaging 13 to 15 km/h. Peak wind gusts in every month originated from the west-southwest, southwest, and south-southwest. However, the summertime drainage winds from the northwest frequently exceed speeds of 13 m/s. The maximum speed of the drainage winds (and their frequency of occurrence) tends to decrease as one moves toward the southeast across the Hanford Site.

3.2 Geology

The Hanford Site lies within the Columbia Plateau, which is formed from a thick sequence of basalt flows. These flows have been folded and faulted over the past 17 million years, creating broad structural and topographic basins separated by asymmetric anticlinal ridges. The Hanford Site lies within one of the larger basins, the Pasco Basin. The Pasco Basin is bounded on the north by the Saddle Mountains and on the south by Rattlesnake Mountain and the Rattlesnake Hills. Yakima Ridge and Umtanum Ridge trend into the basin and subdivide it into a series of smaller anticlinal ridges and synclinal basins. The largest syncline, the Cold Creek syncline, lies between Umtanum Ridge and Yakima Ridge and is the principal structure containing the DOE waste management areas.

The IDF site is situated on the Cold Creek bar, a geomorphic remnant of the cataclysmic floods of the Pleistocene epoch. As the floods raced across the lowlands of the Pasco Basin and Hanford Site, the flood waters lost energy and began leaving behind deposits of gravels. The IDF site is about 3 km north of the axis of the Cold Creek syncline, which controls the structural grain of the basalt bedrock and Ringold Formation. The basalt surface and Ringold Formation trend roughly southeast-northwest parallel to the major geologic structures of the site. As a result, the Ringold Formation and the underlying basalt dip gently to the south off the Umtanum Ridge anticline into the Cold Creek syncline. Geologic mapping at the Hanford Site has not identified any faults in the vicinity of the IDF site. The closest faults are along the Umtanum Ridge-Gable Mountain structure north of the site and the May Junction fault east of the site.

The stratigraphy of the IDF site consists of the basalt flows overlain by the Ringold Formation, the Hanford formation, and Holocene eolian deposits. All recharge-related measurements and estimates occur within the Hanford formation and eolian deposits; they are described in the following paragraphs.

Hanford Formation. The Hanford formation is an informal name that represents all the deposits of the cataclysmic floods of the Pleistocene (1.6 million to 13,000 years ago). Glacial Lake Missoula formed in the Clark Fork River valley in Montana behind continental glaciers that spread south as far as the present Columbia Plateau. The lake may have given way as many as 40 times in the late Pleistocene, allowing the impounded water to spread across eastern Washington and form the Channeled Scablands. These flood waters collected in the Pasco Basin and formed Lake Lewis, which slowly drained through the narrow valley in the Horse Heaven Hills called Wallula Gap.

Three principal types of deposits were left behind by the Missoula Floods: (1) high-energy deposits consisting of gravel; (2) coarse to fine sand deposits representing an energy transition environment; and (3) low-energy, slackwater deposits consisting of rhythmically bedded silt and sand of the Touchet Beds. Gravel-dominated strata consist of coarse-grained sand and granule-to-boulder gravels that display massive bedding, plane to low-angle bedding, and large-scale cross-bedding in outcrop. Sometimes the gravel strata lack a matrix material; such gravel strata have an open-framework appearance. The sand-dominated facies consists of fine- to coarse-grained sand and granules that display plane lamination and bedding and, less commonly, plane and trough cross-bedding in outcrop. Small pebbles and pebbly interbeds (<20 cm thick) may be encountered. The silt content of these sands varies, although where its content is low, an open-framework texture may occur. The silt-dominated facies consists of fine- to

coarse-grained sand grading up to silt to form normally graded rhythmites 0.07 to 1.0 m thick. Plane lamination and ripple cross-lamination is common in outcrop.

According to Reidel (2004), the Hanford formation is as much as 116 m thick in and around the IDF site. It thickens in the erosional channel cut into the Ringold Formation and thins to the southwest along the margin of the trough. The Hanford formation reaches its greatest thickness along a NW-SE trending trough under the eastern part of the IDF site. Reidel (2004) described the Hanford formation at the IDF site as consisting of two major units: a lower gravel-dominated facies and an upper sand-dominated facies. Hanford formation units seen elsewhere (e.g., upper gravelly facies; silt-dominated, slackwater facies (Touchet Beds); interbedded sand- and silt-dominated facies) appear to be thin or absent in parts of the IDF area.

The sand-dominated facies is about 84 m thick and contains fine to coarse-grained sand with minor amounts of silt and clay and some gravelly sand. The texture becomes somewhat coarser as one moves from the west to the northeast, reflecting the higher-energy environment of the floodwater that occurred in the northeast. The sand dominated facies can be subdivided into layers, each with a capping paleosol (Reidel 2004). The basal Layer 1 thickness ranges from 26 to 64 m and may be 1 to 1.7 million years old. Layer 2 is about 28 m thick and is between 13,000 and 720,000 years old. Layer 3, the uppermost of the three layers, is 16 to 24 m thick. Layer 3 is interpreted to consist of the upper gravelly sequence and the upper part of the sandy sequence defied in previous studies. Ash from the eruption of Mt. St. Helens (Set S Ash) 13,000 years ago is typically found near the top of Layer 3 about 100 m west of the IDF, but the ash layer has not been detected within the IDF site. The paleosol that caps Layer 3 forms much of the surface of the northern end of the IDF site.

At many locations on Hanford, variably oriented sediment features known as clastic dikes cut across the typically horizontal sediment layers (Fecht et al. 1999; Murray et al. 2003). These dikes could act as preferential pathways for water and contaminant transport. Clastic dikes have not been visually observed at the IDF site because most of the area remains largely untouched by construction activities. However, a borehole sample collected in 2002 from about the 47.5-m depth contained portions of a clastic dike (Reidel 2004).

Holocene Deposits. Holocene deposits consisting of silt, sand, and gravel form a thin (<5 m) veneer across much of the Hanford Site as well as the IDF Site. The thickness of the eolian material ranges from less than 0.5 m on the north end of the site to 1.5 m near the southern end before reaching the sand dune. The southern 200 m is covered with a stabilized sand dune that is as much as 8 m high. Appendix D of Fayer et al. (1999) described the nature of the dune and its relationship to the active dune field that lies to the south and southeast. Mature sagebrush is present on the sand dune, indicating that the dune has been stable since the 1940s at least. Clastic dike features are not visible at the soil surface anywhere within the IDF area.

3.3 Soil

The Holocene deposits and exposed Hanford formation sediment have experienced soil development and evolved into identifiable soil types. Hajek (1966) produced a soil map of the Hanford Site.

Figure 3.1 shows that only two soil types cover the IDF site: Rupert sand and Burbank loamy sand. Hajek (1966) described these types of soil as follows:

> ***Rupert Sand***. "This mapping unit represents one of the most extensive soils on the Hanford Project. The surface is a brown to grayish brown (10YR5/2) coarse sand, which grades to a dark grayish brown (10YR4/2) sand at about 36 in. Rupert soils developed under grass, sagebrush, and hopsage in coarse sandy alluvial deposits, which were mantled by wind-blown sand. Relief characteristically consists of hummocky terraces and dune-like ridges. This soil may be correlated as Quincy sand, which was not separated here. Active sand dunes are present. Some dune areas are separated; however, many small dunes, blow-outs, and associated small areas of Ephrata and Burbank soils are included."

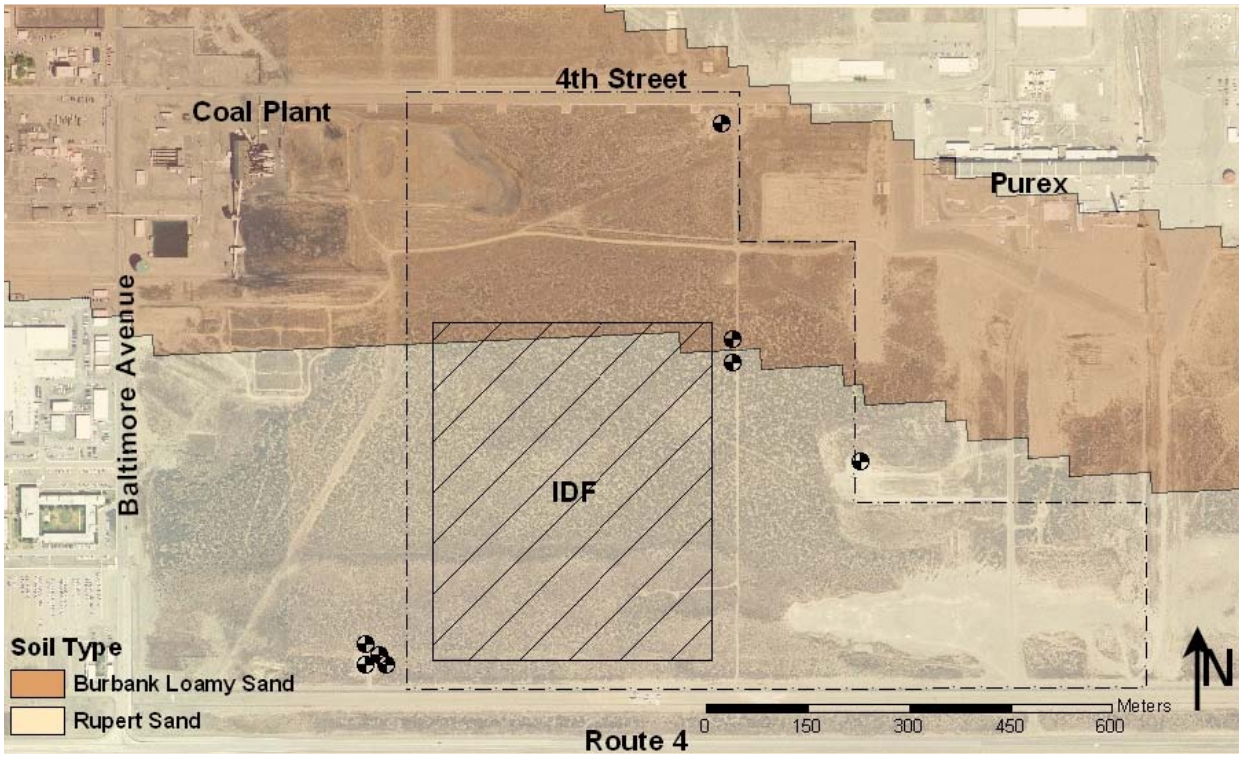

Figure 3.1. Soil Types at the Integrated Disposal Facility Site

> ***Burbank Loamy Sand***. "This is a dark-colored [surface is very dark grayish brown (10YR3/2); subsoil is dark grayish brown (10YR4/2)], coarse-textured soil which is underlain by gravel. The surface soil is usually about 16 in. thick but can be 30 in. thick. The gravel content of the subsoil may range from 20 to 80 volume percent. Areas of Ephrata and Rupert are included."

The soil map produced by Hajek (1966) was based largely on the soil survey work conducted around 1910 to 1915 and reported by Kocher and Strahorn (1919). The focus of these surveys was primarily agricultural use and not estimation of natural recharge. Recent evidence suggests that the soil conditions at the IDF are unique and not easily classified into either Rupert sand or Burbank loamy sand. For example, Figure 3.2 shows the side of a pit that was excavated about 175 m west of the IDF site. The profile shows a 1.2-m-thick set of nearly horizontal layers of alternating sands, gravels, and fines that were deposited during the waning period of the last cataclysmic flooding. Above this sequence of layers lies eolian material; below this sequence lies the coarse sand of the Hanford formation.

Anecdotal information suggests the sequence of layers in Figure 3.2 exists across much of the IDF Site. The contrasting textures within that sequence create capillary breaks that impede the movement of unsaturated liquid water. The water storage capacity of the eolian material residing above the layers will influence the potential deep drainage rate. Depths of eolian material between 1.0 and 2.0 m may be ideal for storing all precipitation till it can be removed by evapotranspiration, thus significantly reducing deep drainage rates. If thinner than 1.0 m, the eolian material may not be able to store all winter precipitation. If thicker than 2.0 m, the eolian material can store the precipitation, but the water stored near the deep capillary break may be too deep to be removed by evapotranspiration. In either case, the result is an increased potential for higher drainage rates.

The depth of eolian material at the IDF Site varies from less than 1.0 m in the north to 1.5 m just to the north of the dune. In and around the dune, the depth can range as high as 5 m. Whether the soil at a particular location at the IDF Site is formally classified as Burbank loamy sand, Rupert sand, or, in the south, dune sand, is debatable. What is important for this recharge data package is that deep drainage rates be estimated using the observed soil profile conditions (e.g., Figure 3.2) rather than the idealized soil conditions reported by Hajek (1966).

3.4 Topography

Figure 3.3 shows that the topography of the IDF site is relatively flat with elevations that range between 219 and 222 m. The dune along the southern edge rises above the surrounding terrain by as much as 9 m, with a peak elevation of about 229 m. The eastern most portion of the dune has been excavated for other construction purposes. The remaining portion of the dune is not expected to exist once construction is completed. The relative flatness of the IDF site means that the final topography will be determined by the surface cover and grading of the surrounding soil.

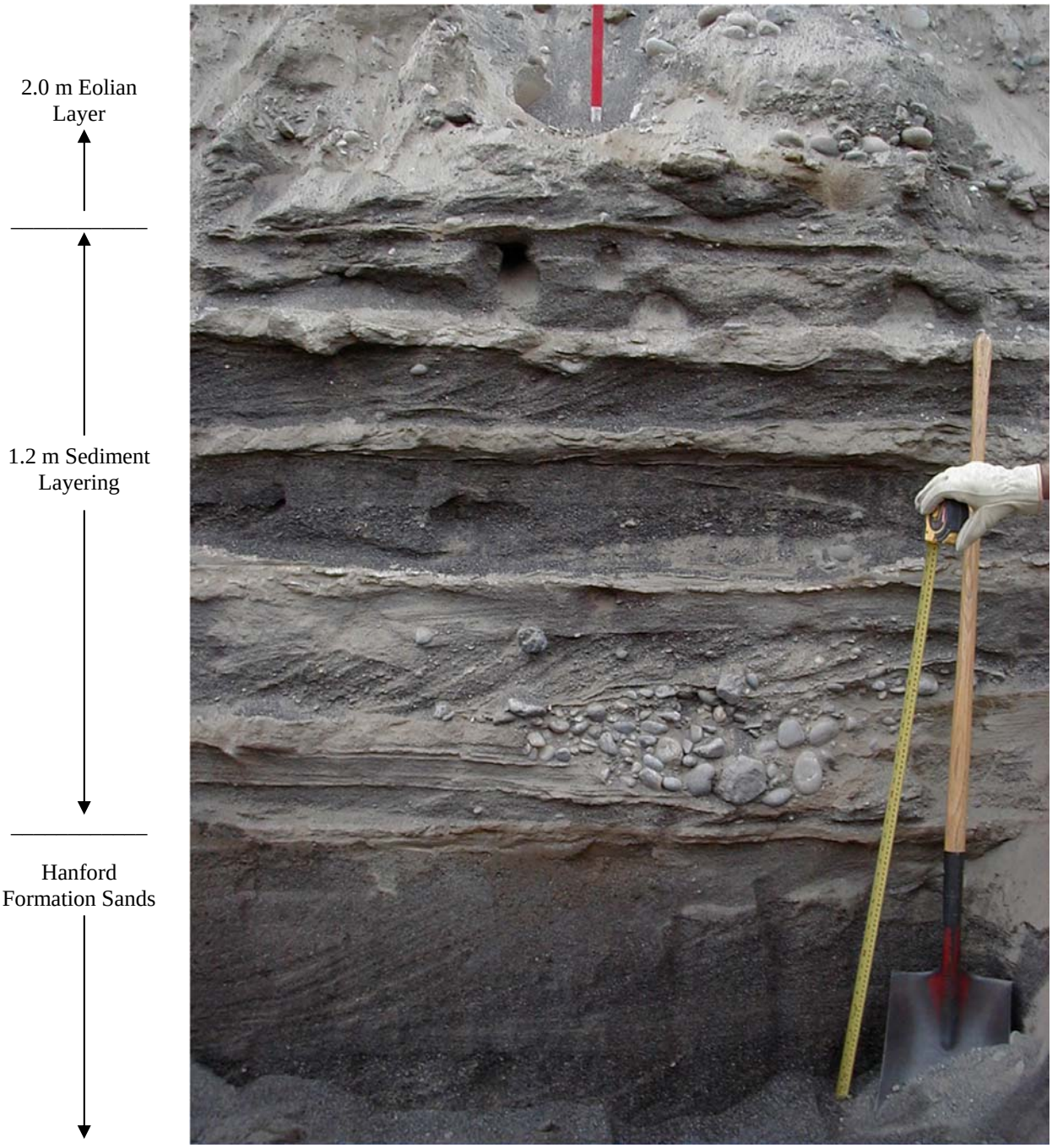

Figure 3.2. Sediment Layering in a Pit Excavated 175 m West of the Southwest Corner of the Integrated Disposal Facility. The pronounced sediment layering is the result of multiple flood events that deposited alternating layers varying from fine sand to coarse sand and gravel. (Photo courtesy of Dr. John Selker, Oregon State University).

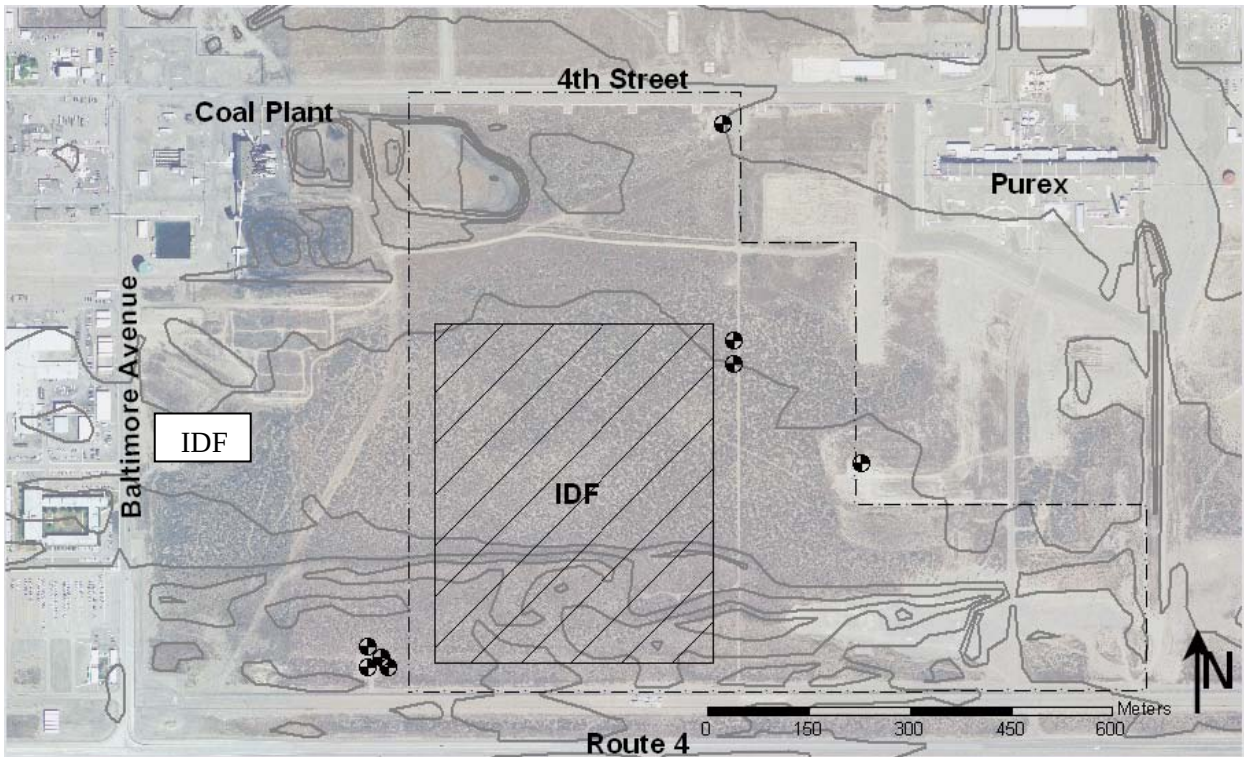

Contour Intervals = 2.5 m

Figure 3.3. Topography at the Integrated Disposal Facility Site. The highest point (229 m) is on the sand dune in the southern end of the Integraged Disposal Facility. From there, the ground surface slopes down to 219 m at the north end.

3.5 Hydrology

The primary surface-water features associated with the Hanford Site are the Columbia and Yakima Rivers. The Columbia River is the second largest river in the contiguous United States in terms of total flow and is the dominant surface-water body on the Hanford Site. Cold Creek and its tributary, Dry Creek, are ephemeral streams within the Yakima River drainage system. Both streams drain areas along the western part of the Hanford Site. Surface flow, which may occur during spring runoff or after heavier-than-normal precipitation, infiltrates and disappears into the surface sediments. The IDF site is located well above and away from these surface-water features and is unaffected by them in any direct manner.

Natural recharge rates across the Hanford Site range from near 0 to more than 100 mm/yr, depending on surface conditions (Gee et al. 1992). Low recharge rates occur in fine-textured sediments where deep-rooted plants occur. The larger values occur in areas having a coarse gravelly surface and no vegetative cover (e.g., disturbed areas such as around the tank farms).

The unsaturated zone beneath the land surface at the IDF site ranges from 94 m thick on the north end of the IDF Site to 101 m thick in the south. This vadose zone lies entirely within the Hanford formation and eolian sediment.

The Pasco Basin has several confined aquifers within the basalt flows and one unconfined aquifer above the basalt flows. In the 200 Areas, the aquifer above the basalt is unconfined to locally semi-confined and is contained largely within the sediments of the Ringold Formation and Hanford formation. In some locations, the aquifer does not exist above the basalt.

The water table beneath the IDF site occurs within the Hanford formation. Normally, groundwater flows from west to east. However, artificial recharge from wastewater disposal activities has perturbed the flow directions. Currently, the water table is flat beneath the IDF site, so a groundwater flow direction cannot be determined. As wastewater discharges decrease and eventually cease, the general west-to-east flow is expected to resume.

3.6 Ecology

The Hanford Site is characterized as a shrub-steppe ecosystem that is adapted to the region's mid-latitude semiarid climate (Neitzel 2003). Such ecosystems are typically dominated by a shrub overstory with a grass understory. In the early 1800s, dominant plants in the area were big sagebrush (*Artemisia tridentata*) and an understory consisting of perennial Sandberg's bluegrass (*Poa sandbergii*) and bluebunch wheatgrass (*Pseudoregneria spicata*). Other species included three-tip sagebrush (*Artemisia tripartite*), bitterbrush (*Purshia tridentate*), gray rabbitbrush (*Ericameria nauseosa*), spiny hopsage (*Grayia spinosa*), needle-and-thread grass (*Hesperostipa comata*), Indian ricegrass (*Achnatherum hymenoides*), and prairie Junegrass (*Koeleria cristata*).

With the advent of settlement, livestock grazing and agricultural production contributed to colonization by non-native vegetation species that currently dominate portions of the landscape. Although agriculture and livestock production were the primary subsistence activities at the turn of the century, these activities ceased when the Site was designated in 1943. Range fires that historically burned through the area during the dry summers eliminate fire-intolerant species (e.g., big sagebrush) and allow more opportunistic and fire resistant species to establish. Of the 727 species of vascular plants recorded for the Hanford Site, approximately 25% are non-native. The dominant non-native species, cheatgrass (*Bromus tectorum*), is an aggressive colonizer and has become well established across the site. Over the past decade, several knapweed species have also become persistent invasive species in areas not dominated by shrubs.

Approximately 300 species of terrestrial vertebrates have been observed on the Hanford Site, including approximately 42 species of mammals, 246 species of birds, 5 species of amphibians, and 12 species of reptiles. Terrestrial wildlife include Rocky Mountain elk (*Cervus elaphus*), mule deer (*Odocoileus hemionus*), coyote (*Canis latrans*), bobcat (*Lynx rufus*), badger (*Taxidea taxus*), deer mice (*Peromyscus maniculatus*), harvest mice (*Riethrodontonomys megalotis*), grasshopper mice (*Onychomys leucogaster*), ground squirrels (*Spermophilus washingtonii*), voles (*Microtus montanus*), and black-tailed jackrabbits (*Lepus californicus*). The most abundant mammal on the Hanford Site is the Great Basin

pocket mouse (*Perognathus parvus*). Bird species commonly found in the shrub-steppe habitats at Hanford include the western meadowlark (*Sturnella neglecta*), horned lark (*Eremophila alpestris*), long-billed curlew (*Numenius americanus*), vesper sparrow (*Pooecetes gramineus*), sage sparrow (*Amphispiza belli*), sage thrasher (*Oreoscoptes montanus*), loggerhead shrike (*Lanius ludovicianus*), and burrowing owls (*Athene cunicularia*).

Butterflies, grasshoppers, and darkling beetles are among the more conspicuous of the approximately 1,500 species of insects that have been identified from specimens collected on the Hanford Site. The actual number of insect species occurring on the Hanford Site may reach as high as 15,000. Insects are more readily observed during the warmer months of the year.

The side-blotched lizard (*Uta stansburiana*) is the most abundant reptile species that occurs on the Hanford Site. Short-horned (*Phrynosoma douglassii*) and sagebrush lizards (*Sceloporus graciosus*) are reported, but occur infrequently. The most common snake species includes gopher snake (*Piteriphis melanoleucus*), yellow-bellied racer (*Coluber constrictor*), and Western rattlesnake (*Crotalus viridis*). The Great Basin spadefoot toad (*Scaphiopus intermountanus*), Woodhouse's toad (*Bufo woodhousei*), Pacific tree frog (*Hyla regilla*), tiger salamander (*Ambystoma tigrinum*) and bullfrogs (*Rana catesbeiana*) are the only amphibians found on the Hanford Site.

The above summary of Hanford ecology (from Neitzel 2003) is based on data collected across the entire Hanford Site. Very few studies, however, have been conducted specifically at the IDF site. The assumption, which is considered reasonable, is that the ecology at the IDF site is a subset of the Hanford ecology. In addition to the common species identified by Neitzel (2003), some species may be important not for their numbers, but for their potential impacts to waste sites. For example, harvester ants (*Pogonomyrmex* spp.) have been observed at Hanford and can burrow and bring waste material to the surface.

4.0 Disposal Facility Design

The IDF will be a large trench in the southeast quadrant of the 200 East Area at Hanford (Figure 1.2). Once completed, the IDF will receive a final surface barrier and surrounding land will be re-vegetated. The following discussion is taken from DOE (2003) and Fayer et al. (1999).

4.1 Waste Destined for the Integrated Disposal Facility

Four categories of waste are destined for disposal in the IDF:

Immobilized Low-Activity Waste (ILAW). More than 209,000 m^3 of radioactive and mixed waste stored in 177 buried single- and double-shell tanks in the Hanford Site 200 Areas (Mann et al. 1998). This waste will be retrieved and separated into two fractions: high-level waste to be sent to a federal geologic repository and low-activity waste to be immobilized (i.e., ILAW) and placed in the IDF. Immobilization will be accomplished through the vitrification process, which will turn the waste slurry into a glass product. Some of the more important radionuclides include ^{90}Sr, ^{99}Tc, ^{129}I, ^{126}Sn, and ^{137}Cs, as well as isotopes and progeny of uranium, plutonium, neptunium, and americium (Mann et al. 1998).

Low-Level Waste (LLW). This waste contains manmade radionuclides that are not classified as high-level or transuranic waste and do not contain materials regulated under the *Resource Conservation and Recovery Act* (RCRA) or the corresponding dangerous waste management laws of the state of Washington.

Mixed Low-Level Waste (MLLW). This waste contains manmade radionuclides that are not classified as high-level or transuranic waste and which contain materials regulated under RCRA or the corresponding dangerous waste management laws of the state of Washington.

Melters. These contaminated pieces of equipment are the high-level and low-activity waste melters used to vitrify tank waste.

4.2 Subsurface Facility

Figure 4.1 shows the footprint of the entire IDF trench and support structures if built to its maximum extent. The subsurface component will be a 15-m-deep lined trench that will be filled until the contents are level with the existing grade. The prepared subgrade material beneath the liner is assumed to be composed of backfill material. A 0.9-m-thick admix layer will be placed on the prepared subgrade. Figure 4.2 shows that the east-west width of the lined trench bottom is 375 m; the depth is 13.2 m. The north-south length of the trench will be sized to accommodate waste added to IDF; the length could approach 400 m. Figure 4.2 also shows that a RCRA-compliant double lined system will be installed. A leachate collection and recovery system is part of each liner. Both the primary and secondary drainage

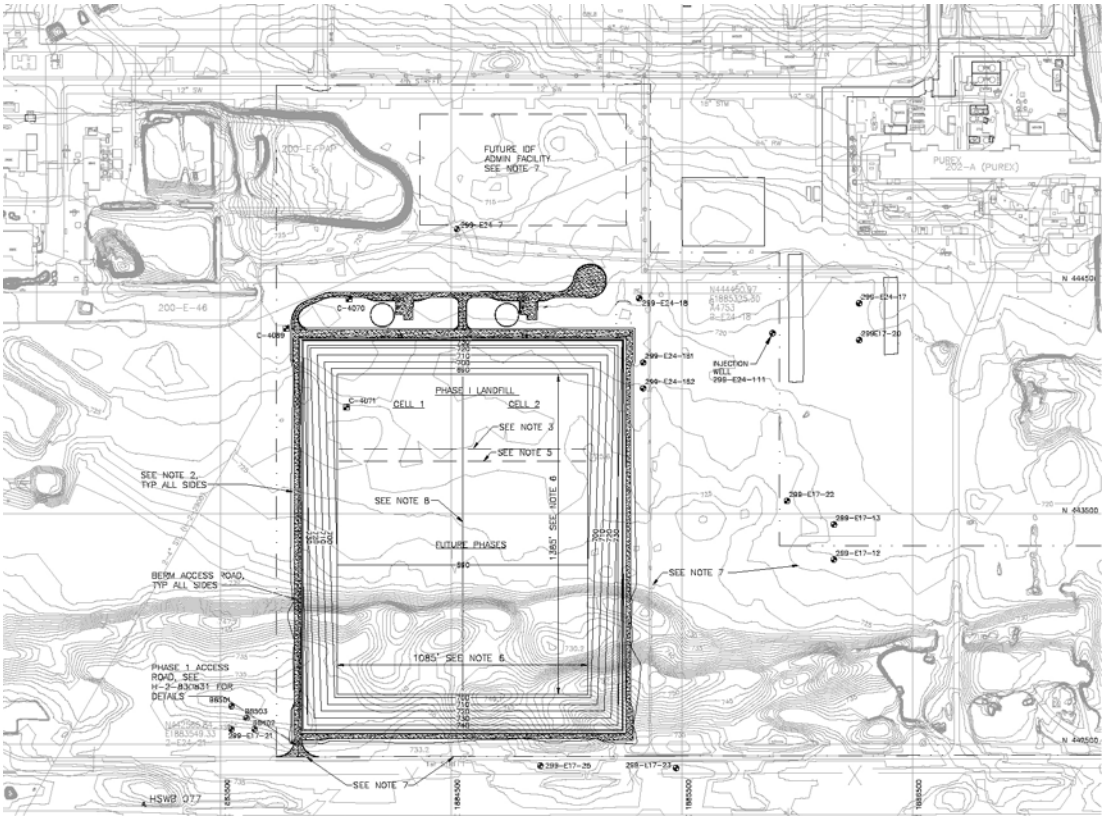

Figure 4.1. Integrated Disposal Facility Footprint (after DOE 2003)

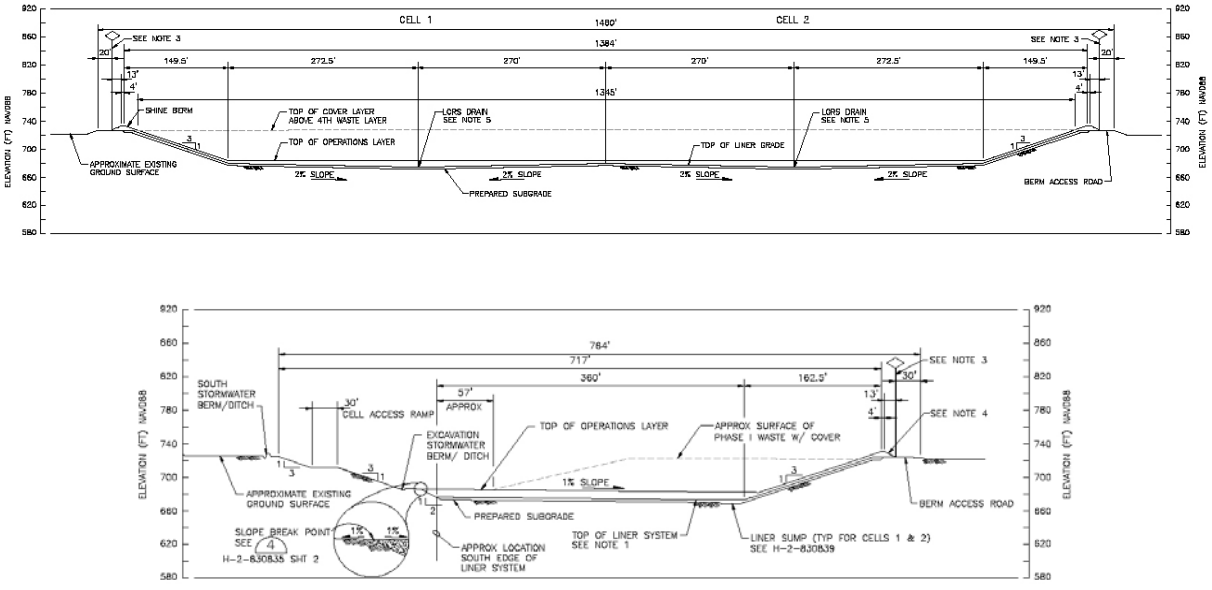

Figure 4.2. Cross Sections of the Integrated Disposal Facility Trench (after DOE 2003)

layers consist of a geocomposite drainage layer on top of high-density polyethylene (HDPE). The trench side slopes will be 3H:1V, and the liner will be anchored at the top of the slope. The 0.9-m layer on the liner is assumed to be backfill material.

The operational plans for the IDF are to fill the trench in stages. The first two cells to be filled will be on the north end of the trench. The length of the trench will be increased to the south to accommodate additional waste as needed. As waste is added to the trench, backfill soil will be added around and on top of the waste containers to minimize voids that could destabilize the surface barrier and to provide radiation shielding for the facility workers. The IDF is expected to be closed by 2046.

4.3 Surface Barrier

The objective of a surface barrier is to isolate and protect buried waste for an extended period of time using natural materials. The surface barrier for the IDF has not yet been designed. At a minimum, the barrier must minimize the amount of water that reaches the trench, and it must be sufficiently thick to ensure a minimum of 5 m of material between the top of the waste and the barrier surface. The barrier is assumed to extend 10 m beyond the inner dimension of the trench. The barrier surface is assumed to have a 2% slope.

The current preconceptual design is the modified RCRA-compliant subtitle C design proposed by DOE (1996). The following description is taken loosely from that report (titled *Focused Feasibility Study of Engineered Barriers for Waste Management Units in the 200 Areas*).

The Modified RCRA Subtitle C Barrier (RCRA barrier) is the baseline design for sites containing dangerous waste and several categories of low-level and mixed waste. This barrier was designed to provide long-term containment and hydrologic protection for a performance period of 500 years. The performance period was based on radionuclide concentration and activity limits for Category 3 low-level waste. The feature thought most likely to be affected during the performance period was the thickness of the silt loam layer. A very conservative calculation of erosion rates showed that, at most, only 15 cm of silt loam would be eroded in 500 years. DOE (1996) concluded that this loss would not compromise the performance of the barrier.

Table 4.1 lists the design criteria. The RCRA barrier is composed of eight layers of durable material with a combined minimum thickness of 1.7 m. Table 4.2 provides the layer thicknesses and descriptions. This design incorporates RCRA “minimum technology guidance,” with modifications for extended performance. One major change is the elimination of the clay layer, which may desiccate and crack over time in an arid environment. The geomembrane component also has been eliminated because of its uncertain long-term durability. The design incorporates provisions for biointrusion and human intrusion control. However, the provisions are modest relative to the corresponding features in the 200-BP-1 Prototype Hanford Barrier (prototype barrier) design, reflecting the reduced toxicity of the subject waste and reduced design-life criterion.

Surface barriers sometimes need to be elevated above the surrounding terrain to provide sufficient coverage above the waste. In such cases, a steep armored side slope may be required to blend the barrier into the surrounding terrain. Based on the trench and liner specifications in Figures 4.2 and 4.3, the

proposed barrier design (2% slope; 10 m extension beyond the waste; 200 m length from crest to edge) can easily be blended into the surrounding terrain without the need for armored side slopes.

Table 4.1. Summary of Design Criteria for the Modified RCRA Subtitle C Barrier

1.	Minimize moisture infiltration through the barrier.
2.	Design a multilayer barrier of materials that are resistant to natural degradation processes.
3.	Design a durable barrier that needs minimal maintenance during its design life.
4.	Design a barrier with a functional life of 500 years.
5.	Prevent plants from accessing and mobilizing contamination (i.e., prevent root penetration into the waste zone).
6.	Prevent burrowing animals from accessing and mobilizing contamination.
7.	Ensure that the top of the waste is at least 5 m below final grade or include appropriate design provisions to limit inadvertent human intrusion.
8.	Facilitate drainage and minimize surface erosion by wind and water.
9.	Design the low-permeability layer of the barrier to have a permeability less than or equal to any natural subsoils present.
10.	Design the barrier to prevent the migration and accumulation of topsoil material within the lateral drainage layer (i.e., clogging of the lateral drainage layer).
11.	For frost protection, the lateral drainage layer and the low-permeability asphalt layer must be located at least 0.75 m below final grade.

4.4 Closure Conditions Around the Surface Barrier

Burbank and Klem (1997) indicated that the disturbed land around the barrier would be re-contoured and re-vegetated with native plant species. It is assumed that some effort will be made to promote any surface water drainage away from the barrier and also that the topsoil used will be similar to the existing topsoil to promote re-vegetation. As noted in Section 3.3, this means 1.0 to 1.5 m of fine sand atop coarse sands and gravels. An alternative conceptual model is that the Hanford formation sand from the excavation will be used for the topsoil.

Table 4.2. Summary of Modified RCRA Subtitle C Barrier Layers

Layer No.	Thickness cm (in.)	Layer Description	Specifications	Function
1	50 (20)	Silt loam topsoil with pea gravel admix	McGee Ranch silt loam containing 15 wt% pea gravel, 2.36 to 9.5 mm in diameter, conforming to ASTM D448 No. 8 aggregate; to be placed at a bulk density of approximately 1.46 g/cc.	The topsoil material was identified for optimal water retention properties and should provide a good rooting medium for cover vegetation. The pea gravel is designed to minimize wind erosion of the silt loam without significantly affecting its moisture retention capabilities.
2	50 (20)	Compacted topsoil	McGee Ranch silt loam without pea gravel, compacted to 90% of optimum dry density as determined by standard Proctor test; in-place bulk density will be approximately 1.76 g/cc.	Same as Layer 1. Layer 2 provides a supplemental soil moisture storage capacity. Compaction of this layer is intended to retard the rate of infiltration of soil moisture. The extended residence time of moisture in Layer 2 will increase the amount of moisture removed by evapotranspiration.
3	15 (6)	Sand filter	Clean, screened sand meeting the following particle sizes: D15 = 0.15 to 0.50 mm, D50 = 0.375 to 1.2 mm, and D85 = 0.70 to 2.5 mm.	This layer is part of a two-layer graded filter designed to prevent the migration of topsoil particles into Layer 5.
4	15 (6)	Gravel filter	Clean, screened aggregate meeting the following particle sizes: D15 = 1.5 to 2.0 mm, D50 =15 to 20 mm, and D85 <37.5 mm.	Same as Layer 3.
5	15 (6)	Lateral drainage aggregate	Naturally occurring aggregate, minus 32-mm material, conforming to the grading identified in WDOT M41-10, 9-03.9(3) for base course, with D10 >1 mm and k >1 cm/s.	The lateral drainage layer will intercept and divert moisture along a 2% slope to the margin of the barrier for collection and/or discharge.
6	15 (6)	Asphaltic concrete with spray-applied asphalt coating	Asphaltic concrete, consisting of asphalt conforming to WDOT M41-10, 9-02.1(4) - Grade AR-4000W, and aggregate with particle size gradation conforming to ASTM C 136. Asphalt will make up 7.5 wt% of total mixture. A spray-applied, styrene-butadiene asphalt material will be sprayed onto the asphaltic concrete surface in two layers, each 100 mils thick minimum.	This layer will function as a hydrologic barrier and as a biointrusion barrier.
7	10 (4)	Asphalt base course	Crushed aggregate, minus 16-mm diameter material, conforming to WDOT M41-10, 9-03.9(3) for top course surfacing material.	This layer will provide a stable base for placing and supporting the asphalt layer.
8	Variable	Grading fill	Clean, bank run sand and gravel conforming to WDOT M41-10, 9-03.18.	This layer will provide a smooth, level subgrade for construction of the overlying layers.

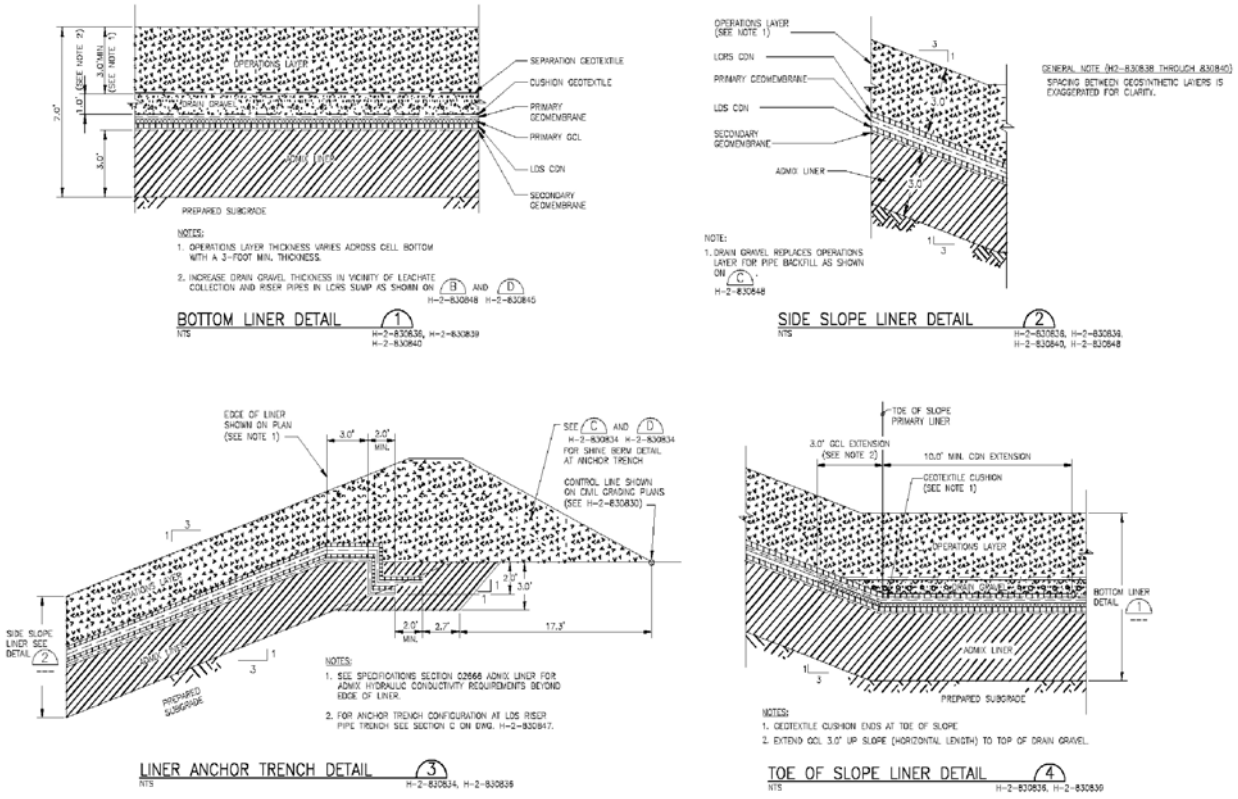

Figure 4.3. Details of the Integrated Disposal Facility Liner (after DOE 2003)

5.0 Analysis Cases and Tests

The mandate for the recharge task was to identify the scenarios that must be evaluated for the 2005 IDF PA and provide estimates of appropriate recharge rates. These scenarios must be framed within the categories of the best estimate case and reasonable bounding cases. In addition, sensitivity tests must be conducted and alternative conceptual models evaluated to demonstrate our understanding of the system. The analysis cases and tests described in this section are nearly identical to those used for the 2001 ILAW PA (Fayer et al. 1999). Section 6.0 describes the methods used to estimate recharge. Section 7.0 describes the estimates and their assignment to the best estimate case and the bounding cases.

5.1 Best Estimate Case

The best estimate case represents the situation in which all disposal facility features function as expected assuming a shrub-steppe plant community, current climate, no major change in land use (e.g., irrigated farming), and no significant subsidence impact on the barrier. This case represents the baseline condition, which is what is reasonably expected to occur. What this case is not is an estimate of the *best* case, i.e., the case in which all components worked perfectly to minimize recharge.

Based on the facility design, there are five surface features that need separate evaluations:

- Modified RCRA Subtitle C Barrier
- Barrier side slope
- Rupert sand
- Burbank loamy sand
- Hanford formation sediment

The relatively impermeable asphaltic concrete (Layer 6 in Table 4.2) was not included in the analysis. Any recharge-related benefits from this layer would be an addition to the benefits provided by the capillary break (i.e., Layers 1 to 5 in Table 4.2). As discussed in Section 4.0, a barrier side slope should not be required. However, the final barrier has not yet been designed, so this feature was retained for evaluation.

The five surface features were evaluated for conditions that existed during four time periods: prior to Hanford, during disposal facility operations, during the design life of the surface barrier, and following the design life of the surface barrier. Table 5.1 shows which features were evaluated for each time period of interest to the 2005 IDF PA.

For the period prior to Hanford, the soils were assumed to be undisturbed and similar to what exists currently. The vegetation was assumed to be a healthy shrub-steppe with a mixture of grasses and shrubs. During the past few thousand years, the IDF site was assumed to have experienced normal weather cycles, vegetation changes in response to fire, drought, disease, and pests, and soil development. The water and geochemical conditions observed in the present-day vadose zone were assumed to be a consequence of these assumptions about past soil and plant conditions.

For the period during disposal operations, the IDF trench will be open and Hanford formation sediment will be exposed. This sediment is coarser than the natural soil and is expected to lead to a higher recharge rate. Plant activity in this construction zone was assumed to be minimal, which will also contribute to a higher recharge rate. The surrounding soils, where undisturbed, were assumed to behave in a fashion similar to their pre-Hanford state.

Table 5.1. Surface Features Evaluated During Each Period of Interest for the Integrated Disposal Facility 2005 Performance Assessment

Surface Feature	Time Period of Recharge Evaluation			
	Pre-Hanford	During Disposal Operations	During Surface Barrier Design Life	After Surface Barrier Design Life
Modified RCRA Subtitle C Barrier			√	√
Barrier Side Slope			√	√
Rupert Sand	√	√	√	√
Burbank Loamy Sand	√	√	√	√
Hanford Formation Sediment		√		

For the period during the surface barrier design life, the barrier was assumed to function as designed. Any benefits that might accrue from an impermeable layer (e.g., asphalt) were not considered. Normal weather variability, variations in plant activity, and soil development were assumed to occur and have no significant impact on barrier performance. The surrounding soils, where undisturbed, were assumed to behave in a fashion similar to their pre-Hanford state. Where disturbed, the soils were assumed restored to their pre-Hanford state.

For the period after the surface barrier design life, external changes in climate and vegetation were assumed to continue to influence the surface barrier and surrounding soils but not measurably change the recharge rates. An important feature of the surface barrier that could change significantly after the design life is the composition of the silt loam layer. Biotic turbation has the potential to mix the underlying sand layer with the silt loam to create a silt loam/sand mix. The post design-life performance of the surface barrier would then be a function of this modified surface layer. The bioturbation process operates independently of the "design life," so changes in barrier function were assumed to occur in a timeframe related to that process rather than the design life. The surrounding soils were assumed to behave in a fashion similar to their pre-Hanford state.

5.2 Reasonable Bounding Cases

To specify that a bounding case is "reasonable" presumes some knowledge of its probability of occurrence. Some cases, such as complete replacement of shrub-steppe by cheatgrass, are theoretically

possible but not probable (or reasonable). These cases were considered as alternative conceptual models and are discussed in Section 5.4. Some cases, such as renewed glacial activity, were considered too speculative for consideration.

For the reasonable bounding cases, assumptions included a shrub-steppe plant community, current climate, and no irrigated farming. A single lower reasonable bounding case was identified that represents the situation in which recharge rates may be at their lowest values. Two upper reasonable bounding cases were identified in which recharge rates may be at their highest values. These bounding cases represent possible variations in how the system might work and give an indication of the level of uncertainty in the recharge estimates.

5.2.1 Lower Bounding Case

This case is interpreted to be a fully functional surface barrier and a dense shrub-steppe community on the barrier and surrounding soil.

5.2.2 Upper Bounding Cases

These cases are interpreted to be situations in which recharge is potentially higher than the best estimate case because of degradation of the barrier. In both cases, the shrub-steppe plant community is relatively unaffected. The impacts of soil and plant variations are addressed in Section 5.3.

- ***Erosion of the Surface Barrier***. Wind and water erode 0.2 m of silt loam from the surface of the barrier, leaving a silt layer that is 0.8 m thick. This change decreases the water storage capacity of the silt loam layer.

- ***Dune Sand Deposition on the Surface Barrier***. Wind deposits a 0.2-m layer of dune sand on top of the silt loam layer. This change does not affect the water storage capacity of the silt loam layer. Instead, it decreases the evaporation potential of the barrier because the sand is less effective than the silt loam at sustaining evaporation.

5.3 Sensitivity Tests

Recharge sensitivities can be determined through the controlled manipulation of selected parameters and processes. Sensitivity tests in this report elected to vary vegetation (type, presence, and density), soil hydraulic properties, and climate.

5.4 Uncertainty Tests

The conceptual model of recharge assumes a shrub-steppe plant community, current climate conditions, and no irrigated farming. Three alternative conceptual models were prepared and tested to demonstrate the impact of these assumptions on recharge estimates:

- ***Vegetation Change***. Through fire, disturbance, disease, or successful competition with the native species, the shallow-rooted alien species cheatgrass becomes the dominant plant. Cheatgrass is so successful that it precludes the vast majority of deep-rooted plants from re-establishing.

- ***Climate Change***. Precipitation rates increase and temperatures decrease to the maximum levels inferred from a pollen record that covers the last 100,000 years. The seasonal distribution of precipitation remains constant.

- ***Irrigation***. If farming is ever allowed on or near the disposal sites, irrigation will be a necessity.

A fourth assumption was that subsidence would be insignificant. This assumption is based on knowledge that the glass waste forms would be very solid and that best engineering practices (compact as much as possible to minimize void space and increase stability) would be used.

6.0 Recharge Estimation Methods

Recharge rates at the Hanford Site can range from near zero to more than 100 mm/yr (Gee et al. 1992). To effectively cover this range, three complementary methods were used to estimate recharge rates for the 2005 IDF PA: lysimetry, the tracer technique, and computer simulations. For a discussion of these and other methods, see the January-February 1994 issue of the *Soil Science Society of American Journal*, which contains a series of papers that were presented at a symposium titled "Recharge in Arid and Semiarid Regions." Rockhold et al. (1995) and Fayer et al. (1999) described how these methods were used at Hanford and presented additional considerations relevant to the presence of the subsurface ILAW disposal facility. Much of those discussions is included here along with updates to reflect activities conducted since 1999.

6.1 Lysimetry

The goal of lysimetry is to provide both performance data and model testing data for specific combinations of soil, vegetation, and precipitation. A lysimeter is a system that can be used to collect water that has flowed through and below the reach of the evaporation process and plant roots to become deep drainage and eventually recharge. Lysimetry is one of only two methods available (the other being drainage flux meters) to directly measure recharge. One of the strengths of lysimetry is that it can provide a control volume in which a number of water balance components can be measured directly. This control volume provides the data needed to calibrate numerical models that can then be used to forecast recharge.

The Hanford Site has used lysimeters for multiple purposes (Hsieh et al. 1973; Gee and Jones 1985; Freeman and Gee 1989; Wittreich and Wilson 1991; Gee et al. 1993; Ward et al. 1997). The lysimeters used to provide data for this report include containers that isolate the soil from its surroundings and field-scale pads that collect drainage but do not isolate the soil.

The primary source of lysimeter data is the Field Lysimeter Test Facility (FLTF). Appendix A describes this facility, which was constructed in FY 1987 to test the performance of capillary barrier designs (Gee et al. 1989). The FLTF contains 18 large lysimeters (surface areas of 2.3 and 3.1 m^2; depth from 1.5 to 3.0 m) and six smaller lysimeters (surface area is 0.07 m^2; depth 3.0 m). Treatments include variations of material types and thicknesses, the presence of vegetation, and the use of irrigation to mimic the increased precipitation of a possible future climate. Data from this facility include drainage, water content, matric potential, temperature, and vegetation observations.

Another source of lysimeter data for this report is the Prototype Hanford Barrier, a full-scale barrier constructed above an actual waste site (Wittreich et al. 2003). The Prototype Hanford Barrier design differs slightly from most of the tests in the FLTF in that the surface silt loam layer is 2 m thick (rather than 1.5 m) and the upper meter contains gravel for erosion control (only two FLTF lysimeters contained gravel in the silt loam layer, and only in the upper 0.3 m). More importantly, the Prototype Hanford Barrier differs from the FLTF tests in that it is a full-scale test that includes side slope effects.

The Prototype Hanford Barrier was instrumented to measure variables such as water content, matric potential, temperature, and drainage. One of the unique and valuable features of the Prototype Hanford Barrier is the presence of asphalt collection pads to collect drainage. These pads are part of the asphalt layer that underlies the entire barrier. Individual collection pads were constructed using asphalt curbing to separate the different collection zones. Four 322-m^2 collection zones underlie the main portion of the prototype barrier. Two similar zones lie beneath each of the two different side slope designs (one is sandy gravel, the other is basalt riprap). In addition, a collection lysimeter was constructed beneath the northeast portion of the barrier, under the asphalt layer that lies beneath the basalt side slope treatment. This lysimeter provides a measure of the effectiveness of the asphalt layer in preventing drainage.

Although they provide the only direct measure of recharge, lysimeters have disadvantages. Lysimeters are usually fixed in space, which limits their ability to quantify the effects of spatial variability. The soil filling the lysimeter may not represent the natural stratification or layering that may be present. The length of record is much shorter than time periods of interest. The lysimeter walls and base alter the natural gradients of temperature, air flow, and vapor flow that could be of importance when trying to measure recharge rates less than 1 mm/yr. Lysimeter walls restrict lateral root growth and promote downward growth. When they involve irrigation, the lysimeter tests are subject to the "oasis effect," in which heat from the un-irrigated surroundings increases the evapotranspiration rate above what it would have been if the entire area had been irrigated. Finally, one of the issues with using lysimeters is verifying that no leaks of drainage water have occurred.

6.2 Tracers

The goal of the tracer method is to estimate historical recharge using measurements of tracer distributions in the soil and sediment of the vadose zone. The vertical distribution of tracers represents the integration of many recharge events and can be used to estimate the mean recharge rate for the time scale of interest for a performance assessment. Several tracers are available that enable estimates of recharge rates for durations of tens to thousands of years. The tracers used for the 2001 ILAW PA were chloride and chlorine-36 (Fayer et al. 1999). The tracers used for this report were chloride and the stable isotopes deuterium and oxygen-18 (e.g., DePaolo et al. 2004; Singleton et al. 2004).

Chloride originates from sea water, is deposited naturally, and can provide recharge estimates spanning hundreds to thousands of years. Chlorine-36 originates from two sources: cosmic irradiation of atmospheric chloride and nuclear weapons testing. The quantities of chlorine-36 created by the testing were far higher than natural production rates and, thus, serve as a marker in the environment. The chlorine-36 data can be used to estimate the average recharge rate over the last 50 years. Deuterium and oxygen-18 are inert isotopes of hydrogen and oxygen that occur naturally. Their concentration increases as the lighter components evaporate disproportionately. The increased concentration can be used to observe seasonal variations in water flux, identify the depth of evaporative enrichment, and roughly estimate recharge.

Both chloride and chlorine-36 are conservative, nonvolatile, and almost completely retained in the soil when water evaporates or is transpired by plants (Phillips 1994). Some chloride is taken up by plants (e.g., Rickard and Vaughan 1988; Sheppard et al. 1998). Over hundreds to thousands of years, plant

cycling is expected to have a minimal impact on the evolution of the chloride distribution in the soil profile beneath plants. Recharge rates determined with this method reflect conditions that existed hundreds to thousands of years ago and are sometimes called paleorecharge or paleofluxes. When using such paleofluxes to represent current or future IDF conditions, the assumption is that the climate, soil, and vegetation conditions are similar. In contrast, bomb-pulse chlorine-36 has been around only ~50 years, so caution must be exercised when interpreting such data. In soils with high pH and high adsorption of other anions, anion exclusion can result in faster movement of chloride. Previous studies strongly suggest a relationship between soil surface area, which is primarily determined by clay content, and anion exclusion (e.g., Thomas and Swoboda 1970). Most of the sandy soil on the Hanford Site have relatively low percentages of clay, so the effects of anion exclusion in this soil should be relatively minor.

Two other issues that affect chloride-based estimates of recharge are mineral dissolution and the chloride dilution that is part of the measurement technique. Both issues can be significant when recharge rates exceed a few millimeters per year (Tyler et al. 1999).

Phillips (1994) suggested that systematic uncertainties in estimated chloride deposition rates can be as great as 20% if the chloride mass balance technique is extended to estimate recharge rates prior to the Holocene epoch (approximately 10,000 years ago). Scanlon (2000) suggested the uncertainty was as high as 38%. Because the Hanford Site was flooded by glacial melt water about 13,000 years ago, the interpretation is not extended beyond that time. Therefore, the uncertainty in chloride deposition rates at the Hanford Site is expected to be less than 38%.

There is some uncertainty about the local influence that Hanford Site operations may have had on the time-dependent concentrations of both chloride and chlorine-36 deposited at Hanford (Fayer et al. 1999). Murphy et al. (1991) examined the issue relative to chlorine-36 and concluded there was no nearby source that would confuse the chlorine-36 signal in the sediment.

Appendix B describes the tracer data collected for the 2005 IDF PA. These data originated from the analyses of samples collected from boreholes that were drilled by the IDF PA activity in 2001 and 2002. The data were supplemented with data from the 2001 ILAW PA (Fayer et al. 1999) and other projects at the Hanford Site (Murphy et al. 1996; Prych 1998). Descriptions of the measurement procedures can be found in Appendix B, Murphy et al. (1991), Murphy et al. (1996), and Prych (1998).

6.3 Modeling

The goals of modeling are to estimate recharge rates when there are little to no data and to leverage the existing short-term data into improved estimates of long-term recharge rates. Simulations of recharge at Hanford have been successful at highlighting the important factors that affect recharge and predicting recharge rates for specific cases. Modeling is the primary tool for forecasting recharge rates for future climate and land use scenarios. The simulations also allow the results of the lysimetry and tracer methods to be merged on a consistent basis. Appendix C describes the modeling activity undertaken to estimate recharge rates for this report.

The UNSAT-H computer code was used to estimate recharge rates for this report (Fayer 2000). UNSAT-H can simulate nonisothermal water flow processes in both liquid and vapor phases and

hysteresis in the soil hydraulic properties. This model has been tested using data from several of the lysimeter experiments at Hanford and elsewhere (Fayer et al. 1992; Fayer and Gee 1992; Khire et al. 1997; Andraski and Jacobson 2000; Scanlon et al. 2002). Fayer and Gee (1997) tested UNSAT-H and a simpler model and concluded that UNSAT-H provided far better estimates of drainage through a surface barrier. Scanlon (1992) used a similar unsaturated flow model to estimate recharge rates in the Chihuahuan Desert of Texas. Scanlon et al. (2002) tested the model with lysimeter data from two sites.

One of the disadvantages of numerical modeling is that it requires numerous parameters to represent climate, soil, and vegetation characteristics. In many instances, these parameters are unknown or only marginally known. Another disadvantage is the use of conceptual simplifications to make the modeling tractable. Numerical modeling with a code such as UNSAT-H is the most flexible method for estimating recharge rates, but its data-intensive needs and conceptual simplification could lead to recharge estimates that have the most uncertainty.

6.4 Additional Considerations

Several features of the IDF could affect the analysis of recharge rates, including physical effects, water consumption, temperature, and preferential flow. Physically, the top of the disposed waste will be located at least 5 m below the top of the surface barrier. At this depth, no direct physical effect on recharge rates is anticipated. The very low permeability of the liner system could affect the flow of air through the vadose zone, but it is assumed that any air exchange with the deep vadose zone is too small to affect recharge rates significantly. The lined trench could also affect the overall temperature gradient within the vadose zone, but the effect is assumed to be too small to affect recharge rates significantly.

Silicate glasses such as the ILAW undergo corrosion when in water. The rate of corrosion depends on factors such as glass composition and the availability of water, which is consumed in the corrosion process. The maximum consumption rate was calculated to be 0.34 g of water per gram of glass.[(a)] This level of water consumption will set up a matric potential gradient that causes water to move toward the ILAW. This consumption might increase water flow through the barrier; however, it was assumed that, because the water was consumed in the corrosion process, the overall effect of this increased downward water movement was not significant to the analysis of recharge.

Radionuclides within the ILAW will undergo radioactive decay and, thus, generate heat. McGrail and Bacon (1998) reasoned that the long half-life and small concentration of radionuclides in ILAW would minimize any temperature increase over ambient conditions. Using the proposed inventory of strontium-90 and cesium-137 in the ILAW, McGrail and Bacon (1998) estimated the maximum temperature increase would be 0.25°C between the disposal facility center and the immediately surrounding soil. They concluded that this small temperature rise was within the expected seasonal

(a) BP McGrail, personal communication with the author, 1998.

temperature fluctuations at the site (about 2°C) and, therefore, not a significant factor affecting the performance of the disposal facility. This small temperature perturbation was assumed to not affect recharge rates significantly.

Preferential flow paths such as clastic dikes could affect recharge under the right conditions. However, the vadose zone in and around the disposal facility will be excavated, thus, eliminating any dikes that may be present near the soil surface. Therefore, the assumption was made that dikes would not be a factor in recharge. Preferential flow could also occur as a result of focused overland flow, such as at the toe of the barrier side slope. The current configuration of the IDF trench suggests that a side slope will not be needed. Finally, preferential flow can occur at a very local scale as a result of flow instabilities that lead to "fingering." Hendricks and Yao (1996) found that, for a sand dune in New Mexico, instabilities occurred during a precipitation event only when the total precipitation exceeded 4 cm. At Hanford, total precipitation in a 24-hour period has exceeded 4 cm only twice between 1947 and 2002 (by less than 1 cm in both cases). Therefore, flow instabilities were assumed to not be a dominant phenomenon affecting recharge at Hanford.

7.0 Results

The process to estimate recharge rates used data from multiple and sometimes conflicting sources. The process was an effort to maximize the value of the information in hand without forgetting the limitations of that information. This section provides an analysis of the data and recharge estimates for the best estimate and bounding cases, demonstrates some recharge sensitivities, estimates recharge for three alternative conceptual models, and summarizes the known issues. This section is an updated version of the Section 7.0 in Fayer et al. (1999) that includes data and analyses obtained since 1999.

7.1 Analyses for the Best Estimate Case

The best estimate case represents what is reasonably expected; it is not the estimate of the best (or perfect) case. For each of the surface features identified in Section 5.0, the data available for estimating recharge rates was assessed. Where data are conflicting, alternate recharge estimates are presented.

7.1.1 Modified RCRA Subtitle C Barrier

The surface barrier for the IDF will control the flux of water directly down to and around the waste. The FLTF drainage data collected under ambient precipitation conditions suggested that recharge rates beneath a barrier would be zero (Appendix A). When lysimeter drainage rates are seemingly this low, caution should be exercised because other factors could affect the results and ought to be considered (e.g., temperature gradients, leaks, and water storage within the basalt). Simulations of the barrier (see Appendix C) indicated recharge rates would be less than 0.1 mm/yr, but no attempt was made to see if the rate might be lower. In the 2001 ILAW PA (Mann et al. 2001), a recharge rate of 0.1 mm/yr was assigned to the barrier. The data and analyses reported by Fayer et al. (1999) and Appendixes A and C of this report support the continued use of this recharge estimate for the barrier. Although there are indications of lower rates, a rate of 0.1 mm/yr was used for an intact surface barrier during its design life.

For the period following the barrier design life, the recharge rate beneath the barrier will be a function of the nature and rate of long-term ecological processes that might alter the barrier configuration and properties. Perhaps the most critical feature is the silt loam layer and its water storage capacity. One of the processes likely to affect the silt loam is bioturbation, which is the excavation and mixing of soil by burrowing animals. Such mixing is normal, expected, and should not affect the performance of a thick silt loam layer. However, if the silt loam layer is too thin, the burrowers may access coarser sediment beneath the silt. The long-term consequence is that the surface layer will become a mixture of materials with less desirable properties.

Wing (1993) summarized the state of knowledge as it related to the functional performance requirements for the Hanford Barrier. With respect to bioturbation, all animals currently at Hanford, or expected to inhabit Hanford in the next 1000 years, normally do not have a need to burrow deeper than 1 m. Food is much scarcer at deeper depths and the energy requirements to reach it become prohibitive. According to Wing (1993), the top meter of silt loam would be completely turned over (bioturbated) within 1,500 years. Bioturbation of surface barriers has been evaluated elsewhere. Shafer et al. (2004) studied the issue at the Nevada Test Site (NTS). They examined four locations on the NTS that were analogs for

various barrier "ages" ranging from 30 to 125,000 years old. On all four analog sites, small mammal bioturbation was largely limited to the upper 0.7 m. As stated earlier, turnover and mixing of the silt loam is expected and not detrimental to performance. Assuming bioturbation is confined to the upper meter, the surface barrier should remain unaffected by the mixing. This assumption could be tested at Hanford by conducting analog studies similar to those by Shafer et al. (2004).

The other process likely to impact the silt loam layer is the loss of material through water and wind erosion. The low precipitation, the low intensity of precipitation events, and the absence of water erosion features at Hanford all support the assumption that water erosion will not be a significant factor at the IDF. Wind erosion, however, has been observed at Hanford, primarily in exposed sandy areas and in the sand dunes to the south of the IDF. The U.S. Department of Energy (DOE 1996) evaluated the potential for wind erosion for surface barriers. DOE calculated that the worst-case potential erosion rate would be to lose 15 cm of silt loam in 500 years. The analysis method was derived for agricultural soils and did not consider the benefits of the pea gravel admix. As related by Wing (1993), pea gravel admix can reduce the wind erosion of silt loam surfaces by 96% to 99%. With the lower reduction value (96%), the wind erosion potential would be 15 cm in 12,500 years. The experience at the Prototype Hanford Barrier suggests that wind erosion will be negligible within months after the barrier surface is vegetated (DOE 1999). For all intents and purposes, wind erosion of the silt loam should be minor and was assumed to be so for this data package.

In summary, for the period after the barrier design life, the recharge rate was projected to be 0.1 mm/yr, the same rate used to represent a fully-function surface barrier.

7.1.2 Barrier Side Slope

The surface barrier is not expected to require side slopes for stability or to blend into the terrain. However, no specific barrier design has yet been chosen, so recharge estimates for side slopes are provided. The ongoing tests of the prototype barrier provide useful performance data on two side slope designs: basalt riprap and sandy gravel. The high cost of basalt riprap makes the use of sandy gravel attractive. Wittreich et al. (2003) reported annual drainage rates through the sparsely vegetated sandy gravel side slope that indicated 21.5% of the precipitation became recharge in 7 years of monitoring (1995-1998, 2000-2002). That percentage is somewhat biased by the first few years during which there was little vegetation and drainage was sometimes 30% to 50% of the precipitation received. During the last 3 years of data collection (from 2000 to 2002) when vegetation began to establish on the side slope, drainage dropped to 12.7% of precipitation received (Wittreich et al. 2003). This change represents a 50% decrease from the first four years. As more vegetation establishes on the side slope in the years to come, the drainage rate ought to decrease further. A complicating aspect of drainage measurements beneath side slopes at the prototype barrier is that about 25% of the collection area lies beneath the gravel road that runs along the top edge of the barrier surface. Because of the road, the side slope drainage measurement is biased high given that drainage rates through graveled surfaces can be high (e.g., 48% for lysimeter C1; see Appendix A). Without knowledge of drainage rates specifically beneath the road surface, it is difficult to separate out the road drainage from the side slope drainage. If the lysimeter value of 48% is used to represent the road, then side slope drainage during the years 2000 to 2002 would

amount to 1% of the precipitation received, or just 1.7 mm/yr. That value is much lower than expected, but it indicates how much bias the road may be exerting on the overall drainage measurement.

For the period during the barrier design life, recharge through the side slope will be high initially but gradually decrease as plants become established. To simplify the analyses, the change in recharge rate was treated as a step function: high initially when plants are not established and low once plants are established. The data from the prototype barrier suggested a 50% decrease in drainage between consecutive 4-year periods. Using that observation, the recharge rate was estimated to be 47.5 mm/yr during the first 4 years (27.6% of 172 mm/yr precipitation). During the subsequent three 4-year periods, the rate was estimated to be 23.8, 11.9, and 5.9 mm/yr. These four 4-year periods could be represented individually, but for the 2005 PA, the analysis was simplified by averaging them to yield a single recharge estimate of 22.3 mm/yr for the entire first 16 years. The recharge rate was assumed to be 4.2 mm/yr thereafter. The rate of 4.2 mm/yr is the average of two recharge estimates for Burbank loamy sand about 1 km north of the IDF Site (Prych 1998). Of the soil types for which recharge estimates exist, Burbank loamy sand, with its high gravel content, most closely resembles the sandy gravel used for side slopes.

Side slope designs that perform as recommended are conceivable but have not yet been tested and demonstrated. If such side slopes are proposed for the IDF, they will need to be tested and their performance verified.

The asphalt layer terminates under the side slope. The water draining through the side slope will be collected and routed laterally and infiltrate just beyond the edge of the asphalt. Ward et al. (1997) detected this infiltration zone at the prototype barrier. In addition to the side slope drainage water, the asphalt layer will also convey any water that drains through the barrier's surface layer. This additional water should be inconsequential relative to the quantity of side slope drainage water.

For the period following the barrier design life, the side slope will continue to experience ecological processes such as soil development. Given the armoring provided by the pea gravel and the presence of a mature shrub-steppe plant community, the long-term average recharge rate is assumed to remain at 4.2 mm/yr. This assumption is supported by observations made at NTS that millennial-scale soil development processes enhance the ability of soils to limit recharge (Shafer et al. 2004).

7.1.3 Rupert Sand

Rupert sand covers nearly all of the IDF trench and most of the surrounding area. The chloride tracer data summarized in Appendix B suggest a range of recharge rates depending on location and depth. Using the shallow chloride peak data, the calculated recharge rates range from 0.02 to 0.05 mm/yr. There is some concern about chloride contamination from nearby facilities. The presence of facility-generated chloride within the soil profile would cause, if unrecognized, an underestimate of the recharge rate using the traditional chloride method. Deposition of facility emissions near the source has been documented at Hanford. For example, Waugh et al. (1998) showed increasing carbon-14 in sagebrush wood as sampling moved from 12.5 to within 0.5 km of the PUREX smokestack (Figure B.2). Analysis of the sagebrush growth rings revealed the elevated carbon-14 coincided with the PUREX operational period. The 200 East Area coal-fired power plant and water purification plant are suspected to have released chloride

(Figure B.1). The coal plant, in particular, is a likely source because it began operations in late 1944 and did not use emission controls until 1980, when a bag house was installed to trap particulates. The IDF site is directly downwind of the prevailing wind direction, which is from the northwest. To date, the issue of facility deposition has not been resolved, so the focus remains on using the deeper chloride that should be unaffected. Using the deep chloride data, the calculated recharge rates range from 0.05 to 2.1 mm/yr.

Fayer et al. (1999) showed that bomb-pulse chlorine-36 still resided entirely within the root zone (the upper 2 m of soil) at a location on the eastern edge of the IDF. While it is still in the root zone, chlorine-36 cannot be used to estimate recharge. The absence of chlorine-36 below 2 m suggests a very low recharge rate, which is in accordance with the recharge estimates derived using chloride data. The chlorine-36 data can also be used to examine the issue of facility deposition. Elevated chlorine-36 levels are a modern phenomenon and, if found in the peak chloride zone, its presence would suggest the peak chloride is modern and, thus, likely came from an anthropogenic source(s). The chloride profiles from the nearby boreholes E24-161 and E24-162 suggest that the chlorine-36 is at the top of the peak chloride zone rather than mixed within it. Unfortunately, the depth resolution in the nearby boreholes was inadequate in the peak zone and, more importantly, chloride was not measured in the same samples used to measure chlorine-36.

There are two other estimates of recharge in Rupert sand. One of those estimates was derived from the simulations in Appendix C, which suggested a recharge rate of 1.8 mm/yr. The other estimate came from Murphy et al. (1996), who measured chloride concentrations in Rupert sand located near the Wye Barricade. The Wye Barricade is about 13 km to the southeast of the IDF site. At that distance, the site should be unaffected by any emissions from the coal plant or other facilities. The shrub density in that general area is far less than at the IDF site. Using the chloride tracer method, Murphy et al. (1996) estimated a recharge rate of 4 mm/yr. This value is much higher than the estimates for the IDF site despite both sites being classified as shrub-steppe on Rupert sand. The distinctly different recharge estimates likely reflect differences in soil hydraulic properties (e.g., Section 3.1) and vegetation between the two sites.

Figure 3.1 shows that the two IDF boreholes located in Burbank loamy sand are near the border with Rupert sand. As the discussion in Section 3.3 indicates, neither of the two soil types quite represents the soil conditions at the IDF. Instead of estimating separate recharge rates for the two soil types, a single recharge rate was estimated for the IDF soil using all of the borehole data. For ease of communication and continuity with the existing soil map; however, the estimated recharge rate will be assigned to both Rupert sand and Burbank loamy sand.

If all eight boreholes in Table B.4 of Appendix B are treated equally (no local averaging or area weighting), the average recharge rate is 0.75 mm/yr. If borehole B8503 is excluded (B8503 had unusually high chloride all the way to the base of the borehole), the average rate is 0.85 mm/yr. If the boreholes are segregated into the four associated with the sand dune (i.e., B8500-B8503) and the four north of the dune, the averages are 1.07 and 0.43 mm/yr, respectively. Appendix B discusses these and other averaging schemes and concludes that, given the limited number of boreholes, the best approach is to use simple averaging of all boreholes except B8503. The rationale for using this method is that the soil conditions that will surround the IDF surface barrier are unknown at this time. Therefore, for the 2005

PA, the recommended recharge rate estimate for soil at the IDF is 0.9 mm/yr (rounded up from 0.85 mm/yr) for the pre-Hanford period. The value of 0.9 mm/yr is fortuitous because it is the value used to represent Rupert sand in the 2001 PA. This value is lower than the 4.2 mm/yr used for Burbank loamy sand.

During the operations period and the barrier design life, the recharge rate for undisturbed Rupert sand is assumed to be equivalent to the pre-Hanford rate. After the barrier design life, the nature of Rupert sand (as well as Burbank loamy sand and the surface barrier and its side slope) will change as a result of the inexorable soil development that will occur. Rupert sand is a relatively young soil. As it matures, this soil type should see increased levels of organic matter, increased levels of fine-textured materials such as silt and clay, and a deepening of the soil profile. All of these changes suggest that recharge rates under Rupert sand will slowly decrease. However, for this report, the recharge rate for the period after the barrier design life is assumed to be equal to the pre-Hanford rate.

7.1.4 Burbank Loamy Sand

Appendix B describes the chloride data from two boreholes that were drilled and sampled for the IDF project in areas designated as Burbank loam sandy (Figure 3.1). The recharge rates were estimated using the deep chloride data; the estimates were 0.16 mm/yr for E24-161 and 0.24 mm/yr for E24-21. Both are much less than the estimate of 4.2 mm/yr that was used for the 2001 PA (Mann et al. 2001). The value of 4.2 mm/yr was the average of two rate estimates (2.8 and 5.5 mm/yr) derived from chloride data collected from two boreholes about 1.5 km northeast of the IDF site. The soil in that area is classified as Burbank loamy sand and is more reflective of that soil type than is the soil at the IDF.

One option for representing the recharge rate in Burbank loamy sand at the IDF is to use the average rate for the two boreholes (i.e., 0.2 mm/yr); however, it is based on only two estimates. As discussed in Section 3.3, the soil at the IDF should be treated as a continuum of a single soil. Thus, as discussed in the previous section on Rupert sand, all borehole data were considered in arriving at a single recharge rate for IDF soil of 0.9 mm/yr for the pre-Hanford period. This value represents a 79% reduction relative to the value used for the 2001 PA and is equivalent to the value used for Rupert sand in the 2001 PA and recommended here for the 2005 PA.

Assumptions about recharge during and after the surface barrier design life are the same for Burbank loamy sand as they are for the surface barrier and side slope and Rupert sand. Basically, the recharge rate for undisturbed Burbank loamy sand at the IDF is assumed to be equivalent to the pre-Hanford rate. After the barrier design life, the nature of Burbank loamy sand will change as a result of the inexorable soil development that will occur. Such development is expected to include increased levels of organic matter, increased levels of fine-textured materials such as silt and clay, and a deepening of the soil profile. All of these changes suggest that recharge rates under Burbank loamy sand will slowly decrease. However, for this report, the recharge rate for the period after the barrier design life is assumed to be equal to the pre-Hanford rate.

7.1.5 Hanford Formation Sediment

During construction and filling of the IDF, Hanford formation sand will be exposed and vegetation will likely not be allowed to establish. Fayer and Walters (1995) reported that an unvegetated 7.6-m-deep lysimeter containing Hanford sand drained 443 mm from July 1985 to June 1993 for an average rate of 55.4 mm/yr. For the conditions envisioned during facility construction, a recharge rate of 55.4 mm/yr is proposed.

During construction and filling of the IDF, water will be used for dust control and compaction. The most likely period for water application will be late spring to early fall when the soil is typically driest. Under these conditions, the added water is not expected to drain deep enough to impact recharge rates.

Construction activities tend to compact soil, which decreases its infiltration capacity and, in turn, increases its potential for generating overland flow. During winter months, rainfall or a quick snowmelt on frozen soil can sometimes generate overland flow. In both cases, the overland flow collects in topographic low spots and infiltrates, becoming what is commonly called focused recharge. The impact of this type of recharge is increased vadose zone water contents prior to emplacement of the liner; it is not a recharge issue once the liner is in place. The occurrence of this type of focused recharge is so highly episodic and dependent on construction activities and weather that it is not amenable to prediction, thus, estimates are not provided for this data package. Fortunately, such focused recharge can be monitored and quantified should it occur during IDF operations.

Once the surface barrier is emplaced, the disturbed soils surrounding the IDF barrier are assumed to be restored to their pre-Hanford condition. No coarse-textured Hanford sediments are expected to be left exposed at the surface once the IDF is completed.

7.1.6 Summary of Best Estimates

The data and analyses just discussed were used to assign recharge rates to each of the scenarios identified in Section 5.0. Table 7.1 shows the estimated recharge rates for each surface feature during each phase of the disposal evaluation. As discussed above, the barrier, barrier side slope, and Hanford formation estimates are based on lysimeter data. The Rupert sand and Burbank loamy sand estimates are based on chloride data.

7.2 Analyses for the Reasonable Bounding Cases

The lower bounding case represents the situation in which recharge rates may be at their lowest reasonable values. The upper bounding cases represent situations in which recharge rates may be at their highest reasonable values. Table 7.2 summarizes the rate assignments for both cases. Climate change, sand dune migration, or irrigation effects were not used to set the bounding estimates.

The lower bounding case was a fully functional surface barrier and a dense shrub-steppe community on the barrier and surrounding soil. A recharge rate of 0.008 mm/yr was used for the barrier. This rate is the lowest value reported by Prych (1998) for silt loam soil. A rate of 2.8 mm/yr was used for the barrier side slope. This rate is the lower estimate for Burbank loamy sand derived from borehole samples

collected about 1.5 km northeast of the IDF. This soil type has a large fraction of gravel (similar to a sandy gravel side slope) and a shrub-steppe plant community (which side slope tests to date have not included). A recharge rate of 0.16 mm/yr was assumed for Rupert sand. This rate is the lowest of the seven rates estimated from site-specific deep chloride data (borehole B8503 was excluded; the lower rates based on shallow peak chloride data were not used). A recharge rate of 0.16 mm/yr was also used for the Burbank loamy sand because both soil types are being treated identically at the IDF. A recharge rate of 47.5 mm/yr was used for the Hanford formation sediment during construction. This rate comes from first 4 years of drainage data collected from the sandy gravel side slope test at the prototype barrier. The side slope test had no shrubs and an extremely sparse cover of annuals.

Table 7.1. Recharge Estimates for the Best Estimate Case for Disposal Facility Features During Each Period of Interest for the 2005 Integrated Disposal Facility Performance Assessment. The surface barrier and side slope, Rupert sand, and Burbank loamy sand have shrub-steppe vegetation.

Surface Feature	Estimated Recharge Rate (mm/yr)			
	Time Period of Recharge Evaluation			
	Pre-Hanford	During Disposal Operations	During Surface Barrier Design Life	After Surface Barrier Design Life
Modified RCRA Subtitle C Barrier	NA	NA	0.1	0.1
Barrier Side Slope	NA	NA	22.3 for years 1 to 16; 4.2 for years >16	4.2
Rupert Sand[(a)]	0.9	0.9	0.9	0.9
Burbank Loamy Sand[(a)]	0.9	0.9	0.9	0.9
Hanford Formation Sediments	NA	55.4	NA	NA

NA = Not applicable.
(a) The soil at the IDF does not exactly fit the description of either official soil type, so it was treated as a single unique soil. Recharge rates were determined for the IDF soil and assigned to both soil types.

The upper bounding case was a degraded surface barrier and a sparse shrub-steppe community on the barrier and surrounding soil. The simulation results in Appendix C show the recharge rate beneath a surface barrier is less than 0.1 mm/yr for both bounding cases. To demonstrate some level of performance reduction, an alternative rate of 0.2 mm/yr (twice the best estimate) was assumed as the upper bounding case for the surface barrier during its design life. After the design life, the upper bounding estimate was increased to 0.9 mm/yr. Using the value of 0.9 mm/yr (which is the rate assumed for the IDF soil) implies that the surface barrier degrades to the point of resembling the surrounding soil (but with a silt loam subsurface layer). A rate of 47.5 mm/yr was assumed for the first 16 years of the barrier side slope and 21.8 mm/yr thereafter. The initial rate of 47.5 mm/yr was based on the first 4 years of data from the prototype barrier. The rate after 16 years comes from the sandy gravel side slope test at the prototype barrier during the last 3 years of monitoring (2000-2002) when the side slope was just

beginning to develop a shrub-steppe plant community. Prior to and during operation as well as during the surface barrier design life, the upper boundary estimate for Rupert sand and Burbank loamy sand was set to 2.1 mm/yr. This value represents the highest paleorecharge rate measured at the IDF. After the design life, recharge rate for the two soils was increased to 4.0 mm/yr to reflect increased uncertainty. This rate was the estimate derived from chloride data collected near the Wye Barricade in Rupert sand with a sparse shrub cover. A recharge rate of 99.8 mm/yr (58% of 172 mm/yr precipitation) was used for the Hanford formation sediment during construction. This rate comes from drainage data collected from an unvegetated sandy gravel test in lysimeter D4 at the FLTF (Appendix A).

Table 7.2. Recharge Estimates for the Reasonable Bounding Cases during Each Period of Interest to the 2005 Integrated Disposal Facility Performance Assessment

Surface Feature	Estimated Recharge Rates (mm/yr) for Reasonable Lower and Upper Bounding Cases			
	Time Period of Recharge Evaluation			
	Pre-Hanford	During Disposal Operations	During Surface Barrier Design Life	After Surface Barrier Design Life
Modified RCRA Subtitle C Barrier	NA	NA	0.008, 0.2	0.008, 0.9
Barrier Side Slope	NA	NA	2.8, 47.5 for years 1 to 16 and 21.8 thereafter	2.8, 21.8
Rupert Sand[(a)]	0.16, 2.1	0.16, 2.1	0.16, 2.1	0.16, 4.0
Burbank Loamy Sand[(a)]	0.16, 2.1	0.16, 2.1	0.16, 2.1	0.16, 4.0
Hanford Formation Sediments	NA	47.5, 99.8	NA	NA

NA = Not applicable.
(a) The soil at the IDF does not exactly fit the description of either official soil type, so it was treated as a single unique soil. Recharge rates were determined for the IDF soil and assigned to both soil types.

7.3 Sensitivity Tests

Some of the modeling results in Fayer et al. (1999) indicated the sensitivity of certain parameters and processes. These include vegetation presence, type, and abundance; soil properties; and climate. Although these simulations did not address the unique soil conditions at the IDF (Section 3.3), they serve as a demonstration of the sensitivity to vegetation, soil properties, and climate for Rupert sand as described by Hajek (1966).

7.3.1 Vegetation

The simulation results showed that the recharge rate through the surface barrier was not sensitive to the type of plant or even to the presence of plants, at least to the model precision level of 0.1 mm/yr that was achieved. In contrast, recharge under the Rupert sand increased from 2.2 mm/yr under shrub-steppe

to 33.2 mm/yr under cheatgrass and 44.3 mm/yr when plants were absent. Similar results were obtained for the Burbank loamy sand.

The sensitivity of the simulation results to the robustness of the shrub vegetation was demonstrated using Rupert sand. For this demonstration, the leaf area index was varied to encompass the range of values measured at the IDF site in 1998. Increasing the shrub leaf area index by 60% reduced the predicted recharge from 2.2 to 1.6 mm/yr. Decreasing the shrub leaf area index by 60% increased the predicted recharge from 2.2 to 5.6 mm/yr. In both cases, the variation in recharge was within a factor of two to three of the base estimate of 2.2 mm/yr.

7.3.2 Soil Properties

The sensitivity of the simulation results to soil properties was demonstrated using Rupert sand (Fayer et al. 1999). Two alternate hydraulic property descriptions for Rupert sand were obtained from a field infiltration test conducted at the IDF site. The resulting predicted recharge rates were 2.7 and 3.3 mm/yr, compared to the base case estimate of 2.2 mm/yr.

Simulations were used to demonstrate the sensitivity of the surface barrier to variability in the properties of the silt loam admix. The results showed no impact (i.e., drainage was zero in all sixteen cases).

7.3.3 Climate

The simulation results showed that the surface barrier would be unaffected by any envisioned change in climate. In contrast, the simulation results showed that recharge in the soil would be significantly affected. Using Rupert sand, the nine combinations of three temperature regimes and three precipitation regimes yielded estimated recharge rates that ranged from less than 0.1 to 27 mm/yr. When precipitation was 50% of modern levels, recharge was less than 0.1 mm/yr regardless of the temperature scenario. For modern precipitation levels, estimated recharge ranged from 0.6 to 7.5 mm/yr for the high to low temperature regimes, respectively. For the high precipitation regime (128% of modern levels), the recharge rates increased, ranging from 5.2 to 27 mm/yr.

7.4 Uncertainty Tests

One method to gauge the uncertainty in recharge estimates is to analyze alternative conceptual models. The model results in Fayer et al. (1999) were used to address a change in the vegetation, a change in the climate, and irrigation. Although these simulations did not address the unique soil conditions at the IDF and discussed in Section 3.3, they serve as a demonstration of the sensitivity to vegetation on Rupert sand as described by Hajek (1966).

One of the two barrier degradation scenarios was that 20% of the silt loam layer was eroded. The simulation results in Fayer et al. (1999) showed that the eroded barrier with shrub-steppe vegetation performed as well as the intact barrier, i.e., it limited drainage to less than 0.1 mm/yr. The second degradation scenario involved the deposition of 20 cm of dune sand on the barrier. The simulation results showed that the barrier with dune sand and shrub-steppe vegetation also performed as well the intact

barrier. The simulation results also showed that the replacement of shrubs with cheatgrass for this particular situation resulted in drainage of 18.4 mm/yr, and the removal of all plants caused drainage to increase to 32.7 mm/yr. Because deep-rooted plants like sagebrush are expected to be present, a rate of 0.1 mm/yr was assumed for the degraded barrier scenario.

7.4.1 Vegetation Change

The simulation results in Fayer et al. (1999) showed that a surface barrier without vegetation limited recharge to less than 0.1 mm/yr. This level of performance is as good as a barrier with shrub-steppe vegetation. Because a barrier with no vegetation was shown to limit recharge to less than 0.1 mm/yr, a barrier with cheatgrass was assumed to limit recharge to less than 0.1 mm/yr. The same simulation results were obtained for an eroded barrier without plants, showing how robust the silt loam barrier is at reducing recharge, even in the absence of plants.

The results in Fayer et al. (1999) indicate that a shift from shrub-steppe to cheatgrass on the Rupert sand will raise the recharge rate from 2.2 to 33.2 mm/yr. This higher estimate of recharge is not unreasonable. Fayer and Walters (1995) used water content measurements to estimate recharge rates for a cheatgrass community growing on Rupert sand in the 300 Area. For an 8-year period, they estimated the average recharge rate was 25.4 mm/yr.

7.4.2 Climate Change

The prediction of climate change is a current research topic. Because the future cannot be foretold, the past was used to see what has happened and possibly could happen again. Fayer et al. (1999) described the analysis used to identify specific climate change scenarios. Under climate change conditions most likely to promote recharge (i.e., higher precipitation and lower temperature), the surface barrier continued to limit drainage to less than 0.1 mm/yr as did the eroded surface barrier. With 20 cm of dune sand on the barrier, this climate scenario resulted in a recharge rate of 16.9 mm/yr. Recharge in the Rupert sand jumped from 2.2 to 27 mm/yr and in the Burbank loamy sand from 5.2 to 36.8 mm/yr. In all cases, a shrub-steppe community was present.

The climate analysis by Fayer et al. (1999) did not explicitly address specific changes in the seasonality of precipitation. Their simulation results suggested that an alteration of the current seasonal distribution of precipitation would not alter surface drainage rates. However, the impact of future climate scenarios was not evaluated. Fayer et al. (1999) also did not explicitly evaluate the impact of climate shifts such as the El Niño Southern Oscillation (ENSO) and the Pacific Decadal Oscillation (PDO). However, they used weather data, collected between 1957 and 1997 that includes several of these events, and they used chloride profiles developed over thousands of years that presumably contained many ENSO and PDO events. In summary, ENSO and PDO events are not outside the ordinary range of climate variability and are not expected to affect barrier drainage rates.

7.4.3 Irrigation

All of the land use options currently being considered for Hanford exclude farming on and near the waste disposal sites. Because such institutional controls cannot be guaranteed to survive forever, the

impact of irrigated agriculture on recharge was evaluated (Fayer et al. 1999). For a potato crop grown on the surface barrier, recharge was 26.4 and <0.1 mm/yr for irrigation efficiencies of 75% and 100%, respectively. For Rupert sand, the rates were 57 and 30 mm/yr for the same efficiencies. The effect of irrigation on the other soil types was not evaluated. Evans et al. (2000) evaluated the agricultural potential of Hanford and concluded that Hanford had significant potential if irrigated. They estimated that, with new technology in 50 years, between 2 and 15% of the applied amount would become deep drainage (this does not include water applied for frost protection or leaks). Depending on the crop, the deep drainage rates would range from 6 mm/yr for sweet onions (assuming 2% deep loss) to 169 mm/yr for pasture (assuming 15% loss).

7.5 Remaining Issues

As with any estimate involving multiple data sources, spatial variability, and time frames of thousands of years, there are issues that could be more fully evaluated. These issues include climate change, bioturbation, unstable and preferential flow, flaws in the barrier (e.g., differential settling and cracking; discontinuities; points of flow convergence), possible facility deposition of chloride, and the importance of temperature and water vapor flow when recharge rates are lower than 1 mm/yr. Most importantly, the longevity of the surface barrier deserves attention. For this data package, key processes such as bioturbation and wind erosion were assumed to have minimal effect on the barrier based on a limited set of field observations and wind tunnel analyses. Given that surface barriers are about to be deployed at numerous individual waste sites at Hanford, opportunities will be available to test these assumptions more rigorously under field conditions. The knowledge gained from such tests will be invaluable to improving the predictions of surface barrier performance hundreds to thousands of years from now. In addition, analog sites could be identified that represent mature stages of soil and barrier. Studies of these analogs could strengthen the understanding of long-term changes and help to reduce the uncertainty embodied in the predictions. The same approach could be used to study and understand the impacts of dune sand deposition. A good analog might be the soil type called Hezel sand. Hajek (1966) describes it as similar to Rupert sand but with a silt loam subsoil within 1 m of the surface.

8.0 Conclusions

CH2M HILL is designing and assessing the performance of a near-surface disposal facility at Hanford for radioactive and hazardous waste (the 2005 IDF PA). PNNL assists CH2M HILL by providing estimates of recharge rates for current conditions and long-term scenarios involving disposal at the IDF location.

The elements of this report compose the Recharge Data Package, which provides estimates of recharge rates for the scenarios being considered in the 2005 IDF PA. The estimates were derived from modeling studies and lysimeter and tracer data collected by the IDF Project and other projects.

For the best estimate case, a recharge rate of 0.1 mm/yr is proposed for the surface barrier with a shrub-steppe plant community. This rate is the same one used in the 2001 ILAW PA and the data collected since then support its continued use. If side slopes are part of the surface barrier design, a two-step recharge rate is proposed: 22.3 mm/yr for the first 16 years while plants get established and 4.2 mm/yr thereafter. These rates are lower than the 50 mm/yr used in the 2001 ILAW PA because they better reflect the data collected from the prototype barrier. The case was made in this data package that the soils at the IDF should be considered a single soil type. Therefore, a single recharge rate of 0.9 mm/yr is proposed for the soil at the IDF site. This rate is identical to that used for Rupert sand in the 2001 PA. This rate is much lower than the rate of 4.2 mm/yr used for Burbank loamy sand in the 2001 ILAW PA. The lower rate is the result of using site-specific chloride data rather than chloride data from a site 1.5 km to the northeast. For Hanford formation sediment during construction, a recharge rate of 55.4 mm/yr is proposed (same as for the 2001 ILAW PA). Using the available recharge estimates, a set of reasonable bounding rates was also identified.

The sensitivity tests conducted for the 2001 ILAW PA are still applicable. The results showed that the surface barrier limited recharge to less than 0.1 mm/yr regardless of the plant type, the presence of plants, or any of the climate change conditions. Additional simulations conducted for this report showed the surface barrier performance (i.e., drainage <0.1 mm/yr) was unaffected by variability in the hydraulic properties of the silt loam admix. In contrast, recharge in the Rupert sand showed a significant sensitivity to vegetation type and climate change conditions, but less sensitivity to small variations in hydraulic properties.

The conceptual model evaluations for the 2001 ILAW PA are still applicable. Replacement of the shrub cover with cheatgrass had no impact on recharge through the surface barrier, but it increased recharge in Rupert sand from 2.2 to 33.2 mm/yr. Deposition of dune sand on the barrier reduced evaporation. The barrier still performed as expected but only if the shrub-steppe plant community remained. In essence, the dune sand makes the barrier performance sensitive to vegetation conditions such as fire removal and species replacement. Under the climate change condition most likely to promote recharge (i.e., increased precipitation and decreased temperature), recharge through the barrier remained <0.1 mm/yr in contrast to recharge in Rupert sand, which increased from 2.2 to 27 mm/yr.

Land use restrictions are expected to preclude farming at the IDF. To understand the consequences of farming, a simulation was conducted of irrigated potatoes. The results showed that irrigation on the surface barrier significantly increased recharge.

Remaining issues concern assumptions about climate change, bioturbation, unstable and preferential flow, variability of the properties of the barrier materials and surrounding soil, longevity of the barrier, flaws in the barrier, possible facility deposition of chloride, and the importance of temperature and water vapor flow when recharge rates are lower than 1 mm/yr.

The recharge estimates provided in this report were based on a pre-conceptual design of the surface barrier. The final barrier design and the materials that will be used to construct it have not yet been identified. When they are, the final design should be re-evaluated to confirm that its performance is acceptable. In the same vein, the properties of the soil that will surround the final barrier will depend on the plan for reclamation following construction. Once identified, the proposed reclaimed soil should be re-evaluated to confirm that its performance is acceptable. Lastly, the recharge estimates provided in this report were based on a set of assumptions regarding future climate, vegetation, and land use. As new information and understanding (e.g., improved climate predictions) are developed, the assumptions should be re-evaluated and, if needed, the recharge estimates should be revised accordingly.

9.0 References

Andraski BJ and EA Jacobson. 2000. "Testing a Full-Range Soil-Water Retention Function in Modeling Water Potential and Temperature." *Water Resources Research* 36(10):3081-3089.

Bacon DH and BP McGrail. 2002. *Effect of Design Change on Remote-Handled Trench Waste Form Release Calculations*. PNNL-13947, Pacific Northwest National Laboratory, Richland, Washington.

Burbank DA and MJ Klem. 1997. *Analysis of Alternatives for Immobilized Low-Activity Waste Disposal*. HNF-SD-TWR-AGA-004, Rev 0, SGN Eurisys Services Corporation, Richland, Washington.

DePaolo DJ, ME Conrad, K Maher, and GW Gee. 2004. "Evaporation Effects on Oxygen and Hydrogen Isotopes in Deep Vadose Zone Pore Fluids at Hanford, Washington." *Vadose Zone Journal* 3:220-232.

DOE. 1987. *Final Environmental Impact Statement: Disposal of Hanford Defense High-Level Transuranic and Tank Wastes*. DOE/EIS-0113, U.S. Department of Energy, Washington, D.C.

DOE. 1996. *Focused Feasibility Study of Engineered Barriers for Waste Management Units in the 200 Areas*. DOE/RL-93-33, Rev. 0, U.S. Department of Energy, Richland Operations Office, Richland, Washington.

DOE. 1999. *200-BP-1 Prototype Barrier Treatability Test Report*. DOE/RL-99-11, Rev. 0, U.S. Department of Energy, Richland Operations Office, Richland, Washington.

DOE. 2003. *Annual Summary of the Immobilized Low-Activity Waste Performance Assessment for 2003, Incorporating the Integrated Disposal Facility Concept*. DOE/ORP-2000-19, Rev. 3, U.S. Department of Energy, Office of River Protection, Richland, Washington.

Evans RG, MJ Hattendorf, and CT Kincaid. 2000. *Evaluation of the Potential for Agricultural Development at the Hanford Site*. PNNL-13125, Pacific Northwest National Laboratory, Richland, Washington.

Fayer MJ. 2000. *UNSAT-H Version 3.0: Unsaturated Soil Water and Heat Flow Model, Theory, User Manual, and Examples*. PNNL-13249, Pacific Northwest National Laboratory, Richland, Washington.

Fayer MJ and GW Gee. 1992. "Predicted Drainage at a Semiarid Site: Sensitivity to Hydraulic Property Description and Vapor Flow." In *Proceedings of the International Workshop on Indirect Methods for Estimating the Hydraulic Properties of Unsaturated Soils*. M Th van Genuchten, FJ Leij, and LJ Lund, (eds.), Riverside, California, October 11-13, 1989, University of California, Riverside, California.

Fayer MJ and TB Walters. 1995. *Estimated Recharge Rates at the Hanford Site*. PNL-10285, Pacific Northwest Laboratory, Richland, Washington.

Fayer MJ and GW Gee. 1997. "Hydrologic Model Tests for Landfill Covers using Field Data." In *Landfill Capping in the Semi-Arid West: Problems, Perspectives, and Solutions*," TD Reynolds and

RC Morris (eds.), May 21-22, 1997. Jackson, Wyoming. ESRF-019, Env. Sci. Res. Foundation, Idaho Falls, Idaho.

Fayer MJ, ML Rockhold, and MD Campbell. 1992. "Hydrologic Modeling of Protective Barriers: Comparison of Field Data and Simulation Results." *Soil Sci. Soc. Am. J.* 56:690-700.

Fayer MJ, EM Murphy, JL Downs, FO Khan, CW Lindenmeier, and BN Bjornstad. 1999. *Recharge Data Package for the Immobilized Low-Activity Waste 2001 Performance Assessment.* PNNL-13033, Pacific Northwest National Laboratory, Richland, Washington.

Fecht KR, KA Lindsey, BN Bjornstad, DG Horton, GV Last, and SP Reidel. 1999. *An Atlas of Clastic Injection Dikes of the Pasco Basin and Vicinity*. BHI-01103 Rev. 0, Bechtel Hanford, Inc., Richland, Washington.

Freeman HD and GW Gee. 1989. *Hanford Protective Barriers Program Asphalt Barrier Studies-FY 1988.* PNL-6874, Pacific Northwest Laboratory, Richland, Washington.

Gee GW. 1987. *Recharge at the Hanford Site: Status Report*. PNL-6403, Pacific Northwest Laboratory, Richland, Washington.

Gee GW and TL Jones. 1985. *Lysimeters at the Hanford Site: Present Use and Future Needs.* PNL-5578, Pacific Northwest Laboratory, Richland, Washington.

Gee GW, RR Kirkham, GL Downs, and MD Campbell. 1989. *The Field Lysimeter Test Facility (FLTF) at the Hanford Site: Installation and Initial Tests.* PNL-6810, Pacific Northwest Laboratory, Richland, Washington.

Gee GW, MJ Fayer, ML Rockhold, and MD Campbell. 1992. "Variations in Recharge at the Hanford Site." *Northwest Science* 66:237-250.

Gee GW, DG Felmy, JC Ritter, MD Campbell, JL Downs, MJ Fayer, RR Kirkham, and SO Link. 1993. *Field Lysimeter Test Facility Status Report IV: FY 1993.* PNL-8911, Pacific Northwest Laboratory, Richland, Washington.

Hajek BF. 1966. *Soil Survey Hanford Project in Benton County, Washington.* BNWL-243, Pacific Northwest Laboratory, Richland, Washington.

Hendricks JMH and T Yao. 1996. "Prediction of Wetting Front Stability in Dry Field Soils Using Soil and Precipitation Data." *Geoderma* 70:265-280.

Hoitink DJ, KW Burk, JV Ramsdell, and WJ Shaw. 2003. *Hanford Site Climatological Data Summary 2002 with Historical Data.* PNNL-14242, Pacific Northwest National Laboratory, Richland, Washington.

Hsieh JJC, LE Brownell, and AE Reisenauer. 1973. *Lysimeter Experiment Description and Progress Report on Neutron Measurements.* BNWL-1711, Battelle Pacific Northwest Laboratories, Richland, Washington.

Khire MV, CH Benson, and PJ Bosscher. 1997. "Water Balance Modeling of Earthen Final Covers." *J. Geotech. Geoenviron. Engr*. 123(8):744-754.

Kincaid CT, JW Shade, GA Whyatt, MG Piepho, K Rhoads, JA Voogd, JH Westsik, Jr, MD Freshley, KA Blanchard, and BG Lauzon. 1995. *Volume 1: Performance Assessment of Grouted Double-Shell Tank Waste Disposal at Hanford.* WHC-SD-WM-EE-004, Rev. 1, Vol. 1, Westinghouse Hanford Company, Richland, Washington.

Kocher AE and AT Strahorn, 1919. *Soil Survey of Benton County, Washington*. U.S. Government Printing Office, Washington, D.C.

Mann FM, CR Eiholzer, NW Kline, BP McGrail, and MG Piepho. 1995. *Impacts of Disposal System Design Options on Low-Level Glass Waste Disposal System Performance.* WHC-EP-0810, Rev. 1, Westinghouse Hanford Company, Richland, Washington.

Mann FM, KC Burgard, WR Root, RJ Puigh, SH Finfrock, R Khaleel, DH Bacon, EJ Freeman, BP McGrail, SK Wurstner, and PE Lamont. 2001. *Hanford Immobilized Low-Activity Waste Performance Assessment: 2001 Version*. DOE/ORP-2000-24, Rev. 0, U.S. Department of Energy, Office of River Protection, Richland, Washington.

Mann FM, RJ Puigh, II, PD Rittmann, NW Kline, JA Voogd, Y Chen, CR Eiholzer, CT Kincaid, BP McGrail, AH Lu, GF Williamson, NR Brown, and PE LaMont. 1998. *Hanford Immobilized Low-Activity Tank Waste Performance Assessment.* DOE/RL-97-69, U.S. Department of Energy, Richland, Washington.

McGrail BP and DH Bacon. 1998. *Selection of a Computer Code for Hanford Low-Level Waste Engineered-System Performance Assessment.* PNNL-10830, Rev. 1, Pacific Northwest National Laboratory, Richland, Washington.

Murphy EM, TR Ginn, and JL Phillips. 1996. "Geochemical Estimates of Paleorecharge in the Pasco Basin: Evaluation of the Chloride Mass-Balance Technique." *Water Resources Research* 32(9):2853-2868.

Murphy EM, JE Szecsody, and SJ Phillips. 1991. *A Study Plan for Determining Recharge Rates at the Hanford Site Using Environmental Tracers.* PNL-7626, Pacific Northwest Laboratory, Richland, Washington.

Murray CJ, AL Ward, and JL Wilson, III. 2003. *Influence of Clastic Dikes on Vertical Migration of Contaminants in the Vadose Zone at Hanford*. PNNL-14224, Pacific Northwest National Laboratory, Richland, Washington.

Neitzel, DA. (ed.). 2003. *Hanford Site National Environmental Policy Act (NEPA) Characterization*. PNL-6415, Rev. 15, Pacific Northwest National Laboratory, Richland, Washington.

Phillips FM. 1994. "Environmental Tracers for Water Movement in Desert Soils of the American Southwest." *Soil Sci. Soc. Am. J.* 58:15-24.

Prych EA. 1998. *Using Chloride and Chlorine-36 as Soil-Water Tracers to Estimate Deep Percolation at Selected Locations on the U.S. Department of Energy Hanford Site, Washington.* Water-Supply Paper 2481, U.S. Geological Survey, Tacoma, Washington.

Puigh RJ. 1999. *Disposal Facility Data for the Hanford Immobilized Low-Activity Waste.* HNF-4950, Rev. 0, Fluor Daniel Northwest, Richland, Washington.

Puigh RJ and FM Mann. 2002. *Statement of Work for FY 2003 to 2008 for the Hanford Low-Activity Tank Waste Performance Assessment Program*. RPP-6702, Rev. 2, CH2M HILL Hanford Group, Inc., Richland, Washington.

RCRA – *Resource Conservation and Recovery Act*. 1976. Public Law 94-580, as amended, 90 Stat. 2795, 42 USC 6901 et seq.

Reidel SP and KD Reynolds. 1998. *Characterization Plan for the Immobilized Low-Activity Waste Borehole.* PNNL-11802, Pacific Northwest National Laboratory, Richland, Washington.

Reidel SP. 2004. *Geologic Data Package for 2005 Integrated Disposal Facility Waste Performance Assessment*. PNNL-14586, Pacific Northwest National Laboratory, Richland, Washington.

Rickard WH and BE Vaughn. 1988. "Chapter 6: Plant Communities: Characteristics and Responses." in *Shrub-Steppe, Balance and Change in a Semi-Arid Terrestrial Ecosystem*, WH Rickard, LE Rogers, BE Vaughn, and SF Liebetrau (eds.), Elsevier, New York.

Rockhold ML, MJ Fayer, GW Gee, and CT Kincaid. 1995. *Estimation of Natural Groundwater Recharge for the Performance Assessment of a Low-Level Waste Disposal Facility at the Hanford Site.* PNL-10508, Pacific Northwest Laboratory, Richland, Washington.

Scanlon BR. 1992. "Evaluation of Liquid and Water Vapor Flow in Desert Soils Based on Chlorine-36 and Tritium Tracers and Nonisothermal Flow Simulations." *Water Resour. Res*. 28:285-298.

Scanlon BR. 2000. "Uncertainties in Estimating Water Fluxes and Residence Times using Environmental Tracers in an Arid Unsaturated Zone." *Water Resources Research* 36(2):395-409.

Scanlon BR, M Christman, RC Reedy, I Porro, J Simunek, and GN Flerchinger. 2002. "Intercode Comparisons for Simulating Water Balance of Surficial Sediments in Semiarid Regions." *Water Resources Research* 38(12):1323.

Shafer DS, MH Young, SF Zitzer, E McDonald, and T Caldwell. 2004. *Coupled Environmental Processes and Long-Term Performance of Landfill Covers in the Northern Mojave Desert.* DOE/NV/13609-32, U.S. Department of Energy, Las Vegas, Nevada.

Sheppard SC, WG Evenden, and CR Macdonald. 1998. "Variation Among Chlorine Concentration Ratios for Native and Agronomic Plants." *J. Environ. Rad.* 43:65-76.

Singleton MJ, EL Sonnenthal, ME Conrad, DJ DePaolo, and GW Gee. 2004. "Multiphase Reactive Transport Modeling of Stable Isotope Fractionation in Unsaturated Zone Pore Water and Vapor: Application to Seasonal Infiltration Events at the Hanford Site, WA." *Vadose Zone Journal* (in press).

Thomas GW and AR Swoboda. 1970. "Anion Exclusion Effects on Chloride Movement in Soils." *Soil Science* 110(3):163-166.

Tyler SW, BR Scanlon, GW Gee, and GB Allison. 1999. "Water and Solute Transport in Arid Vadose Zones." In *Vadose Zone Hydrology*, MB Parlange and JW Hopmans (eds.). Oxford University Press, New York, p. 334-373.

Ward AL, GW Gee, and SO Link. 1997. *Hanford Prototype-Barrier Status Report: FY 1997.* PNNL-11789, Pacific Northwest National Laboratory, Richland, Washington.

Waugh WJ, J Carroll, JD Abraham, and DS Landeen. 1998. "Applications of Dendrochronology and Sediment Geochronology to Establish Reference Episodes for Evaluation of Environmental Radioactivity." *J. Environ. Radioactivity* 41(3):269-286.

Wing NR. 1993. *Permanent Isolation Surface Barrier: Function Performance.* EHC-EP-0650, Westinghouse Hanford Company, Richland, Washington.

Wing NR. 1994. *Permanent Isolation Surface Barrier Development Plan.* WHC-EP-0673, Westinghouse Hanford Company, Richland, Washington.

Wittreich CD and CR Wilson. 1991. "Use of Lysimeters to Monitor a Sanitary Landfill." In *Proceedings of the Conference on Lysimeters for Evapotranspiration and Environmental Measurements, Honolulu, Hawaii, July 23-25, 1991,* Irrigation Division, American Society Civil Engineers, pp. 397-405.

Wittreich CD, JK Linville, GW Gee, and AL Ward. 2003. *200-BP-1 Prototype Hanford Barrier Annual Monitoring Report for Fiscal Year 2002.* CP-14873, Rev. 0, Fluor Hanford, Richland, Washington.

Appendix A

Field Lysimeter Test Facility Data to Support the 2005 Integrated Disposal Facility Performance Assessment

Appendix A

Field Lysimeter Test Facility Data to Support the 2005 Integrated Disposal Facility Performance Assessment

MJ Fayer and CE Strickland

A.1 Introduction

CH2M HILL Hanford Group, Inc. (CH2M HILL) is designing and assessing the performance of a near-surface disposal facility at Hanford for radioactive and hazardous wastes. The CH2M HILL project to assess the performance of this disposal facility is known as the Integrated Disposal Facility (IDF) Performance Assessment (PA), hereafter called the IDF PA activity. One of the requirements of the IDF PA activity is to estimate the fluxes of water moving through the sediment within the vadose zone around and beneath the disposal facility. These fluxes, loosely called recharge rates, are the primary mechanism for transporting contaminants to the groundwater.

Pacific Northwest National Laboratory (PNNL) assists CH2M HILL in their performance assessment activities. One of the PNNL tasks is to provide estimates of recharge rates for current conditions and long-term scenarios involving disposal at the IDF location (Puigh and Mann 2002). Recharge estimates are needed for a fully functional surface cover, its sideslope, and the immediately surrounding terrain. In addition, recharge estimates are needed for conditions after the cover's design life and for scenarios involving irrigated farming directly on the cover. DOE (2003) suggests that the temporal scope of the 2005 immobilized low-activity waste (ILAW) PA is at least 10,000 years and may be longer if some contaminant peaks occur after 10,000 years.

One of the primary methods for measuring recharge rates is lysimetry. The recharge task uses the lysimeters at the Field Lysimeter Test Facility (FLTF) near the 200 West Area to collect recharge-related data. The two goals of the lysimeter work are to accurately quantify the recharge flux for scenarios pertinent to the IDF PA activity and provide a set of long-term monitoring data with which to test the recharge model (Fayer 2000). This model will be used to extend the observations and estimate recharge rates for potential future scenarios. Fayer et al. (1999) provided details on the FLTF design and the data collection methods and frequency employed from initiation of the facility in November 1987 up to March 1999. This appendix summarizes lysimeter data that have been collected from the FLTF through March 31, 2004.

A.2 Background

The Protective Barrier Program constructed the FLTF in FY 1987 to test the performance of capillary barrier cover designs (Gee et al. 1989; Wing 1994). Figure A.1 shows the location of the FLTF within

the 200 Areas. In 1994, the emphasis of the Protective Barrier Program switched from monitoring the FLTF to constructing and monitoring a prototype barrier in the 200 East Area (Gee et al. 1993a). The change in program emphasis created an opportunity for the ILAW Project (the pre-cursor to the IDF PA activity) to conduct testing in the facility for soil-vegetation-climate treatments of importance to ILAW disposal.

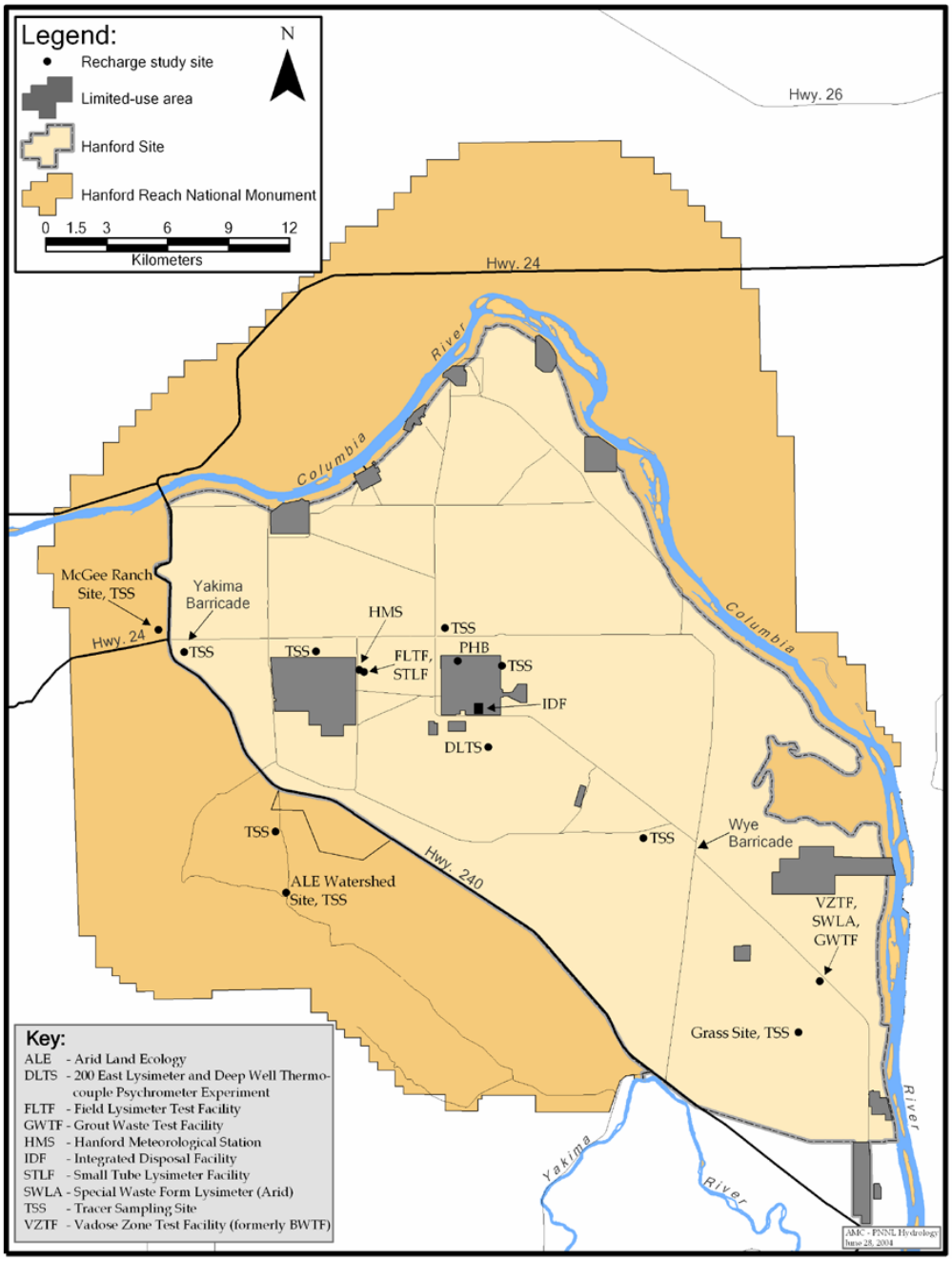

Figure A.1. Location of the Field Lysimeter Test Facility

Figure A.2 shows that the FLTF contains a total of 24 lysimeters of three types: 14 drainage, 4 weighing, and 6 small-tube lysimeters. The drainage lysimeters are vertical cylinders that are 3 m deep and 2 m in diameter (surface area of 3.1 m^2). The drainage lysimeters compose the walls of the FLTF. The weighing lysimeters are boxes with length and width dimensions of 1.5 m and a depth of 1.7 m (surface area of 2.3 m^2). The boxes rest on platform scales to enable hourly weight measurements of water gain and loss. The small-tube lysimeters are vertical cylinders that are 3 m deep and 0.3 m in diameter (surface area of 0.07 m^2). Unlike the others, the small-tube lysimeters are clear Plexiglas to facilitate root and soil observations. These lysimeters are arrayed along the inner walls of the FLTF.

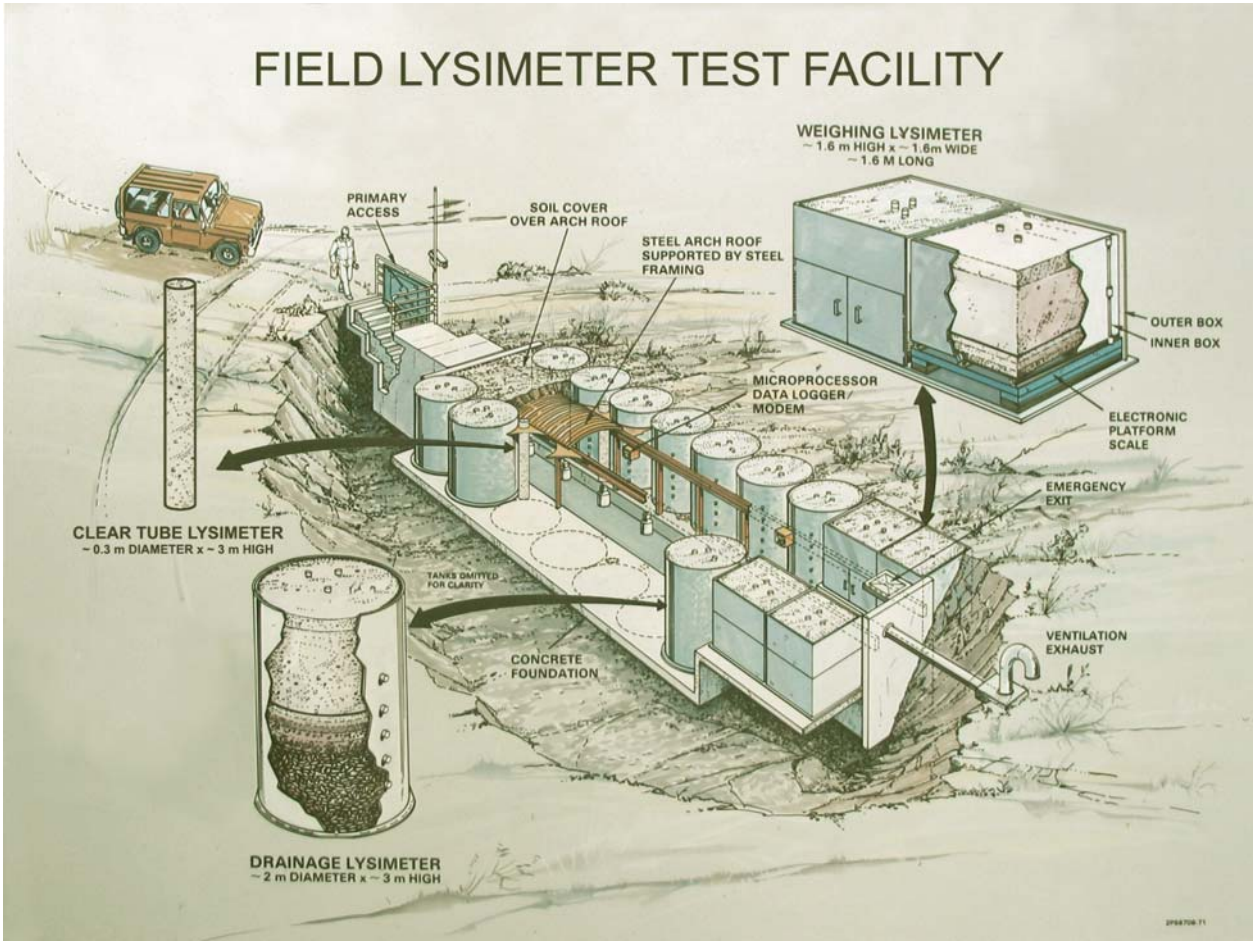

Figure A.2. Artistic Rendering of the Field Lysimeter Test Facility

Treatments include variations of material types and thickness, presence of vegetation, and the use of irrigation to mimic the possible increased precipitation of future climate. The data collected from this facility have included drainage, water content, matric potential, temperature, and vegetation observations. Discussions of the early data from this facility can be found in Gee et al. (1989), Campbell et al. (1990), Campbell and Gee (1990), Gee et al. (1993b), and Fayer et al. (1999).

A.3 Methods

Since 1987, twelve tests and 26 treatments have been set up in the FLTF to reflect various combinations of soil type and layering, vegetation, and precipitation. Table A.1 summarizes all of the tests and treatments. When testing was completed for some of the lysimeters, those lysimeters were converted to new tests and treatments. As of March 31, 2004, the number of ongoing tests was 10 involving 22 treatments. The 10 tests and associated data collection activities and frequencies are described below. Unless noted, treatment numbers in this report match the treatment numbers in Gee et al. (1993b).

A.3.1 Test Descriptions

Each test is briefly described in the following paragraphs. More details about the construction and data collection as well as a more extensive review and discussion of the data can be found in Gee et al. (1989), Campbell et al. (1990), Campbell and Gee (1990), Gee et al. (1993b), and Fayer et al. (1999).

Hanford Barrier. The objective of this test was to document the performance of a Hanford Barrier. The basic configuration consisted of 1.5 m of silt loam that rested on a sequence of materials grading from sand to gravel filter layers and finally to basalt riprap. This test included shrub-steppe vegetation and no vegetation comparisons. The treatment numbers are 1 to 4, and 7.

Hanford Barrier with Gravel Admix. The objective of this test was to document the impact of a gravel admix on the performance of a Hanford Barrier. The basic configuration was a Hanford Barrier, with the exception that the top 0.2 m of silt loam was amended with pea gravel to protect against possible erosion. The gravel content was 15% by weight. This test included shrub-steppe vegetation but addressed only ambient precipitation. The treatment number was 5; this test was terminated in 1997.

Eroded Hanford Barrier. The objective of this test was to document the performance of an eroded Hanford Barrier. The basic configuration was a Hanford Barrier design, with the exception that the silt loam layer thickness was reduced from 1.5 to 1.0 m. In many respects, this design is similar to that of the Modified RCRA Subtitle C Barrier (RCRA barrier) (see below). This test included shrub-steppe vegetation. The treatment number is 18 in this report and 6 in Gee et al. (1993b).

Gravel Mulch. The objective of this test was to document the performance of a gravel mulch layer above Hanford formation sand. The basic configuration was 0.15 m of coarse gravel above 1.35 m of screened pitrun sand (to remove the gravel), on top of unscreened pitrun sand (described below). This test was conducted only in the clear-tube lysimeters. The test did not include vegetation. The treatment numbers are 8 and 10. Although not its primary purpose, this test may be useful for characterizing deep drainage rates at the tank farms at Hanford.

Pitrun Sand. The objective of this test was to document the performance of a coarse gravelly sand taken from a nearby borrow pit (hence “pitrun” sand). The basic configuration was 1.5 m of screened pitrun sand (to remove the gravel), on top of unscreened pitrun sand. This test was conducted only in the

Table A.1. Summary of Treatments and Applicable Dates at the Field Lysimeter Test Facility as of March 31, 2004

Test Description	Treatment ID No.	Precipitation			Vegetation			Lysimeter ID	Monitoring Period	
		1x	2/ 3x	3x	NV	SRV	DRV		Start	End
Hanford Barrier	1	X					X	D4	4 Nov 1987	22 Apr 1994
		X					X	D7	4 Nov 1987	22 Apr 1994
		X					X	W1	4 Nov 1987	***31 Mar 2004***
		X					X[g]	C3	9 Nov 1988	***31 Mar 2004***
	2	X			X			D1	4 Nov 1987	***31 Mar 2004***
		X			X			D8	4 Nov 1987	27 Feb 1998
		X			X			W2	4 Nov 1987	31 Oct 1997
	3		X				X	D13	4 Nov 1987	27 Feb 1998
			X				X	D14	4 Nov 1987	22 Apr 1994
			X				X	W3	4 Nov 1987	***31 Mar 2004***
			X				X	C6	9 Nov 1988	***31 Mar 2004***
	4		X		X			D10	4 Nov 1987	8 Apr 2002
			X		X			D12	4 Nov 1987	31 Oct 1997
			X		X			W4	4 Nov 1987	31 Oct 1997
	7		X[a]		X			D9	4 Nov 1987	22 Apr 1994
			X[a]		X			D11	4 Nov 1987	22 Apr 1994
Hanford Barrier w/Gravel Admix	5	X					X	D2	4 Nov 1987	22 Apr 1994
		X					X[g]	D5	4 Nov 1987	31 Oct 1997
Eroded Prototype Barrier	6	X					X	D3	4 Nov 1987	***31 Mar 2004***
		X					X	D6	4 Nov 1987	27 Feb 1998
	18			X			X	D13	27 May 1998	***31 Mar 2004***
Gravel Mulch	8	X			X			C1	17 Nov 1989	***31 Mar 2004***
	10		X		X			C4	17 Nov 1989	***31 Mar 2004***
Pitrun Sand	9	X					X[g]	C2	17 Nov 1989	***31 Mar 2004***
	11		X				X	C5	17 Nov 1989	***31 Mar 2004***
Basalt Side Slope	12	X			X			D2	Nov 1994	***31 Mar 2004***
	13			X	X			D9	Nov 1994	Nov 1998
Sandy Gravel Side Slope	14	X			X			D4	Nov 1994	***31 Mar 2004***
	15			X	X			D11	Nov 1994	27 Sep 2001
Prototype Barrier	16	X					X	D7	Nov 1994	Nov 1998
	17			X			X	D14	Nov 1994	31 Aug 2002
Hanford Barrier Erosion/Dune Sand Deposition	19	X				X		D5	17 Nov 1997	***31 Mar 2004***
		X				X		W2	17 Nov 1997	***31 Mar 2004***
	20			X		X		D12	17 Nov 1997	***31 Mar 2004***
				X		X		W4	17 Nov 1997	***31 Mar 2004***
Sand Dune Migration	21	X				X		D6	22 Jul 1998	***31 Mar 2004***
	22			X		X		D8	22 Jul 1998	***31 Mar 2004***
Modified RCRA Subtitle C Barrier	23	X					X	D7	23 Feb 1999	***31 Mar 2004***
	24			X			X	D9	23 Feb 1999	***31 Mar 2004***
Glass Performance	25G1			X	X			D10	25 Sep 2002	***31 Mar 2004***
				X	X			D11	25 Sep 2002	***31 Mar 2004***
	26G2			X	X			D14	25 Sep 2003	***31 Mar 2004***

Vegetation Symbols: NV = no vegetation, SRV = shallow rooted vegetation, and DRV = deep rooted vegetation.
Superscripts: "a" = irrigation accelerated till drainage commenced; "g" = sagebrush planted but died, leaving only grasses; "G1" = HAN-28F glass; "G2" = is LAWA44 glass.
Note 1: Treatment 7 lysimeters received special precipitation and evaporation conditions after March 14, 1988.
Note 2: Dates in bold italics indicate current configurations.
Note 3: The yellow shading indicates active tests.

clear-tube lysimeters. The test included shrub-steppe vegetation initially, but the shrub eventually died and only shallow-rooted plants such as cheatgrass and Sandberg's bluegrass remained. The treatment numbers are 9 and 11.

Basalt Side Slope. The objective of this test was to document the performance of basalt riprap that could be used to construct side slopes for surface barriers. The basic configuration was 1.5 m of unscreened basalt riprap. This material is being tested for side slope use on a larger scale at the prototype barrier in the 200-BP-1 Operable Unit (Ward et al. 1997). Beneath the basalt layer was a 0.15-m thick asphaltic concrete layer that was underlain by gravel and more basalt riprap. Resting on top of the asphaltic concrete was about 2 to 3 cm of silt loam, within which was embedded a 2.54-cm-outside-diameter fiberglass wick. The wick was splayed within the silt loam to maximize contact, but exited through the drain outlet as one piece. This test did not include vegetation. The treatment numbers are 12 and 13.

Sandy Gravel Side Slope. The objective of this test was to document the performance of unprocessed local sandy gravel that could be used to construct side slopes for surface barriers. The basic configuration was 1.5 m of sandy gravel resting on an asphaltic concrete layer in a manner similar to the basalt side slope test. The sandy gravel material was tested for side slope use on a larger scale at the prototype barrier, where it is called clean-fill gravel (Ward et al. 1997). This test did not include vegetation. The treatment numbers are 14 and 15. Although not its primary purpose, this test may be useful for characterizing deep drainage rates at the high-level waste tank farms at Hanford that have similar textures.

Prototype Barrier. The objective of this test was to document the performance of the prototype Hanford Barrier (prototype barrier) (Ward et al. 1997). The basic configuration was 1 m of silt loam amended with pea gravel (15% by weight) above 1 m of silt loam, which gave a combined thickness of 2 m. Beneath the silt layer were sand and gravel filter layers, then the asphaltic concrete layer described in the basalt sideslope test description. Drainage is measured both above and below the asphalt layer. The test at the FLTF included shrub-steppe vegetation. The treatment numbers were 16 and 17. This test was terminated in 2002.

Hanford Barrier Erosion/Dune Sand Deposition. The objective of this test was to document the performance of the Hanford Barrier after experiencing some erosion of the silt loam layer and subsequent deposition of dune sand. The top 20 cm of silt loam was removed from four lysimeters containing a Hanford Barrier. The excavated silt loam was replaced with dune sand obtained from the dune that is aligned along the southern edge of the IDF site (Reidel 2004). This test included shallow-rooted vegetation, primarily cheatgrass; deep-rooted vegetation was kept off to mimic what might happen if fire prevented establishment of shrubs. The treatment numbers are 19 and 20.

Sand Dune Migration. The objective of this test was to document the performance of a sand dune that might migrate into the vicinity of or onto the surface barrier. The basic configuration was 3 m of dune sand obtained from the dune that is aligned along the southern edge of the IDF site (Reidel 2004). This test included shallow-rooted vegetation, primarily cheatgrass; deep-rooted vegetation was kept off to mimic what might happen if fire prevented establishment of shrubs. The treatment numbers are 21 and 22.

Modified RCRA Subtitle C Barrier. The objective of this test was to document the performance of the RCRA barrier design (DOE 1996). This barrier design meets the requirements for a RCRA barrier using only 1 m of silt loam rather than the 2 m of silt loam used for the prototype barrier design. In addition, the silt layer has two modifications. First, the upper 0.5 m of silt loam was amended with pea gravel at the rate of 15% by weight for erosion protection. Second, the lower 0.5 m of silt was compacted to create a low-conductivity layer to impede downward drainage (DOE 1996). Construction of this test required slight design modifications to the sand filter layer, the gravel drainage layer, and the density of the compacted silt layer (Fayer et al. 1999). The layers reside on an asphaltic concrete layer; drainage is measured both above and below the asphalt layer. This test included shrub-steppe vegetation. The treatment numbers are 23 and 24.

Glass. The objective of this test was to document the performance of glass waste forms in a field setting that received enhanced precipitation to accelerate the glass dissolution rate. The lysimeters were packed with vadose zone sediments (predominantly gravelly sand) excavated adjacent to the IDF site. The glass waste forms are in the shape of cylinders (20 cm diameter, 46 cm tall). The glass cylinders were placed in two layers in each lysimeter, three cylinders per layer, for a total of six cylinders per lysimeter. Two glass formulations were used. This test did not include vegetation. This test was designed, implemented, and monitored under a separate project task (Meyer et al. 2001), and the results are not discussed in this report. The treatment numbers are 25 and 26.

A.3.2 Data Collection Methods and Frequency

The types of data needed to estimate recharge and test models include water contents and storage, matric suction, temperature, drainage, and vegetation characteristics. Some measurements were conducted manually, while others were made automatically using the facility data logger system. Each lysimeter has a unique combination of sensors, sensor placement, and measurement frequency. Details were provided by Gee et al. (1989) and Fayer et al. (1999). This appendix provides data collected since 1999 that will support recharge estimation for the IDF PA: weather, irrigation, matric potential, drainage, and vegetation.

Weather. Weather data were collected at the Hanford Meteorological Station (HMS), which is located at the same elevation about 0.5 km west of the FLTF (Hoitink et al. 2003). The HMS is a complete weather station, providing hourly measurements of all variables, including air temperature, dewpoint temperature, solar radiation, wind speed, cloud cover, and precipitation. The station is operated by another project.

Irrigation. A subset of lysimeters received irrigation to mimic an increased precipitation regime. Untreated water from the Columbia River was applied in increments ranging from 3 to 35 mm per application. The rate was typically 4 mm/h. During several years, up to 73 mm of water were applied in a single irrigation event to simulate a 1,000-year storm. The total quantity and frequency of application were determined by the target amount, which was either two or three times the monthly average. The water was delivered through six nozzles spaced 0.41 m apart along a 2.4-m boom that was connected to the water source. The boom was 0.5 m above the ground surface and was moved automatically down the length of the facility at the rate of about 0.7 m/min. Four rain gauges were positioned within the irrigation path and monitored during each application.

Matric Potential. Matric potential was measured intermittently with a pressure transducer and tensiometers in those lysimeters that had potentials in the tensiometer measurement range (above –800 cm). In those lysimeters, two depths were monitored: 100 and 150 cm. In the dune sand treatment, an additional tensiometer was placed at the 210-cm depth and monitored.

Vegetation. Plant activity was monitored monthly for several years beginning in November 1998 and less frequently after 2002. Each lysimeter was surveyed to identify the species present, their areal coverage, and the height of shrubs.

Drainage. Drainage was measured in all lysimeters by collecting free water from the outlet located at the base of each lysimeter. The collected water was weighed immediately at the facility. The nominal collection frequency was bi-weekly. The collection of drainage in this manner (i.e., free drainage) creates a seepage face above which water contents can remain potentially high. Simulation results have shown that seepage face boundaries can reduce drainage rates (Scanlon et al. 2002). If plants roots have access to this zone, the resulting evapotranspiration can remove water that might normally have drained in the absence of the lysimeter bottom. Fortunately, most of the lysimeters have a large gravel zone that does not allow high water contents to develop above the seepage face at the outlet. For the few that do not, the lysimeters are either plant-free or maintained with only shallow-rooted plants.

A.4 Results

The FLTF has been operated for more than 16 years and yielded a significant quantity of data, much of which was presented and discussed by Gee et al. (1993b) and Fayer et al. (1999). Summarized below are the weather, irrigation, vegetation, matric potential, and drainage data. Following the data summary is a synthesis of observations relative to the potential for drainage in each of the eleven tests described in Section A.3.

A.4.1 Data Summary

A.4.1.1 Weather

Figure A.3 shows that monthly average air temperatures for the period of FLTF operation (defined as November 1987 to December 2003) were higher, 0.8°C on average, than the temperatures for the pre-FLTF period (1945 to October 1987). The individual monthly averages for the FLTF period were warmer than those for the pre-FLTF period by amounts ranging from 0.3 to 2.6°C (which occurred in January). The comparison is even starker for the minimum monthly temperatures. Average minimums during the FLTF period were 2.2°C higher and, for January, the difference was an incredible 7.1°C. Six monthly records for maximum temperature were either set or tied during the FLTF period; one monthly minimum record was also set.

Figure A.4 shows that average monthly precipitation amounts during the FLTF period were mostly higher than amounts during the pre-FLTF period. The FLTF monthly averages ranged from 3.7 mm less than pre-FLTF to 8.25 mm greater. Four maximum monthly precipitation records were set. The maximum annual precipitation record of 313 mm was set in 1995. This record was nearly broken in the following year when annual precipitation totaled 310 mm. During the FLTF period, two records for

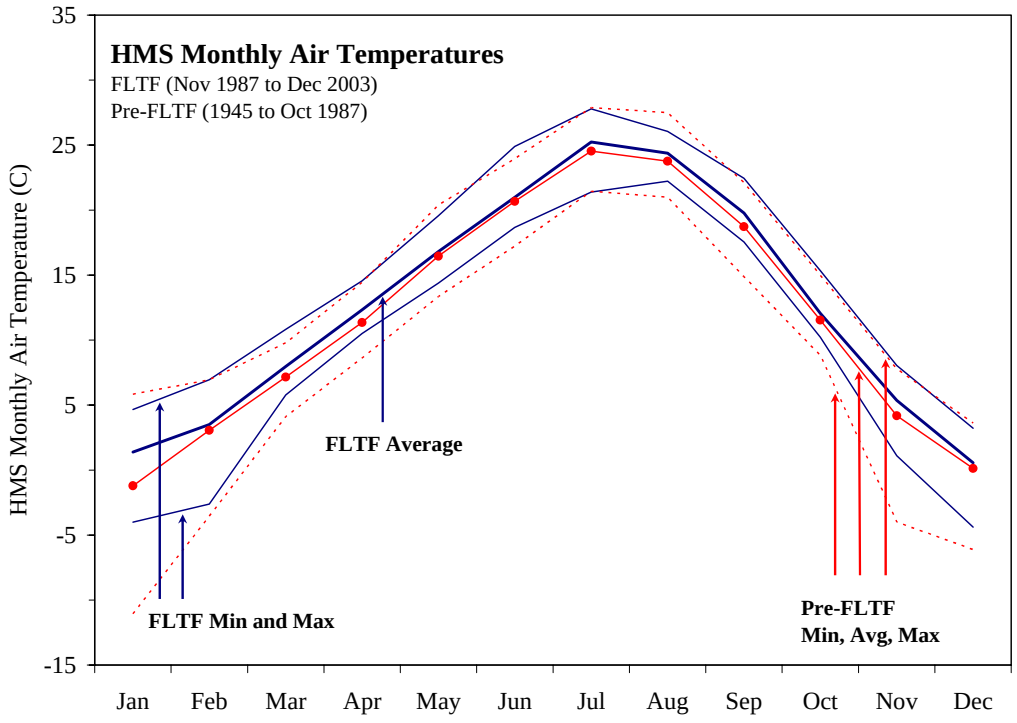

Figure A.3. Monthly Air Temperatures Measured at the Hanford Meteorological Station

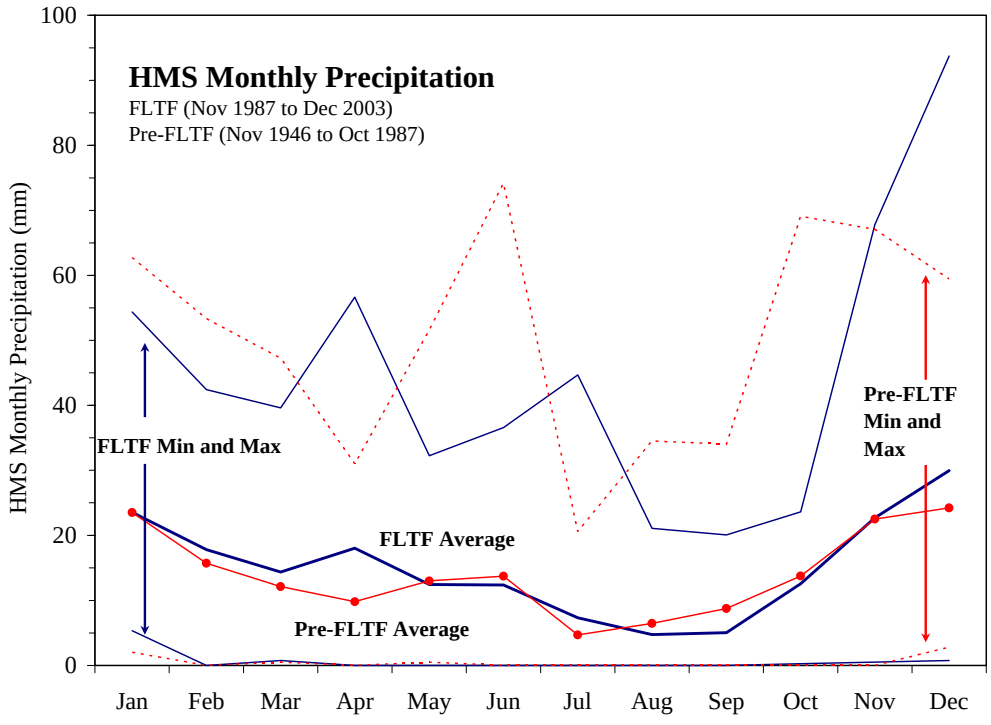

Figure A.4. Monthly Precipitation Measured at the Hanford Meteorological Station

maximum monthly snowfall were set: 57.4 cm in December 1996 and 43.2 cm in February 1989. The annual snowfall record of 142.5 cm was set during the winter of 1992-1993. During the FLTF period, the annual average precipitation was 181 mm, which was 13 mm greater than the pre-FLTF average of 168 mm.

Overall, the weather during the FLTF period could be characterized as warmer and wetter than during the pre-FLTF period. The impact to drainage rates is uncertain. Warmer weather increases potential evaporation and lengthens the season of plant activity, both of which reduce drainage. Higher precipitation can lead to higher drainage, but it could be offset by increased plant growth encouraged by the extra water.

A.4.1.2 Irrigation

Irrigation applications were sufficient to maintain the target rate. Deviations occurred during winter months when it was not feasible to irrigate. Deviations also occurred during lysimeter modifications, when it was not possible to run the system because of open lysimeters and construction material. When conditions prevented irrigation, the amount to be added was applied during subsequent irrigation events such that the long-term rate was maintained.

A.4.1.3 Matric Potential

Only a few lysimeters had matric potentials high enough to measure with a tensiometer. For these, Figure A.5 shows that potentials at the 150-cm depth were quite consistent from 1995 through 1997. In November 1997, D12 and W4 were modified: 20 cm of silt loam was removed and replaced with 20 cm of dune sand (treatment No. 20). In the following summer, potentials in D10 dropped as in previous years, but potentials in D12 and W4 remained above -100 cm. All three lysimeters were mostly unvegetated, so the contrast in potentials was due primarily to the impact of the surface soil. The dune sand was much less able than the silt loam to store water near, and/or transmit water to, the evaporation surface. These lysimeters were intended to have only shallow-rooted vegetation, but deep-rooted tumblemustard (*Sisymbrium altissimum*) invaded D12 in 1999 and covered 30% of the lysimeter surface before being removed in May. The results can be seen in Figure A.5 as the rapid drop in matric potentials in the spring of 1999.

Figure A.6 shows the seasonal variations in matric potential in the two sand dune lysimeters (D6 and D8). After significant drying of D6 in 1999 by deep-rooted bur ragweed (*Ambrosia acanthicarpa*), the potentials steadily increased to the point that they are comparable to the potentials measured in the heavily draining D8. For the first time, in March 2003, drainage was collected from D6.

A.4.1.4 Vegetation

Table A.2 shows the list of common species observed on the FLTF lysimeters. Most are annuals and were present for only a portion of each year. Sagebrush health and survival continues to be problematic on several lysimeters. Shrubs on lysimeters D3 and D13 are effectively dead. C2 lost its only shrub in 1999; C5 lost its shrub in 2001. Shrubs on other lysimeters appear to be somewhat active but not vigorous. These results highlight one of the difficulties with growing plants on lysimeters. Shrubs need

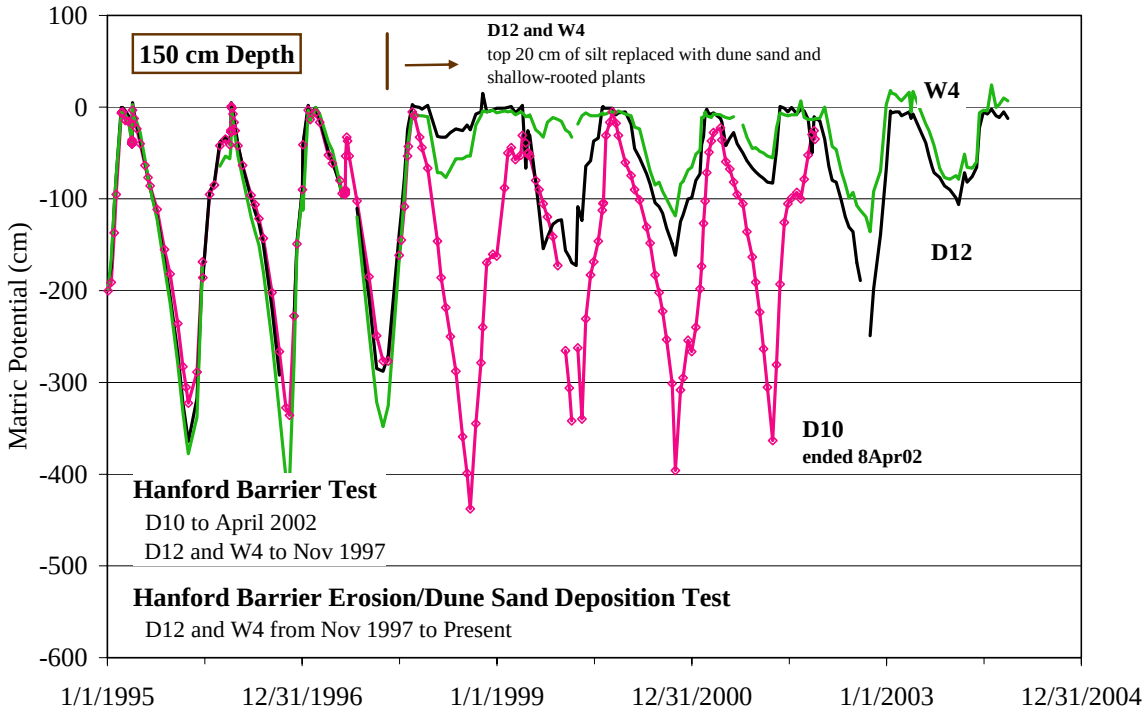

Figure A.5. Matric Potentials at the 150-cm Depth in the Irrigated Prototype Barrier with No Plants

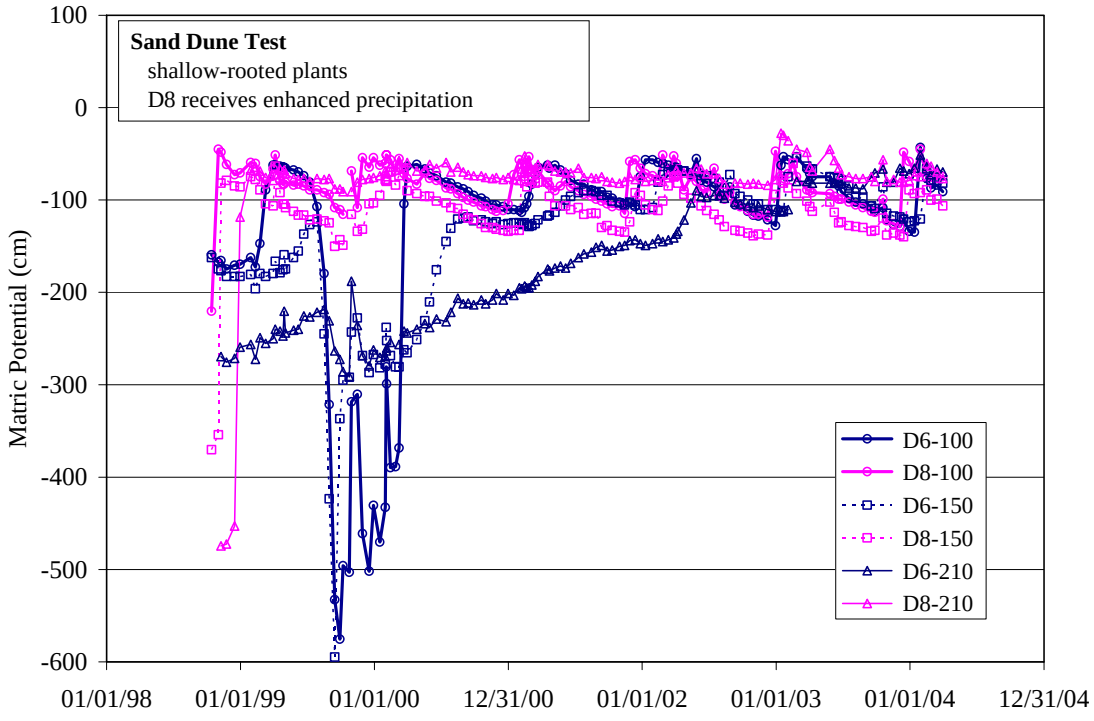

Figure A.6. Matric Potentials at the 150-cm Depth in the Irrigated Prototype Barrier with No Plants

Table A.2. Common Species Observed on Field Lysimter Test Facility Lysimeters. Species bolded and highlighted in yellow covered at least 50% of at least one lysimeter for some portion of a year.

Species Name	Common Name
Agropyron cristatum	Crested Wheatgrass
Artemisia tridentata	Sagebrush
Bromus tectorum	Cheatgrass
Convolvulus arvensis	Field Bindweed
Erodium cicutarium	Storksbill
Helianthus cusickii	Cusick's Sunflower
Machaeranthera canescens	Hoary Aster
Oryzopsis hymenoides	Indian Ricegrass
Poa Sandbergii	Sandberg's Bluegrass
Sitanion hystrix	Bottlebrush Squirreltail
(many)	Cryptogamic crusts and mosses

large areas to harvest sufficient water and nutrients. Small diameter lysimeters like C5 (30-cm diameter) are insufficient in size. The issue of sagebrush health and survival is further complicated by the observation of a general decrease in sagebrush health, and well as some sagebrush die-off, at the Hanford Site. Poston et al. (2000) reported areas totaling 1,776 ha that showed evidence of sagebrush decline, and 280 ha where sagebrush death was 80% or greater. Although shrubs are excellent at reducing drainage, the drainage data presented later in this report show that shrubs are not critical to the performance of the barrier designs that utilize silt loam for the surface layer.

It was difficult to establish shallow-rooted plants on lysimeters having dune sand on the surface (e.g., D6, D5, D8, D12, W2, W4). The maximum cheatgrass coverage has ranged from 2% in 1999 to 80% in 2001. In 2002 and subsequent years, germination was poor; only once did cheatgrass coverage exceed 25%. Such wide variations in plants on the silt loam soil has not been observed. The difficulty of establishing vegetation on the dune sand may be related to nutrient status, which was not evaluated but is suspected to be low. Such year-to-year variability in plant cover on the dune sand could significantly affect the performance.

Lysimeters that are kept free of vegetation have more water stored in the soil throughout the year. One of the most difficult tasks in operating the FLTF has been maintaining the no-vegetation status of those lysimeters. Our experience has been that these lysimeters must be weeded every two weeks in the spring and monthly during the remainder of the year. On several occasions, a one- or two-month hiatus in weeding during the spring resulted in an extensive crop of plants, usually tumbleweed (*Salsola kali*) but also sagebrush seedlings, cheatgrass, and other species. The implication is that a non-vegetated condition (e.g., due to fire, disturbance) will probably not persist for silt loam surface barriers for more than a couple of months, and certainly not for more than 1 year.

A.4.1.5 Drainage

Since the fall of 1989, all of the lysimeters containing vegetated Hanford Barrier treatments had no drainage, even those receiving the 3x precipitation treatment. Data from 1987 and 1988 was not included because of the leak tests (Campbell and Gee 1990), which could not be separated from actual drainage. Through September 1989, two of the vegetated lysimeters drained less than 0.1 kg in 1989, but this is suspected to be residual water from leak testing conducted in 1988. In the years since then, no water has drained from vegetated Hanford Barrier lysimeters. The drainage design specification for the Hanford Barrier was to limit drainage to less than 0.5 mm/yr. The FLTF observations are strong evidence that the Hanford Barrier design functions much better than designed.

The only condition that led to significant drainage from a Hanford Barrier treatment was enhanced precipitation and no vegetation. Figure A.7 shows that, for the first 3 years (under 2x precipitation), the three lysimeters containing an unvegetated Hanford Barrier had no significant drainage. Three years after increasing to 3x precipitation, these lysimeters began to show significant drainage. The onset of drainage coincided with the melting of a large snowpack in February 1993. In early 1997, a similar event occurred that also resulted in significant drainage from these lysimeters. In the intervening years, and in 1998, individual lysimeters had small amounts of drainage, but there was no consistency in amount. Such differences indicate the drainage variability that could be expected in a real cover.

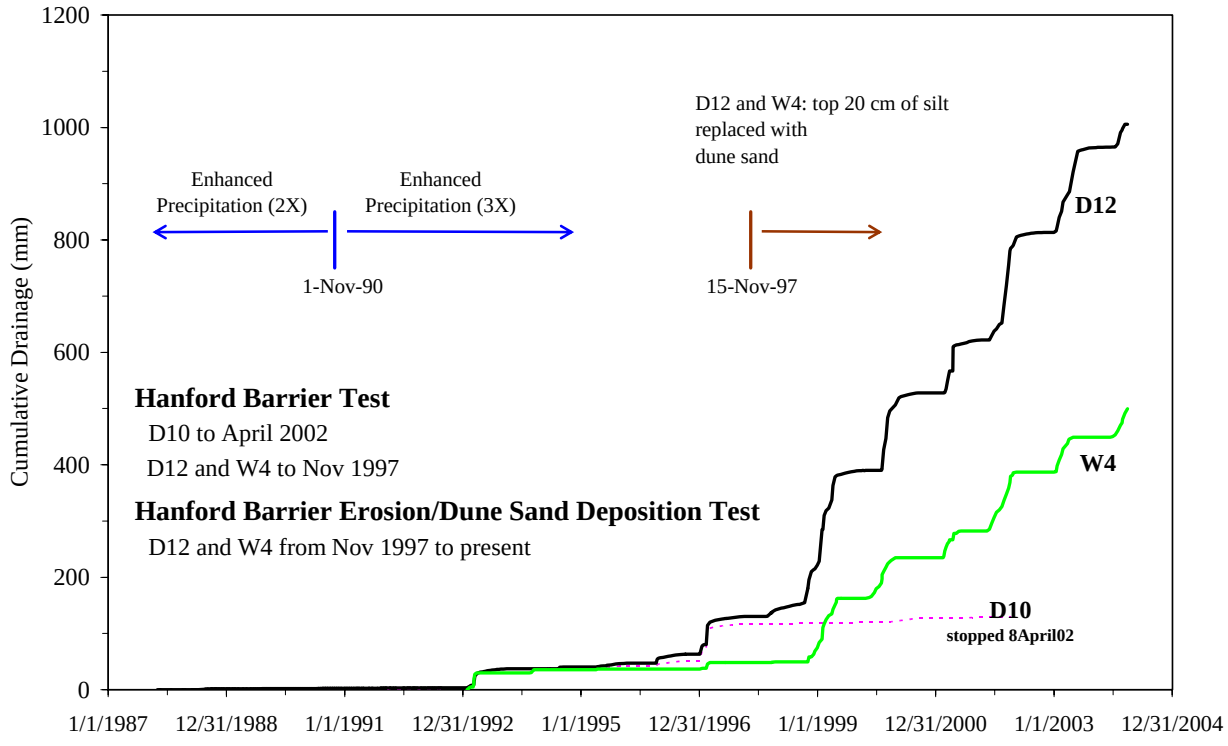

Figure A.7. Cumulative Drainage from Irrigated Lysimeters Containing the Unvegetated Prototype Barrier

After D12 and W4 were modified in November 1997, the drainage pattern of the three lysimeters diverged. D10 continued to have very little drainage, while D12 and W4 began to have more drainage than was collected in all of the previous years combined. The increase in drainage resulted from the replacement of 20 cm of silt loam with dune sand on the surface. This result is consistent with the observed increase in matric potential in D12 and W4. The increased drainage from D12 and W4 is striking because these lysimeters had a reasonable quantity of shallow-rooted vegetation whereas D10 had no vegetation. This observation demonstrates the power of evaporation to limit drainage if the right soil type is at the surface.

Figure A.8 shows that drainage from the side slope treatments was consistently significant in every year. During the 9-year period from 1995 to 2003, the sandy gravel lysimeters drained at the rate of 113 mm/yr under ambient precipitation and 365 mm/yr under enhanced precipitation. These rates represent 58% of the amount of water received under ambient conditions and 76% under enhanced precipitation. If the percentage is robust, then the drainage rate associated with the average precipitation (172 mm/yr from 1946 to 2003) would be 99.8 mm/yr. This rate could also be applied to conditions at the tank farms in the 200 Areas. The precise value for each tank farm would depend on the distribution of sand and gravel on the surface. In addition, this rate does not account for any effects caused by the increased temperature around the tanks.

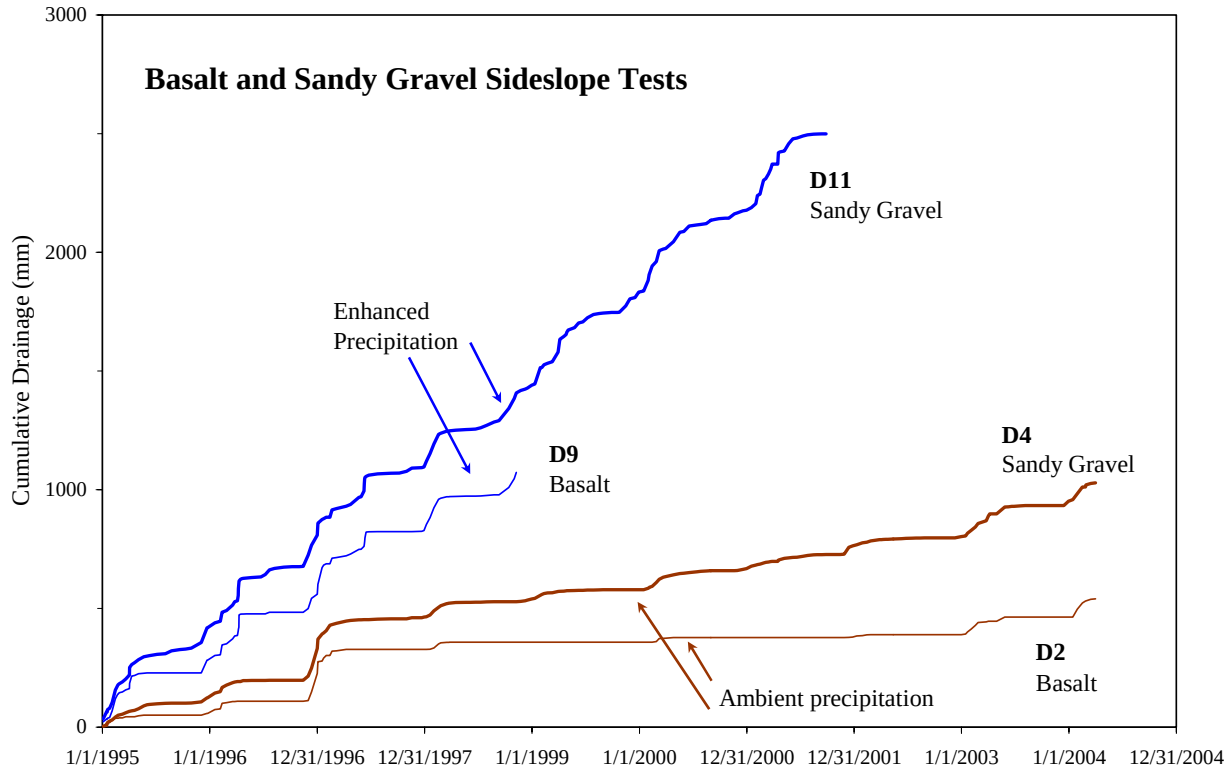

Figure A.8. Cumulative Drainage from the Lysimeters Containing Side Slope Tests

The higher percentage (of precipitation becoming drainage) for the enhanced precipitation treatment may truly reflect what could happen under wetter regimes. It may also be related to the method of applying irrigation water. With this method, 10 to 20 mm of irrigation water were applied in a single event rather than as more numerous smaller events. Large events may penetrate the profile more deeply, where the water would be less susceptible to evaporation.

Under both precipitation regimes, the basalt side slope had less drainage and, in some years, had no drainage. Fayer et al. (1999) discussed design and operational reasons for the lower rates. Wittreich et al. (2003) observed a similar effect (lower drainage rates) on the basalt side slope of the prototype surface barrier. They attributed the lower rates to evaporative drying within the open-work basalt.

Figure A.9 shows that there was significant drainage from four of the clear tube lysimeters, the two with pitrun sand and the two with gravel mulch; drainage was never detected in the clear tube lysimeters containing the Hanford Barrier configuration (C3 and C6). The pitrun sand lysimeters had drainage in some but not all years. Although the lysimeters are vegetated, the plants were unable to prevent drainage. For the 14-year period from 1990 to 2003, drainage rates averaged 25.1 and 79.9 mm/yr for the ambient (C2) and enhanced precipitation (C5) treatments, respectively. These drainage rates represented 13 and 20%, respectively, of the total amount of precipitation and irrigation received.

Figure A.9 also shows that the gravel mulch lysimeters had much more drainage than the pitrun sand lysimeters. For the same 14-year period, drainage rates averaged 89 and 333 mm/yr for the ambient (C1) and enhanced precipitation (C4) treatments, respectively. These drainage rates represented 48 and 83%, respectively, of the total amount of precipitation and irrigation received. Two factors that explain the higher drainage relative to the pitrun sand test are the lack of vegetation and the suppression of evaporation by the gravel mulch. The suppression occurs because water that infiltrates into the sand beneath the gravel can only evaporate by the slow process of diffusion up through the gravel mulch layer. The other mechanism for water to move upward is for water to flow directly in the liquid phase up through the gravel. Such flow is essentially negligible because of the extremely low hydraulic conductivity of unsaturated gravel.

The two lysimeters of the sand dune test have been monitored for nearly 5 years. In that time, drainage from D8 (enhanced precipitation) has been steady and currently averages 234 mm/yr. Under ambient conditions, D6 did not drain prior to 2004, but the steady increasing matric potential data suggested that D6 would eventually drain. True to form, 5.8 mm of drainage was collected in March 2004.

The pattern of drainage is generally predictable. Lysimeters such as C4 drain steadily throughout the year because they receive enhanced precipitation. Lysimeters that receive ambient precipitation tend to drain in the spring following the winter precipitation. In contrast to these usual patterns, some lysimeters have drained very small amounts sporadically but always in late summer and fall when drainage is expected to be the smallest. Figure A.10 shows the annual amounts are variable (some data sets are short because the treatments were ended). This anomalous drainage was attributed to vapor flow (Campbell and Gee 1990). Basically, the warmth of the summer enhanced downward vapor flow. As it penetrated the underlying cooler sands and gravels, the vapor condensed and, in time, became drainage.

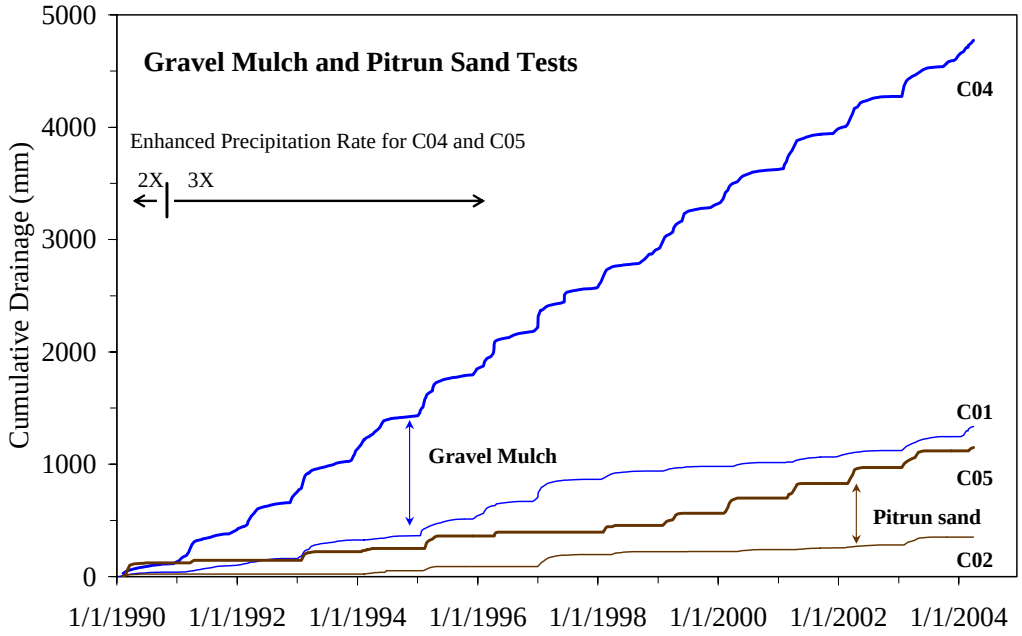

Figure A.9. Cumulative Drainage for the Gravel Mulch and Pitrun Sand Treatments

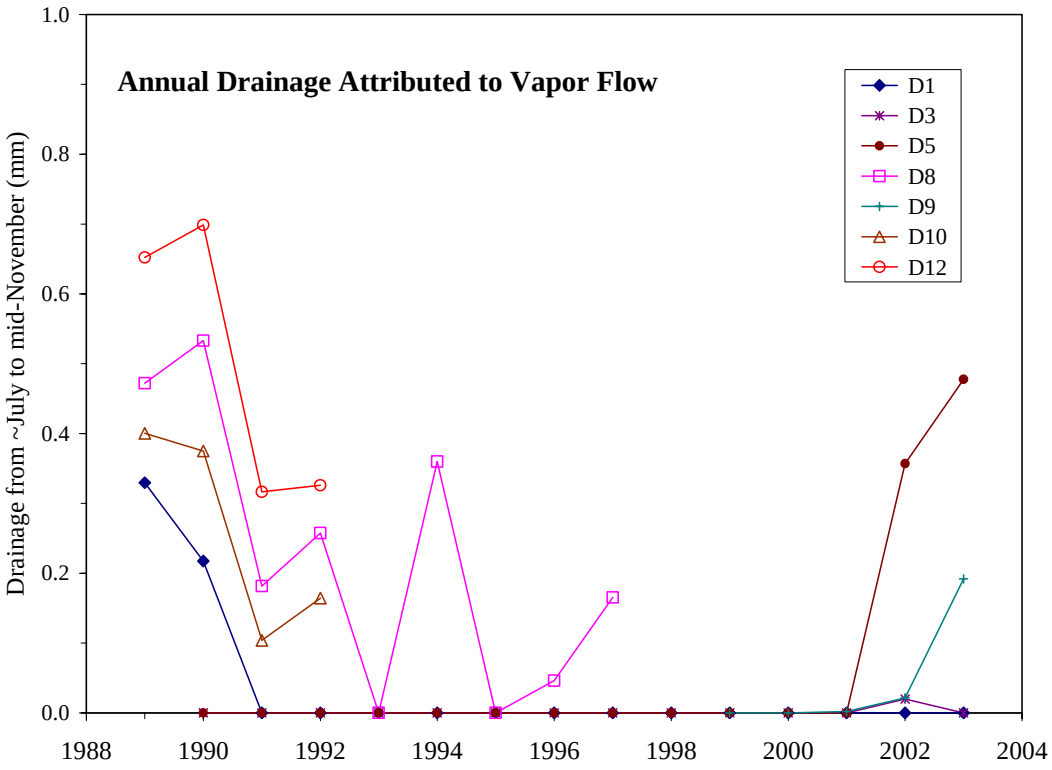

Figure A.10. Annual Drainage from the Lysimeters Containing the Unvegetated Prototype Barrier

Figure A.10 also shows that, recently, late summer drainage was detected in two lysimeters normally thought to be incapable of having drainage. Lysimeter D5 is currently being tested with a 20-cm layer of dune sand on the surface and only shallow-rooted plants. Lysimeter D9 is currently testing a RCRA barrier design with several healthy shrubs and receiving enhanced precipitation. In both cases, the water content at the base of the silt loam layer is much higher than normally occurs at that time of year in a silt loam receiving ambient precipitation and could increase vapor movement.

Two questions arise from these results:

1. If seasonal temperature changes are affecting drainage, is the design of the lysimeter facility in any way responsible?

2. Does the drainage water originate from the basalt riprap and gravel (i.e., residual water from construction and leak testing) or from the silt loam layer above?

Ward et al. (1997) reported "small seasonal discharges" from the prototype barrier test plots. These vegetated test plots were in a full-scale surface cover; thus, avoiding any complications such as might be possible in the FLTF. These results suggest that the FLTF design is not the sole possible cause of seasonal discharge. The Ward et al. (1997) data set covered 3 years of monitoring following construction. Wittreich et al. (2003) did not report any subsequent seasonal discharge. However, the plant community had become well established after 1997, and it may be that the silt loam layer was too dry for significant downward vapor flow to occur. Such a result is consistent with the vegetated lysimeters receiving ambient precipitation at the FLTF.

Answering the second question is more problematic. Currently, no method exists that can identify the source of the seasonal drainage water. Given sufficient years, residual water from construction or leak testing ought to diminish. If so, continued seasonal discharges would imply the drainage water was coming from the silt loam. Fortunately, the observed quantities are less than 0.5 mm/yr and not a barrier performance issue at this time.

Finally, for all lysimeter results, the concern exists that the drainage rates could have been affected by the presence of a seepage face at the base of the lysimeters. Such a condition is created when a thin gravel pack is used at the lysimeter bottom to facilitate drainage collection. As noted in Section A.3, the impact for the FLTF was estimated to be minimal. Furthermore, during the lifetime of the FLTF, four vegetated lysimeters have been excavated and found to have no roots below the silt loam. However, because this phenomenon could affect the key drainage variables, the possibility of an effect ought to be investigated more fully.

A.4.2 Results of the Eleven Tests

The FLTF data (primarily the drainage data) was used to draw conclusions for each of the eleven tests. For each test, the most recent data (Table A.3) confirm what has been observed in previous years, specifically:

Hanford Barrier. With plants, the Hanford Barrier continues to limit drainage to well below the design specification of 0.5 mm/yr. Without plants, the Hanford Barrier continues to function under ambient conditions, and previously collected data showed it performed under 2x precipitation during a 3-year test. Only after 3 years at 2x and 2 years of 3x precipitation, with no plants, has the Hanford Barrier allowed significant drainage. Based on experience trying to keep designated lysimeters plant-free, the Hanford Barriers are predicted to receive 3x normal precipitation, will not remain plant-free for more than a few months at most, and drainage should remain below the 0.5 mm/yr design goal.

Hanford Barrier with Gravel Admix. The two lysimeters containing this configuration with plants and receiving the ambient precipitation treatment showed no drainage after 4 and 7 years, respectively. The gravel admix did not appear to impair the ability of the Hanford Barrier to prevent drainage. There were no recognizable differences in plant community compared to the tests without gravel admix. Although there were no treatments involving enhanced precipitation, a Hanford Barrier with gravel admix and receiving enhanced precipitation is expected to prevent drainage as designed.

Eroded Hanford Barrier. The lysimeter containing 1 m of silt loam above sand and gravel, with plants, and receiving the ambient precipitation treatment showed no drainage after 14 years. This configuration is similar to the RCRA barrier. The results suggest that the RCRA barrier will perform as well (a test of the actual design is discussed below). The single lysimeter receiving the enhanced precipitation treatment (i.e., 3x normal) has averaged 2.4 mm/yr in 5.8 years.

Gravel Mulch. The two small lysimeters used for this test generated a significant amount of drainage in 14 years: 89 mm/yr (48% of received water) for the ambient treatment and 333 mm/yr (83% of received water) for the enhanced precipitation treatment. These results may be useful for describing an upper limit to deep drainage in tank farms. The gravel mulch used at the FLTF contains very few finer particles (except what the wind deposits). Tank farms, in contrast, have 50% or more sand particles (Figure 3 of Smoot et al. 1989).

Pitrun Sand. The two small lysimeters used for this test generated a measurable amount of drainage, although not consistently in every year. In a 14-year period, drainage rates averaged 25.1 mm/yr (13% of received water) for the ambient precipitation treatment and 79.9 mm/yr (20% of received water) for the enhanced precipitation treatment. These lysimeters are vegetated mostly with grasses. Several attempts were made to establish sagebrush, but the plants did not survive for more than a few years. Thus, these deep drainage results are probably higher than for similar sand with a shrub-steppe plant community.

Basalt Side Slope. The two lysimeters used for this test generated a significant amount of drainage: 58.9 mm/yr for 9 years of the ambient treatment and 269 mm/yr for 3.9 years of the enhanced precipitation treatment. As a percentage of total water input, drainage was 30 and 53% for the ambient and

Table A.3. Average Drainage Rates for Selected Periods at the Field Lysimeter Test Facility (as of 31 March 2004)

Test Description	Treatment ID No.	Lysimeter ID	Averaging Period			Average Drainage (mm/yr)
			Start	End	Duration (yr)	
Hanford Barrier	1	D4	4 Nov 1987 ***2 Jan 1990***	19 Apr 1994	6.5 ***4.3***	0.5 ***0.0***[a]
		D7	4 Nov 1987 ***2 Jan 1990***	19 Apr 1994	6.5 ***4.3***	0.7 ***0.0***[a]
		W1	4 Nov 1987	31 Mar 2004	16.4	0.0
		C3	9 Nov 1988	31 Mar 2004	15.4	0.0
	2	D1	4 Nov 1987 ***3 Jan 1991***	31 Mar 2004	16.4 ***13.2***	0.3 ***0.0***[a]
		D8	4 Nov 1987 ***2 Jan 1990***	25 Feb 1998	10.3 ***8.2***	0.3 ***0.2***
		W2	4 Nov 1987	31 Oct 1997	10.0	0.0
	3	D13	2 Jan 1990	7 Jan 1998	8.0	0.0
		D14	2 Jan 1990	5 Jan 1994	4.0	0.0
		W3	2 Jan 1990	31 Mar 2004	14.3	0.0
		C6	2 Jan 1990	31 Mar 2004	14.3	0.0
	4	D10	2 Jan 1990	10 Jan 2002	12.0	10.7
		D12	2 Jan 1990	31 Oct 1997	7.8	16.4
		W4	2 Jan 1990	31 Oct 1997	7.8	6.2
Hanford Barrier w/Gravel Admix	5	D2	4 Nov 1987 ***2 Jan 1990***	19 Apr 1994	6.5 ***4.3***	0.1 ***0.0***[a]
		D5	4 Nov 1987 ***2 Jan 1990***	31 Oct 1997	10.0 ***7.8***	0.4 ***0.0***[a]
Eroded Hanford Barrier	6	D3	4 Nov 1987 ***2 Jan 1990***	31 Mar 2004	16.4 ***14.3***	0.3 ***0.0***[a]
		D6	4 Nov 1987 ***2 Jan 1990***	25 Feb 1998	10.3 ***8.2***	0.0 ***0.0***[a]
	18	D13	27 May 1998	31 Mar 2004	5.8	2.4
Gravel Mulch	8	C1	2 Jan 1990	30 Dec 2003	14.0	89.0
	10	C4	2 Jan 1990	30 Dec 2003	14.0	333
Pitrun Sand	9	C2	2 Jan 1990	30 Dec 2003	14.0	25.1
	11	C5	2 Jan 1990	30 Dec 2003	14.0	79.9
Basalt Side Slope	12	D2	4 Jan 1995	30 Dec 2003	9.0	58.9
	13	D9	4 Jan 1995	24 Nov 1998	3.9	269
Sandy Gravel Side Slope	14	D4	4 Jan 1995	30 Dec 2003	9.0	113
	15	D11	4 Jan 1995	Sep 2001	6.8	365
Prototype Barrier	16	D7	4 Jan 1995	24 Nov 1998	3.9	0.0
	17	D14	4 Jan 1995	28 Aug 2002	7.7	0.0
Hanford Barrier Erosion/Dune Sand Deposition	19	D5	17 Nov 1997	31 Mar 2004	6.4	0.14
		W2	17 Nov 1997	31 Mar 2004	6.4	0.0
	20	D12	17 Nov 1997	18 Nov 2003	6.0	139
		W4	17 Nov 1997	18 Nov 2003	6.0	66.8
Sand Dune Migration	21	D6	26 May 1999	31 Mar 2004	4.8	1.2[b]
	22	D8	26 May 1999	31 Mar 2004	4.8	234
Modified RCRA Subtitle C Barrier	23	D7	23 Feb 1999	31 Mar 2004	5.1	0.0
	24	D9	23 Feb 1999	31 Mar 2004	5.1	0.04

(a) Italicized and bolded drainage rates do not include data that appeared to be influenced by initial conditions.
(b) All drainage occurred in March 2004, so the average value reported should be considered preliminary.

enhanced precipitation treatments. These lysimeters had no vegetation, so the drainage rates should be viewed as upper limits. A field-scale test of this side slope with no vegetation is occurring at the prototype barrier. The results after nearly 8 years indicated a drainage rate of 26.7 mm/yr, or 15.2% of the precipitation received (Wittreich et al. 2003).

Sandy Gravel Side Slope. The two lysimeters used for this test generated a significant amount of drainage: 113 mm/yr for 9 years of the ambient treatment and 365 mm/yr for 6.8 years of the enhanced precipitation treatment. As a percentage of total water input, drainage was 58 and 76% for the ambient and enhanced precipitation treatments. These lysimeters had no vegetation, so the drainage rates should be viewed as upper limits. A field-scale test of this side slope, with vegetation (albeit limited) is occurring at the prototype barrier. The results after nearly 8 years indicated a drainage rate of 37.8 mm/yr, or 21.5% of the precipitation received (Wittreich et al. 2003). The lysimeter and prototype barrier results may be useful to describe deep drainage in tank farms.

Prototype Barrier. The lysimeter receiving enhanced precipitation for this test had no drainage in 7.7 years. In addition, matric potentials were always below the tensiometer range, indicating dry soil. The prototype barrier is expected to perform as designed (to limit drainage to less than 0.5 mm/yr).

Hanford Barrier Erosion/Dune Sand Deposition. The two lysimeters receiving ambient precipitation drained 0.14 and 0.0 mm/yr during the 6.4-year monitoring period. The two lysimeters receiving enhanced precipitation drained 139 and 66.8 mm/yr during a 6-year period. In both treatments, the lower drainage rate occurred in a weighing lysimeter, an effect that has been observed previously in other treatments. All four lysimeters were intended to be vegetated by shallow-rooted plants but the actual vegetation cover has been much less than expected. Because of the limited vegetation, the drainage results may more accurately be said to reflect a sparsely vegetated state. Clearly, sand deposition on a surface barrier has the potential to degrade performance in the sense of allowing drainage rates to increase.

Sand Dune Migration. The two lysimeters used for this test have been monitored for nearly 5 years. The lysimeter receiving ambient precipitation had no measurable drainage until March 2004. The lysimeter receiving 3x normal precipitation generated significant drainage each year. The average rate was 234 mm/yr (49% of the precipitation received). Like the erosion/deposition test above, vegetation was intended to be a reasonable cover of shallow-rooted species like cheatgrass. However, plant activity was marginal, so the results are more nearly like an unvegetated test.

Modified RCRA Subtitle C Barrier. The lysimeter receiving ambient precipitation had no drainage for 5.1 years. The lysimeter receiving the enhanced precipitation treatment drained 0.04 mm/yr, primarily in the early fall of 2002 and 2003. This drainage is attributed to vapor flow. Regardless, under the current climate conditions, this cover is expected to perform as designed for the conditions envisioned for the IDF site. Further, this cover will meet the performance criterion of <0.5 mm/yr even if subjected to 3x precipitation levels.

A.5 Conclusions

The data collected at the FLTF continue to show how soil type, barrier design, vegetation, and precipitation can impact deep drainage rates. The Hanford Barrier described by Wing and Gee (1994)

continues to work successfully. In concert with vegetation, the barrier reduced drainage to zero (compared to the design goal of 0.5 mm/yr). This performance occurred under ambient and 2x precipitation, with or without plants. Even under 3x precipitation, the vegetated Hanford Barrier prevented drainage. Variations of the Hanford Barrier (RCRA barrier; prototype barrier) also reduced drainage to zero. All of the testing conducted to date indicates that the capillary barrier design can be successful if it includes a 1- to 2-m-thick silt loam layer above sand and gravel layers.

The deposition of dune sand on a capillary barrier could impair its ability to limit drainage. The presence of vegetation, especially deep-rooted shrub-steppe plants, could mitigate this problem, but that makes the barrier's success susceptible to plant disturbances and fire. Because a deep-rooted shrub-steppe plant community cannot be guaranteed, deposition of wind-blown sand on the cover is a concern.

The side slope tests continued to show how ineffective these materials are at preventing drainage (rates exceed the barrier drainage goal [0.5 mm/yr] by a factor of more than 100). These tests were not vegetated, so the results represent an upper limit to drainage through such side slopes. Even if vegetation were present, the pitrun sand results show that drainage rates would still exceed the design by a factor of 50. Traditional side slope designs call for coarse-textured geologic material such as gravel for stability purposes. The need exists for new side slope designs that address the desire to minimize drainage while maintaining stability. If the final barrier design for the IDF Site includes side slopes, then an effort ought to be made to identify and evaluate side slope designs that minimize drainage or route the drainage water safely away from the disposal site being protected by the surface barrier.

Two issues were identified for future resolution. First, the mechanism responsible for the late summer occurrence of small quantities of drainage needs to be confirmed. Second, the potential impact of a seepage face at the bottom of the lysimeters needs to be evaluated more fully.

A.6 References

Campbell MD, GW Gee, MJ Kanyid, and ML Rockhold. 1990. *Field Lysimeter Test Facility: Second Year (FY 1989) Test Results*. PNL-7209, Pacific Northwest Laboratory, Richland, Washington.

Campbell MD and GW Gee. 1990. *Field Lysimeter Test Facility: Protective Barrier Test Results (FY 1990, the third year)*. PNL-7558, Pacific Northwest Laboratory, Richland, Washington.

DOE. 1996. *Focused Feasibility Study of Engineered Barriers for Waste Management Units in the 200 Areas*. DOE/RL-93-33, Rev. 0, U.S. Department of Energy, Richland Operations Office, Richland, Washington.

DOE. 2003. *Annual Summary of the Immobilized Low-Activity Waste Performance Assessment for 2003, Incorporating the Integrated Disposal Facility Concept*. DOE/ORP-2000-19, Rev. 3, U.S. Department of Energy, Office of River Protection, Richland, Washington.

Fayer MJ, EM Murphy, JL Downs, FO Khan, CW Lindenmeier, and BN Bjornstad. 1999. *Recharge Data Package for the Immobilized Low-Activity Waste 2001 Performance Assessment*. PNNL-13033, Pacific Northwest National Laboratory, Richland, Washington.

Fayer MJ. 2000. *UNSAT-H Version 3.0: Unsaturated Soil Water and Heat Flow Model, Theory, User Manual, and Examples*. PNNL-13249, Pacific Northwest National Laboratory, Richland, Washington.

Gee GW, LL Cadwell, HD Freeman, MW Ligotke, SO Link, RA Romine, and WH Walters. 1993a. *Testing and Monitoring Plan for the Permanent Isolation Surface Barrier Prototype*. PNL-8391, Pacific Northwest Laboratory, Richland, Washington.

Gee GW, DG Felmy, JC Ritter, MD Campbell, JL Downs, MJ Fayer, RR Kirkham, and SO Link. 1993b. *Field Lysimeter Test Facility Status Report IV: FY 1993*. PNL-8911, Pacific Northwest Laboratory, Richland, Washington.

Gee GW, RR Kirkham, JL Downs, and MD Campbell. 1989. *The Field Lysimeter Test Facility (FLTF) at the Hanford Site: Installation and Initial Tests*. PNL-6810, Pacific Northwest Laboratory, Richland, Washington.

Hoitink DJ, KW Burk, JV Ramsdell, and WJ Shaw. 2003. *Hanford Site Climatological Data Summary 2002 with Historical Data*. PNNL-14242, Pacific Northwest National Laboratory, Richland, Washington.

Meyer PD, BP McGrail, and DH Bacon. 2001. *Test Plan for Field Experiments to Support the Immobilized Low-Activity Waste Disposal Performance Assessment at the Hanford Site*. PNNL-13670, Pacific Northwest National Laboratory, Richland, Washington.

Poston TM, RW Hanf, and RL Dirkes, (eds.). 2000. *Hanford Site Environmental Report for Calendar Year 1999*. PNNL 13230, Pacific Northwest National Laboratory, Richland, Washington.

Puigh RJ and FM Mann. 2002. *Statement of Work for FY 2003 to 2008 for the Hanford Low-Activity Tank Waste Performance Assessment Program*. RPP-6702, Rev. 2, CH2M HILL Hanford Group, Inc., Richland, Washington.

Reidel SP. 2004. *Geologic Data Package for 2005 Integrated Disposal Facility Waste Performance Assessment*. PNNL-14586, Pacific Northwest National Laboratory, Richland, Washington.

Scanlon BR, M Christman, RC Reedy, I Porro, J Simunek, and GN Flerchinger. 2002. "Intercode Comparisons for Simulating Water Balance of Surficial Sediments in Semiarid Regions." *Water Resour. Res.* 38(12):1323.

Smoot JL, JE Szecsody, B Sagar, GW Gee, and CT Kincaid. 1989. *Simulations of Infiltration of Meteoric Water and Contaminant Plume Movement in the Vadose Zone at Single-Shell Tank 241-T-106 at the Hanford Site*. WHC-EP-0332, Westinghouse Hanford Company, Richland, Washington.

Ward AL, GW Gee, and SO Link. 1997. *Hanford Prototype-Barrier Status Report: FY 1997*. PNNL-11789, Pacific Northwest National Laboratory, Richland, Washington.

Wing NR. 1994. *Permanent Isolation Surface Barrier Development Plan*. WHC-EP-0673, Westinghouse Hanford Company, Richland, Washington.

Wing NR and GW Gee. 1994. "The Permanent Isolation Surface Barrier Program at the Hanford Site." pp. 427-440. In *33rd Hanford Science Symposium on In-Situ Remediation*, GW Gee and NR Wing (eds.). Battelle Press, Columbus, Ohio.

Wittreich CD, JK Linville, GW Gee, and AL Ward. 2003. *200-BP-1 Prototype Hanford Barrier Annual Monitoring Report for Fiscal Year 2002*. CP-14873, Rev. 0, Fluor Hanford, Inc., Richland, Washington.

Appendix B

Recharge Estimates Using Environmental Tracers at the Integrated Disposal Facility (IDF) Site

Appendix B

Recharge Estimates Using Environmental Tracers at the Integrated Disposal Facility (IDF) Site

MJ Fayer, JE Szecsody, and CW Lindenmeier

B.1 Introduction

CH2M HILL Hanford Group, Inc., (CH2M HILL) is designing and assessing the performance of a near-surface disposal facility at Hanford for radioactive and hazardous wastes. The CH2M HILL effort to assess the performance of this disposal facility is known as the Integrated Disposal Facility (IDF) Performance Assessment (PA), hereafter called the IDF PA activity. One of the requirements of the IDF PA activity is to estimate the fluxes of water moving through the sediments within the vadose zone around and beneath the disposal facility. These fluxes, loosely called recharge rates, are the primary mechanism for transporting contaminants to the groundwater (Mann et al. 2001).

Pacific Northwest National Laboratory (PNNL) assists CH2M HILL in their performance assessment activities. One of the PNNL tasks is to provide estimates of recharge rates for current conditions and long-term scenarios involving disposal at the IDF location (Puigh and Mann 2002).

To support the analyses by Mann et al. (2001), Fayer et al. (1999) estimated recharge rates using a combination of lysimeter measurements, modeling, and tracer analyses. Several issues relating to the tracer analyses were identified, including a lack of information on the depth of evaporative drying, areal variability of chloride profiles, and the possibility of effects from the deposition of coal emissions.

Since 1999, the goals of the tracer task were to estimate recharge rates for scenarios pertinent to the IDF PA activity and to delineate the depth of long-term evapotranspiration at the IDF site. To provide data to support several of its tasks, the IDF PA activity drilled one borehole in 2001 and another one in 2002. Samples collected from these boreholes were analyzed for a variety of physical, hydraulic, and geochemical properties. This appendix summarizes the data most relevant to the tracer task: water content, chloride concentration, and deuterium and oxygen-18 ratios.

B.2 Tracer Techniques

For the immobilized low-activity waste (ILAW) 2001 PA, Fayer et al. (1999) used the chloride and chlorine-36 tracer techniques to estimate recharge rates. For the 2005 IDF PA, two tracer techniques were used: chloride mass balance (CMB) and deuterium and oxygen-18:

Chloride Mass Balance. The natural tracer method based on CMB is one of the simplest, least expensive, and most useful for determining recharge in arid climates (Allison et al. 1994). In this

approach, water entering the soil column contains meteoric chloride that is treated as an inert tracer. As water percolates downward through the root zone, evapotranspiration removes water, thus enriching the chloride concentration with depth through the root zone. This increase in chloride concentration quantitatively reflects the corresponding reduction in water flux from the infiltration flux to the deep drainage flux beneath the evapotranspiration zone. The CMB method is especially applicable to arid and semiarid regions where evapotranspirative enrichment of the pore water produces a distinct chloride profile in the unsaturated zone.

Application of the CMB method typically involves the following assumptions regarding transport: (1) flow is vertically and uniformly downward at constant water content and (2) the precipitation and accumulation rate of atmospheric chloride are steady over the relevant period. An additional assumption of steady state water flux throughout the column is often invoked, but as shown by Ginn and Murphy (1997) this assumption is not required in application of CMB. Recharge or net deep drainage flux is determined by the relationship

$$J_R = \left(\frac{Cl_o}{Cl_{sw}} \right) P \tag{B.1}$$

where J_R = net downward deep drainage flux (mm/yr)
Cl_o = average atmospheric chloride concentration in local precipitation and dry fallout (mg/L)
Cl_{sw} = average chloride concentration in the soil water (mg/L)
P = average annual precipitation (mm/yr).

Cl_o can be expressed as the total chloride mass deposited at ground surface q_{Cl} (mg $m^{-2}yr^{-1}$) divided by the precipitation. For the ILAW site, q_{Cl} was determined to be 38.4 mg/m^2/yr (Fayer et al. 1999). This value is consistent with previously reported values for the Central Plateau, which range from 32.7 to 49.4 mg/m^2/yr (Murphy et al. 1996). If the complete chloride profile is known, the chloride "age" at a specific depth can be determined as the total chloride above that depth divided by the chloride deposition rate.

Isotopic Tracers. The recharge rate is determined largely by the magnitude of transpiration and evaporation relative to precipitation and overland flow that has infiltrated the soil. Transpiration is the process whereby plants extract water from soil and transmit it to the atmosphere. Evaporation is the flux of water vapor that moves from the soil surface to the atmosphere. Because water consists of several isotopes of hydrogen and oxygen, each with slightly different atomic weights, evaporation tends to remove the lighter isotopes preferentially. The net result is that the residual water contains a higher proportion of the heavier isotopes. Moving down from the soil surface, there is a progressive decrease in the proportion of heavy stable isotopes because evaporation is less and because of mixing with infiltrating water. At some depth, the isotopic profile becomes somewhat uniform; this depth represents the vertical extent of significant water vapor flux. The amount of enrichment (relative to the isotopic signature in precipitation) is suggestive of the recharge rate.

Oxygen-18 and deuterium are the two isotopes of interest because they are stable (and benign) and because they occur in measurable quantities. The oxygen-18 and deuterium ratios ($R = {}^{18}O/{}^{16}O$; $R = {}^{2}H/{}^{1}H$) are used to express isotopic composition in delta (δ) units relative to a standard material as follows:

$$\delta = \left[\frac{R_{Sample}}{R_{Standard}} - 1 \right] \times 1000 \qquad \text{(B.2)}$$

where δ is reported in permil units (‰; a δ value of 10‰ is equivalent to 1%). Typical values for winter precipitation (the primary source of recharge water) are –19 to –16‰ for $\delta^{18}O$ and –142 to –120‰ for $\delta^{2}H$ (Singleton et al. 2004).

The U.S. Geological Survey conducted a study at Beatty, Nevada, that showed heavy isotope enrichment to a depth of 20 m (Prudic et al. 1997). In contrast, Barnes and Allison (1988) and Barnes et al. (1989) showed enrichment to a depth of 3 to 4 m at two sites in New Mexico. The actual depth of enrichment will depend on several factors, including recharge rate, soil properties, meteorological conditions, and the average annual temperature.

Murphy et al. (1991) described how deuterium and oxygen-18 could be used to understand recharge rates at the Hanford Site. There have been no measurements of these tracers at the IDF site, but a separate unrelated project used these tracers at a tank farm in the 200 West Area. DePaolo et al. (2004) used deuterium/oxygen-18 to infer a long-term recharge rate of 10 mm/yr in a disturbed area mapped as Rupert sand.

The Hanford Site receives about 65% more precipitation than the Beatty site (Prudic et al. 1997). A significant fraction of the precipitation received at Hanford is returned to the atmosphere by transpiration from the plant community, a process that does not enrich the soil water. Beatty, in contrast, has an extremely sparse plant cover. Thus, most of the precipitation is lost via evaporation, leading to greater enrichment. Beatty also has a significantly warmer average temperature (approximately 4°C), which further increases enrichment. Taken together, the lower evaporation and lower temperatures at Hanford relative to Beatty suggest the depth of enrichment at the IDF site should be less than the 20-m depth observed at the Beatty site.

B.3 Site Description

The IDF site is located on the south side of the Cold Creek bar, a depositional bar left in the lee of the Umtanum Ridge during Pleistocene cataclysmic flooding. This bar is dominated by gravel on the north side (closest to the main flood channels) grading to fine sand on the south side. Figure B.1 shows that a long, stabilized dune occupies the southern end of the IDF site. The presence of the dune at the IDF site indicates a history of sand dune activity in this area following the last cataclysmic flood (~13,000 years ago). The dune represents the northern fringe of a large dune field that exists below and south of the Central Plateau. The dune is stabilized by a very healthy stand of shrub-steppe vegetation and is not actively growing or migrating (the dune will eventually be removed during construction of the IDF). The

nearest active dune to the IDF site is approximately 3 km south of this area (Gaylord and Stetler 1994). Chapter 3 of this recharge data package describes the geologic setting in more detail.

Figure B.1. Aerial View of the Integrated Disposal Facility Site (outlined by white rectangle) in the 200 East Area of the Hanford Site. Viewing direction is southeast. Inactive coal-fired power plant is in the foreground. Water purification plant is to the right.

B.4 Borehole Descriptions

Table B.1 lists the boreholes and auger holes that have been drilled in and around the IDF site to collect sediment samples for tracer analyses. Figure B.2 shows the location of each borehole. Fayer et al. (1999) discussed the results from analyses conducted prior to 1999. This report addresses data collected in 2001 and 2002.

In 2001, borehole 299-E24-21 was drilled at the northeast corner of the IDF site. Loose samples (i.e., those not contained within a core liner) were collected every 1.5 m between 0 and 13.7 m and continuous core was collected between 13.7 and 77.7 m. A total of 9 loose samples and 30 discrete core samples were analyzed for water content and chloride (Horton et al. 2003).

In 2002, borehole 299-E17-21 (C3826) was drilled east of the midpoint of the IDF site (Reidel 2004). The borehole was drilled adjacent to crib 216-A-45, just south of the PUREX plant. Three other boreholes (C3827, C3828, and C3829) were drilled at the same time on the shoulder of 1st Avenue, which parallels Route 4 where it runs along the southern boundary of the 200 East Area. These three boreholes

were in an area that was graded in the early years of Hanford and were essentially sited near or in the drainage ditch that lies along the road. Samples from these boreholes were not analyzed because the tracer profile in each borehole had the potential to be significantly affected by runoff from the road.

Table B.1. Sampling Locations and Dates for Immobilized Low-Activity Waste Tracer Studies

Borehole ID	Local ID	Northing	Easting	Drilling Start Date
299-E24-161	NA	N135378	E574651	March 1995
299-E24-162	NA	N135344	E574651	March 1995
NA	Plains Trench			1995
299-E17-21	B8500	N134894.21	E574107.02	April 6, 1998
NA	B8501	N134924.68	E574107.02	April 24, 1998
NA	B8502	N134894.21	E574137.48	April 27, 1998
NA	B8503	N134909	E574127	~May 1998
299-24-21	**C3177**	**N135698.20**	**E574635.76**	**2001**
299-17-22	**C3826**	**N135195.92**	**E574841.07**	**2002**
NA	**Hand Auger No. 1**	**~ N135208**	**~E574841**	**2002**
NA	**Hand Auger No. 2**	**~N135423**	**~E574179**	**2002**
Bolded items are discussed in detail in this Appendix; non-bolded items were discussed by Fayer et al. (1999). NA = Not assigned.				

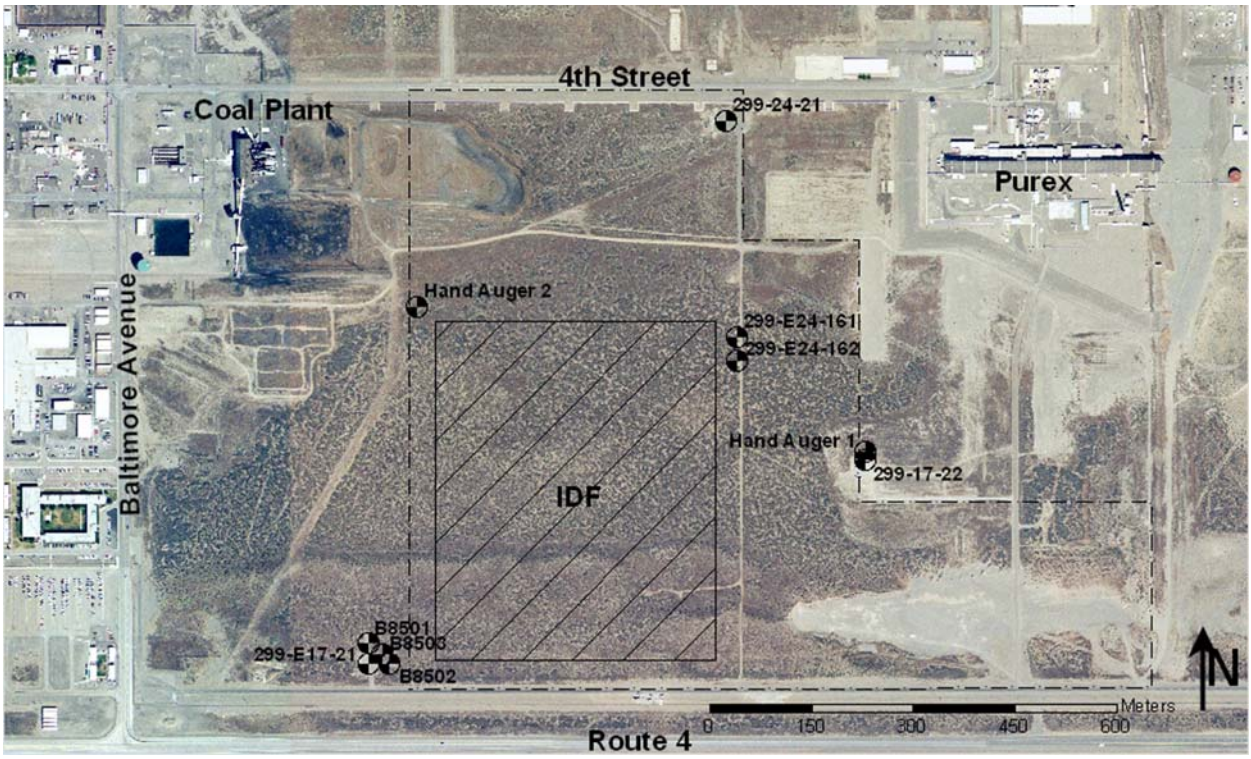

Figure B.2. Layout of the Integrated Disposal Facility Showing Borehole Locations

There was some concern that construction and operation of the nearby crib, in which fluids were discharged at the 13.7-m depth, might affect the tracer profile in C3826. To address the surface disturbance that occurred during crib construction, samples were not collected in the top 3 m. Instead, a second borehole was installed about 11.6 m north of C3826, within an area that had a native shrub-steppe plant community (i.e., an area that appeared to be undisturbed by construction). Sediment samples were collected to a depth of 3 m from this borehole. As for the effects of crib operations, any significant change in stable isotope ratios is expected to occur at a depth shallower than the 13.7-m disposal depth; therefore, the crib location is assumed to create no impact.

Concurrent with the drilling activity in 2002, a second shallow borehole was augered close to the northwest corner of the IDF site. Sediment samples were collected down to a depth of 1.8 m.

In addition to the sediment samples, groundwater samples were obtained from three boreholes (C3826, C3827, and C3829). These water samples were analyzed for deuterium and oxygen-18.

B.5 Methods

All samples were analyzed for water content and anions (including chloride). In addition, the samples from borehole C3826 were analyzed for deuterium and oxygen-18.

B.5.1 Sample Handling and Storage

In general, all samples were sealed once retrieved from the borehole. The sealed samples were brought to the laboratory and stored in a refrigerator to minimize evaporation before analysis. The samples collected in 2002 required special handling to prevent evaporation that might distort the isotopic content of the samples. Drilling of borehole C3826 yielded 89 undisturbed cores in lexan liners. Once each core reached the soil surface, the liner ends were packed, capped, and taped to retain and preserve the undisturbed sample and prevent evaporation of sample moisture (which would alter the isotopic ratio of the sediment water). A subset of the 89 cores was chosen to obtain the greatest coverage near the surface and around the expected depth of maximum enrichment (6 to 11 m). The total amount of material needed for isotopic and anion analyses and moisture content was 650 g, or a 5-cm length of the 10.2-cm diameter core. Because there may have been some evaporation near the ends of cores, at each sample location, a 5-cm length of core was removed and set aside, then the next 5 cm of core material were removed and placed into high-density polyethylene bottles and capped. Slightly drier sediment was observed near the end of cores, as well as a 1-2 mm rind along the inside of the lexan liner. The initial 5 cm of sediment removed from each liner was then placed back into the liner, and the liner was recapped. The sealed cores were then placed into a refrigerator.

The 2002 sediment samples were analyzed for water content and pore water concentrations of the oxygen isotopic ratio $^{18}O/^{16}O$, the hydrogen isotopic ratio $^{2}H/^{1}H$, and a suite of anions.

B.5.2 Moisture Content

The 50-g sediment sample was used to determine the water content of the sediment (standard PNNL laboratory procedures), then used for anion analysis, as described in the following section.

B.5.3 Anion Analysis

The soluble inorganic anions were determined using a one-to-one (1:1) sediment to de-ionized water extract method. This method was chosen because the sediments were too dry to extract vadose zone pore water easily. The extracts were prepared by adding an equal weight of de-ionized water to approximately 50 g of sediment sub-sampled from each sleeve. The amount of de-ionized water needed was calculated based on the weight of the samples and their previously determined moisture contents. The appropriate amount of de-ionized water was added to screw-cap jars containing the sediment samples. The jars were sealed and briefly shaken by hand, then placed on a mechanical orbital shaker for 1 hour. The samples were allowed to settle until the supernatant liquid was fairly clear. The supernatant was carefully decanted and separated into unfiltered aliquots for conductivity and pH determinations, and 0.45 μm-filtered aliquots for anion analyses.

The 1:1 sediment to water extracts were analyzed for anions using an ion chromatograph. Chloride, sulfate, and bromide were separated on a Dionex AS4A column with an eluent of 1.75 mM $NaHCO_3$/ 1.85 mM Na_2CO_3 with an NaOH gradient and measured using a conductivity detector following the standard PNNL laboratory procedure, which is based on U.S. Environmental Protection Agency (EPA) Method 300.0A.

B.5.4 Isotope Analysis

Extraction of water from soil for stable isotopic analysis ($^2H/^1H$, $^{18}O/^{16}O$) was conducted by azeotropic distillation per University of Waterloo Technical Procedure 3.0, Revision 03. The procedure involved the addition of toluene to the low-water content soil, then distillation at 70°C to remove all of the water, with condensation by liquid nitrogen (-210°C) to ensure trapping all of the water with no isotopic fractionation. The addition of toluene results in a lower distillation temperature (i.e., a water/ toluene azeotrope with lower boiling point is formed). This extraction process should remove within ±0.3% of the water within a sediment sample, based on moisture content measurements. Several test samples were submitted, each consisting of dry sediment to which water with a known isotopic composition is added. Isotopic analysis of the extracted water was within ±3.0‰ (parts per thousand) for $^2H/^1H$, ±0.3‰ for $^{18}O/^{16}O$ for these test samples. The University of Waterloo laboratory determined the moisture content of the samples, which was compared with the water content determined from separate samples (used for anion analysis).

Oxygen Isotopes, $^{18}O/^{16}O$ Ratio. Measured the $^{18}O/^{16}O$ ratio in water relative to a standard per University of Waterloo Technical Procedure 13.0, Revision 02. The precision and accuracy of $^{18}O/^{16}O$ ratio measurement was 0.2 parts per thousand or better. With each set of samples run, an isotopic standard water was additionally measured at least 5 times with an average measured value within 0.2 parts per thousand of the published standard value. Replicate analysis for 10% of samples were conducted. Oxygen isotope values are reported as deviation from standard meteoric ocean water (SMOW) in parts per thousand ($\delta^{18}O$).

Hydrogen Isotopes, $^2H/^1H$ Ratio. Measured the $^2H/^1H$ ratio in water relative to a standard per University of Waterloo Technical Procedure 4.0, Revision 02. The precision and accuracy of the $^2H/^1H$

ratio measurement is 3.0 parts per thousand or better. With each set of samples analyzed, an isotopic standard water was additionally measured at least 5 times with an average measured value within 3.0 parts per thousand of the published standard value. Replicate analyses for 10% of the samples were conducted. Hydrogen isotope values are reported as deviation from SMOW in parts per thousand (δ^2H).

A total of 32 sediment samples and 3 water samples were submitted to the Environmental Isotope Laboratory at the University of Waterloo for stable isotope analysis (deuterium; oxygen-18). Splits of the same sediment samples were also submitted to a PNNL analytical laboratory for anion analysis. Complementary to these activities, subsamples of the core material were provided to Mike Singleton, who is a researcher from Lawrence Berkeley National Laboratory (LBNL) working on an unrelated project at Hanford. As part of their project, LBNL analyzed the subsamples for deuterium, oxygen-18, and strontium isotopes. The LBNL results were not required by the IDF project, but will provide confirmatory information.

B.5.5 Presence of Radioactive Contamination

As described earlier, subsamples of each sediment sample were sent to the University of Waterloo and LBNL for isotopic analyses and to the PNNL geochemistry laboratory for anion analyses. Each core was monitored for radioactivity contamination in the field and no contamination was found. However, to be certain the samples contained no unusual radioactivity before they were distributed for analyses, an additional trace analysis was conducted to detect radioactive isotopes. Two composite samples were prepared: (a) 1 g from each of the 20 sediment samples from well C3826 and the 7 sediment samples from hand auger borehole #1, and (b) 1 g from each of the 5 sediment samples from hand auger borehole #2 (within the IDF trench 1 location). A 1:1 ratio of sediment and deionized water was then mixed on a slow rotary mixer for 24 h to extract some radionuclides (if any) into solution. A 1.0-mL water sample was then mixed with 4.5 mL of scintillation fluid and samples were counted for 20 minutes over a broad spectrum (0 to 2000 keV), which covers nearly all isotopes. A background sample (deionized water only) was also counted.

The results of the test for possible sample contamination were:

a) background sample, 26.95 counts per minute (CPM)

b) C3826 location, 22.10 CPM

c) IDF trench location, 21.85 CPM

Given that the sediment extract samples were equal to or lower than the background, no radioactive contamination was detected by this method.

B.6 Results

This section discusses the results of the two tracer techniques used at the IDF site to estimate recharge rates.

B.6.1 Water Content

Tables B.2 and B.3 show that the water contents were very dry and fairly typical of values measured in the vadose zone at other IDF locations (Fayer et al. 1999). The average value for C3177 was 0.022 g/g (range = 0.005 to as high as 0.065 g/g). The average value for C3826 was 0.019 g/g (range = 0.012 to 0.039 g/g). The C3177 site was disturbed decades ago and had only marginal plant cover ever since. The C3826 site has not had shrubs since approximately 1987. With the absence of shrubs from these sites many years ago, somewhat higher water contents was expected. However, deep-rooted annual plants such as tumblemustard and tumbleweed may have been sufficient to limit recharge.

B.6.2 Chloride Mass Balance

Figure B.3 shows that the chloride profiles for C3177 and C3826 are similar but not identical. C3177 shows a distinct chloride peak with a high value of 2,000 mg/L and a depth range between 6 and 14 m, which is well below the expected zone of evapotranspiration. As mentioned above, the site was disturbed years ago, so one possibility may be that recharge rates increased after the disturbance and moved the chloride down. C3826 shows a much shallower chloride peak located between 2 and 5 m with a maximum concentration of 1,800 mg/L. This site may not have been disturbed as long ago as C3177, in which case the chloride peak was not expected to be as deep in the profile.

One of the concerns with using the tracer technique at the IDF site is the possibility of chloride contamination from the nearby coal-fired power plant (which is now dormant). Fayer et al. (1999) avoided this concern by only using the chloride data below the chloride peak, depths at which drainage during the last 60 years should not have reached. With this approach, they estimated rates ranging from 0.16 to 1.8 mm/yr for various locations, yielding an average rate of 0.9 mm/yr. The same approach was applied to C3177 and C3826. The average chloride concentration in the 13.7- to 26.2-m depth range in C3177 was 162 mg/L. The average chloride concentration in the depth range 15.2 to 30.1 m in C3826 was 0.62 mg/L.

Using Equation B.1 and the deposition rate of 38.4 $mg/m^2/yr$, recharge rates were estimated to be 0.24 mm/yr in C3177 and 0.62 in C3826. Both of these rates are comparable with earlier chloride-derived rate estimates; both are below the average rate of 0.9 mm/yr recommended by Fayer et al. (1999) and used in the ILAW 2001 PA (Mann et al. 2001).

The tracer data reported by Fayer et al. (1999) has sufficient depth resolution to allow calculation of chloride age as a function of depth assuming that the deposition rate was constant at 38.4 $mg/m^2/yr$. The amount of chloride detected between the surface and the 4-m depth suggested ages ranging from 750 to 2,400 years for the B8501-B8503 boreholes and 4,900 to 5,700 years for the 161/162 boreholes. Borehole E17-21 had good depth resolution below 2.7 m but had no samples above 2.7m. Even so, the data suggested an age in excess of 2,700 years. The recent boreholes (C3177 and C3826) did not have sufficient depth resolution to make an age determination. However, the chloride profile in C3177 suggested an age significantly less than 750 years and the chloride profile in C3826 suggested an age greater than 4,000 years.

Table B.2. Sample Identification and Depth, Water Contents, and Chloride Concentrations for Sediment Samples Collected from Borehole 299-E24-21 (C3177) in 2001 (adapted from Horton et al. 2003)

Sample ID	Sample Depth (m)	Gravimetric Water Content (g/g)	Chloride Concentration in Pore Water (mg/L)
C3177-5	1.52	0.036	95.1
C3177-10	3.05	0.037	160.3
C3177-15	4.57	0.036	199.9
C3177-20	6.10	0.064	399.7
C3177-25	7.62	0.005	1155.9
C3177-30	9.14	0.006	1996.4
C3177-35	10.67	0.012	1150.9
C3177-40	12.19	0.007	1934.9
C3177-45	13.72	0.006	571.2
C3177 CS-45T	13.72	0.018	204.0
C3177 CS-47T	14.33	0.019	160.7
C3177 CS-47B	14.33	0.015	115.2
C3177 CS-49B	14.94	0.022	80.0
C3177 CS-50	15.24	0.018	143.0
C3177 CS-50T	15.24	0.031	131.0
C3177 CS-51B	15.54	0.019	95.4
C3177 CS-60	18.29	0.005	733.6
C3177_CS-65T	19.81	0.021	85.9
C3177 CS-67B	20.42	0.023	64.8
C3177 CS-85T	25.91	0.020	63.3
C3177 CS-86B	26.21	0.018	67.8
C3177 CS-110T	33.53	0.063	110.0
C3177 CS-111B	33.83	0.018	286.1
C3177 CS-130T	39.62	0.047	47.2
C3177 CS-131B	39.93	0.024	46.8
C3177 CS-150T	45.72	0.023	33.7
C3177 CS-151B	46.02	0.019	44.9
C3177 CS-180T	54.86	0.017	32.1
C3177 CS-181B	55.17	0.025	16.6
C3177 CS-200T	60.96	0.025	50.2
C3177 CS-201B	61.26	0.021	24.0
C3177 CS-215T	65.53	0.015	101.3
C3177 CS-216B	65.84	0.016	105.6
C3177 CS-230T	70.10	0.011	128.7
C3177 CS-231B	70.41	0.017	85.4
C3177 CS-251T	76.50	0.021	28.7
C3177 CS-252B	76.81	0.026	27.9
C3177 CS-253T	77.11	0.011	144.8
C3177 CS-255B	77.72	0.022	38.8

Table B.3. Sample Identification and Depth, Water Contents, and Chloride Concentrations for Sediment Samples Collected from Borehole 299-E17-21 (C3826) in 2002

Sample ID	Borehole	Core Liner Depth (m)		Subsample Location (m)		Gravimetric Water Content (g/g)	Chloride Concentration in Pore Water (mg/L)
		Top	Bottom	Top	Bottom		
ILAW9	C3826	2.74	3.05	2.74	2.83	0.0387	1768.3
ILAW 11	C3826	3.05	3.35	3.29	3.35	0.0232	1917.1
ILAW 11 dup	C3826	3.05	3.35	3.29	3.35	NA	1784.1
ILAW14	C3826	3.96	4.27	4.21	4.27	0.0214	808.1
ILAW160	C3826	4.88	5.18	4.88	4.97	0.0209	1018.5
ILAW20	C3826	5.79	6.10	5.94	6.10	0.0152	100.7
ILAW26	C3826	7.62	7.92	7.77	7.86	0.0115	167.8
ILAW28	C3826	8.53	8.84	8.53	8.60	0.0138	113.6
ILAW33	C3826	9.91	10.21	10.00	10.09	0.0117	104.6
ILAW43	C3826	12.95	13.26	13.11	13.20	0.0139	162.2
ILAW50	C3826	14.94	15.24	15.12	15.21	0.0184	24.7
ILAW50 dup	C3826	14.94	15.24	15.12	15.21	NA	24.3
ILAW65	C3826	19.66	19.96	19.72	19.81	0.0207	95.8
ILAW78	C3826	23.62	23.93	23.77	23.87	0.0174	73.8
ILAW99	C3826	29.87	30.18	30.02	30.11	0.0175	89
ILAW122	C3826	36.88	37.19	37.09	37.19	0.0241	91.7
ILAW152	C3826	46.02	46.33	46.24	46.33	0.0160	36.6
ILAW182	C3826	55.47	55.78	55.47	55.57	0.0151	30
ILAW223	C3826	67.67	67.97	67.82	67.91	0.0185	33.4
ILAW223 dup	C3826	67.67	67.97	67.82	67.91	NA	35.4
ILAW0	Auger 1	NA	NA	0.00	0.15	0.0180	31.5
ILAW0 dup	Auger 1	NA	NA	0.00	0.15	NA	31.4
ILAW1	Auger 1	NA	NA	0.25	0.36	0.0378	6.8
ILAW2	Auger 1	NA	NA	0.51	0.61	0.0338	51.1
ILAW4	Auger 1	NA	NA	1.07	1.24	0.0616	34.1
ILAW6	Auger 1	NA	NA	1.78	1.88	0.0642	577.6
ILAW8	Auger 1	NA	NA	2.39	2.49	0.0216	1505.4
ILAW10	Auger 1	NA	NA	3.05	3.05	0.0264	930.4
ILAW0A	Auger 2	NA	NA	0.00	0.00	0.0387	15.9
ILAW1A	Auger 2	NA	NA	0.25	0.30	0.0331	5
ILAW2A	Auger 2	NA	NA	0.61	0.66	0.0366	2.2
ILAW4A	Auger 2	NA	NA	1.17	1.22	0.0410	12.4
ILAW6A	Auger 2	NA	NA	1.83	1.83	0.0245	121.1
ILAW6A dup	Auger 2	NA	NA	1.83	1.83	NA	116.3

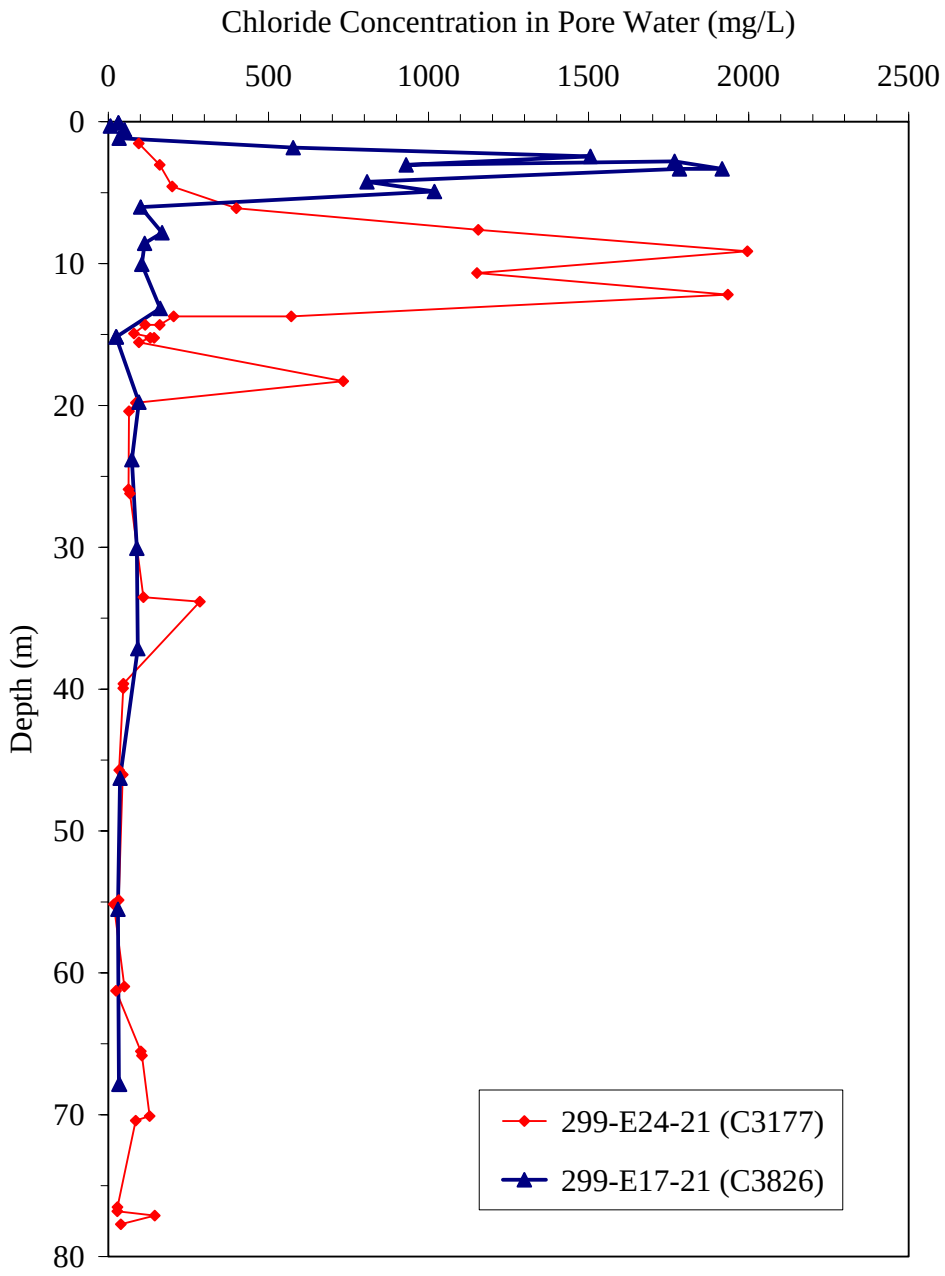

Figure B.3. Depth Profiles of Chloride Concentrations from Boreholes C3177 and C3826

Section 3.3 of this report described the soils at the IDF as not being easily classified into either Burbank loamy sand or Rupert sand and suggested the soils be evaluated as a continuum of a single soil. To that end, Table B.4 summarizes all of the chloride data collected at the IDF since 1995. Shown in the first three data columns are peak chloride concentrations and the associated recharge estimates. Note that the estimates are very low and range from only 0.02 to 0.05 mm/yr. Note also that the peak values occur fairly deep in some boreholes, suggesting that rates may have increased recently and moved the chloride deeper into the profile. The next three data columns are the deep chloride concentrations and the

associated recharge estimates. The rates are higher, ranging from 0.05 to 2.11 mm/yr and averaging 0.75 mm/yr. The data from B8503 show very high chloride deeper than in any of the other nearby boreholes. B8503 was only drilled to 8.4 m, so it is unclear if the deepest data are within the peak or below the peak. Given the uncertainty, the data from this borehole could be excluded. If so, then the average of the remaining boreholes is 0.85 mm/yr, with a range of 0.16 to 2.11 mm/yr, a median of 0.71 mm/yr, and a standard deviation of 0.66 mm/yr.

Table B.4. Summary of Chloride Data Collected from Boreholes Associated with the Integrated Disposal Facility Performance Assessment Activity (Because sampling intervals varied borehole to borehole, depth-weighted concentrations were not used to determine chloride averages.)

Hanford Borehole ID (Local ID)	Soil Type Based on Hajek (1966)	Depth Range of Peak Cl (m)	Avg. Cl Within Peak Cl Range (mg/L)	Recharge Est. from Avg. Cl in Peak (mm/yr)	Depth Range Below Peak Cl (m)	Avg. Cl of Depth Range Below Peak (mg/L)	Recharge Est. from Avg. Cl Below Peak (mm/yr)
E24-161 (NA)	Burbank loamy sand	2.6 to 4.1	1503	0.03	5 to 15.1	240	0.16
E24-162 (NA)	Rupert sand	1.7 to 3.2	2285	0.02	10.3 to 17.4	54.2	0.71
E17-21 (B8500)	Rupert sand	< 4.2 to 4.2	1611	0.02	6.1 to 15.1	38.1	1.01
NA (B8501)[(a)]	Rupert sand	3.7 to 7.9	932	0.04	10.1 to 14.7	34.6	1.11
NA (B8502)	Rupert sand	3.4 to 6.3	747	0.05	8.3 to 13.3	18.2	2.11
NA (B8503)	Rupert sand	5.1 to 5.2	1066	0.04	5.7 to 8.4	704	0.05
E24-21 (C3177)	Burbank loamy sand	7.6 to 13.7	1362	0.03	13.7 to 26.2	162	0.24
E17-22 (C3826)	Rupert sand	1.8 to 4.9	1289	0.03	15.2 to 30.1	61.5	0.62
(a) B8501 had three distinct chloride peaks, but only the deepest was considered for the peak-derived recharge rate.							

Besides simple averaging, other methods exist for coalescing the recharge estimates into a single value. For example, some of the boreholes are close together and could be combined into a localized single value to reduce their weighting on the recharge estimate. The average for the B8500-B8503 boreholes is 1.07 mm/yr. The average for E24-161 and E24-162 is 0.43. Treating these as single values and averaging them with the estimates for C1377 and C3826 yields an overall average of 0.59 mm/yr.

Another method is to ignore the B8500-B8503 data. These boreholes are associated with the sand dune on the southern edge of the IDF site. The sand dune will not exist once the IDF is completed, so data from these boreholes may bias the recharge estimate. Without these boreholes, the overall average recharge rate is 0.43 mm/yr.

Although both of the above methods may seem reasonable and rational, the limited number of boreholes argues that the best approach is to use simple averaging of all boreholes except B8503. The

rationale for using this method is that the soil conditions that will surround the IDF surface barrier are unknown at this time. Therefore, for the 2005 PA, the recommended recharge rate estimate for soil at the IDF is 0.9 mm/yr (rounded up from 0.85 mm/yr). The value of 0.9 mm/yr is fortuitous because it is the value used to represent Rupert sand in the 2001 PA. This value is lower than the 4.2 mm/yr used for Burbank loamy sand.

B.6.3 Deuterium and Oxygen-18 Isotopes

Isotope data from the University of Waterloo and the supplemental analysis by Lawrence Berkeley National Laboratory (LBNL) were analyzed together. The data include the samples from borehole C3826, the shallow samples from the two hand-augered boreholes, and the groundwater samples.

Figure B.4 shows the isotope data for the entire vadose zone; Figure B.5 shows the same data for the uppermost 10 m only.

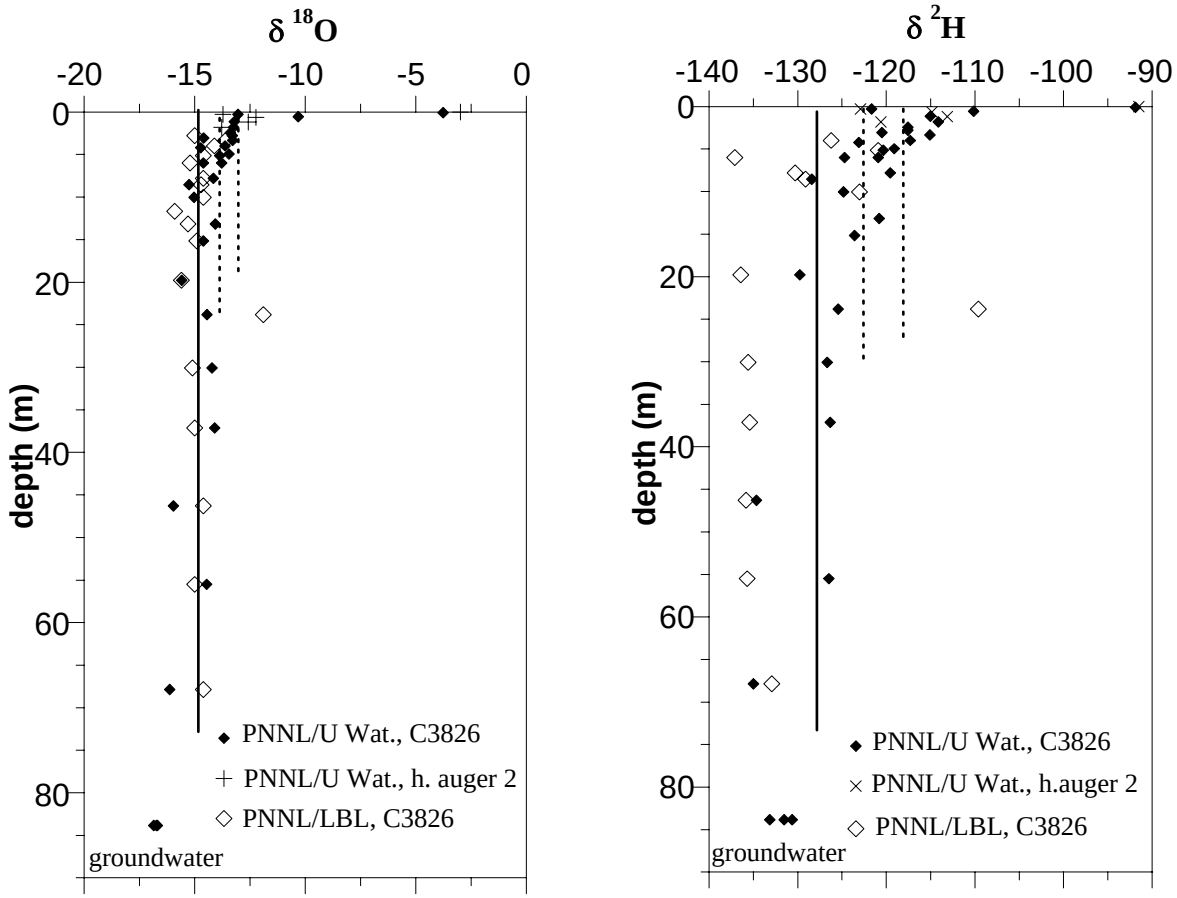

Figure B.4. Water Stable Isotope Data Extracted from Pore Water in Sediment from the C3826 Borehole and Auger Holes. (a) $\delta^{18}O$ profile with depth to groundwater and (b) $\delta^{2}H$ profile with depth to groundwater.

The groundwater (three water wells) averaged -16.85‰ $\delta^{18}O$ and -132‰ $\delta^{2}H$. Water in the deep vadose zone (<15 m) averaged -14.75 ± 0.86‰ $\delta^{18}O$ and -126.7 ± 4.5‰ $\delta^{2}H$ (solid lines in Figures B.4 and B.5), or slightly heavier than groundwater. The heavier isotopic composition of the vadose could imply that water is still evaporating at this extreme depth (i.e., 15 to 76 m), but this is highly unlikely. It is more likely that the isotopic composition of the groundwater at this location is controlled by recharge processes upgradient of the IDF site, such as has been previously hypothesized and confirmed by geochemical and stable isotopic profiles within groundwater wells near the Rattlesnake Mountain foothills.

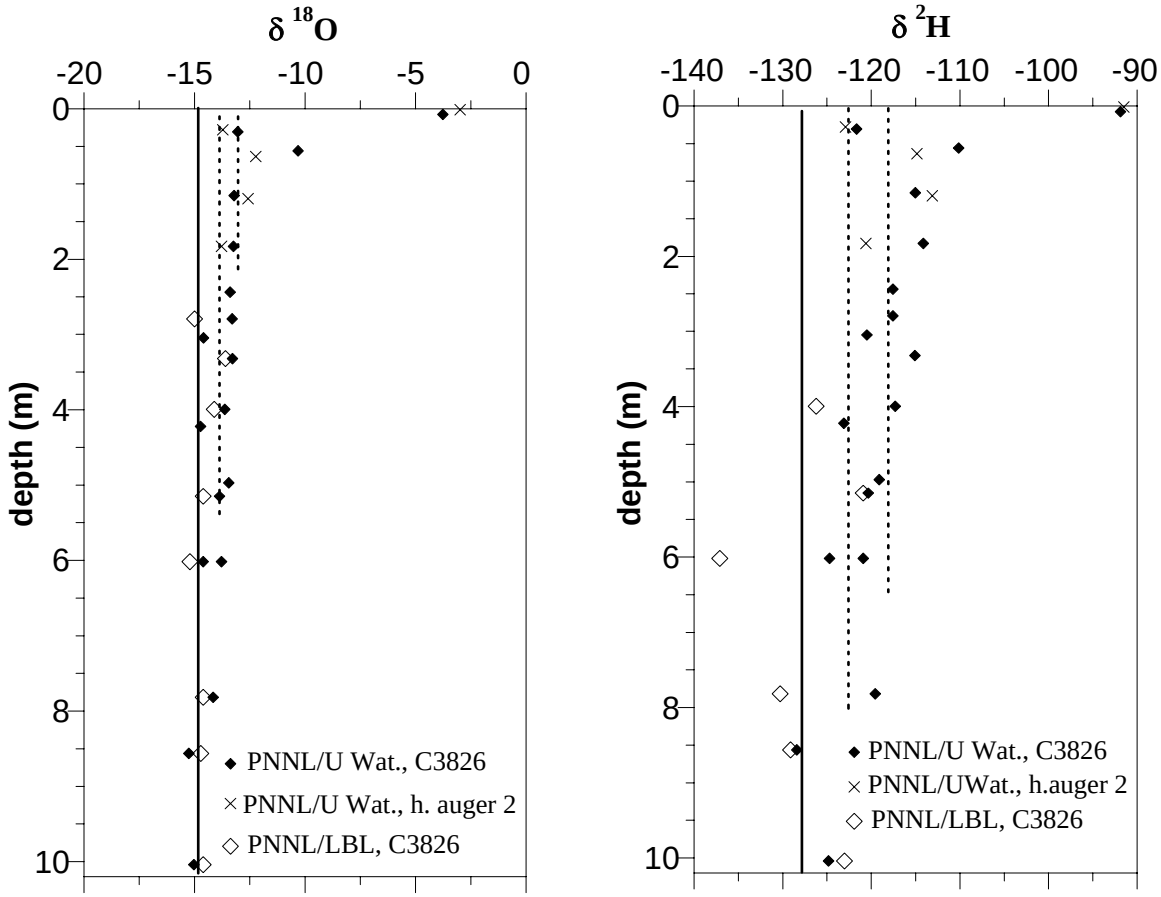

Figure B.5. Water Stable Isotope Data Extracted from Pore Water in Sediment from the C3826 Borehole and Auger Holes. (a) Oxygen 18/16 profile with depth to groundwater, and (b) deuterium profile with depth to groundwater.

Pore water in the shallow vadose zone (i.e., <15 m) shows a dramatic increase in heavy isotopes near the soil surface, which is consistent with a classic profile created by evaporation. The variability of the deep isotope profile is indicated by the standard deviations (±0.86‰ $\delta^{18}O$ and ±4.5‰ $\delta^{2}H$). An "increase" in the isotopic signature is indicated by a statistically significant departure from the deep isotope profile. One and two standard deviation increases from the deep isotope profile are shown in Figures B.4 and B.5 (dashed lines) and indicate statistical significance at the 66% (1 standard deviation)

and 95% confidence intervals. The stable isotope profiles of all of PNNL and LBNL data at shallow depth (Figure B.5) show statistical departure from the deep isotope profile at a 3.7-m depth ($\delta^{18}O$) and 5.2-m depth ($\delta^{2}H$) at an 80% confidence interval (roughly 1.5 standard deviations). This implies that evaporation and vapor transport extends to this 3.7- to 5.2-m depth at this site.

There was no significant difference between the profile taken at the C3826 borehole and the hand auger No. 2 samples taken at the northwest corner of the IDF. This result suggests the two sites share a similar recharge pattern, even though the C3826 borehole location had been cleared of brush for years so may exhibit more recent increased infiltration.

The amount of departure of the surface stable isotope signature from the deep vadose zone can be used to estimate the amount of recharge. Models are typically used to simulate the isotope profile that would result, based on additional data such as the temperature, temperature variability over seasons, and soil texture properties. An empirical relationship between isotopic departure and recharge, based on this type of modeling and field data (Barnes and Allison 1989) was used in this case to estimate recharge. The $\delta^{18}O$ data indicated a maximum enrichment of 11.4‰ $\delta^{18}O$, and the $\delta^{2}H$ data indicated a maximum enrichment of 34.8‰ $\delta^{2}H$ relative to the deep vadose zone values. This provides a crude estimate of 1.3 mm/yr of annual recharge (0.8% of the average annual precipitation), which is comparable with estimates using the chloride method.

Figure B.6 shows $\delta^{18}O$ versus $\delta^{2}H$, which indicates evaporation of samples relative to the worldwide atmospheric isotopic composition ("meteoric water"). The IDF samples produced a relatively good slope ($r = 0.933$) of 3.37, significantly less than the slope of 8.0 for meteoric water. Other comparisons are a slope of 5.80 (Dixie Valley, Nevada; arid environment, snow samples) and 6.03 (Eagle Valley, Nevada; semi-arid environment, snow samples), indicating significant evaporation and isotopic fractionation of the samples, which is consistent with the evaporation calculation. The departure from meteoric water indicates that the source (i.e., precipitation) should have a composition of approximately -18‰ $\delta^{18}O$ and -135‰ $\delta^{2}H$. Precipitation collected at the Hanford site (Graham 1983) indicates precipitation in the Rattlesnake Hills area is as light as -141‰ $\delta^{2}H$ and -18.4‰ $\delta^{18}O$, consistent with the intersection of the evaporated soil water samples with the meteoric water line (Figure B.6).

Figure B.7 compares the isotopic analyses of LBNL and the University of Waterloo. The $\delta^{18}O$ results show no significant difference (average difference was 0.08‰) other than the single anomalously high value reported by LBNL at 21.9 m.

In contrast to the $\delta^{18}O$ results, the $\delta^{2}H$ results show a consistent difference. The average LBNL composition was 4.4‰ $\delta^{2}H$ lighter than the average University of Waterloo composition. Longer retention times for the University of Waterloo samples might have led to some evaporation of these samples (leaving the remaining water heavier isotopically; however, both the $\delta^{18}O$ and $\delta^{2}H$ data should have been affected.

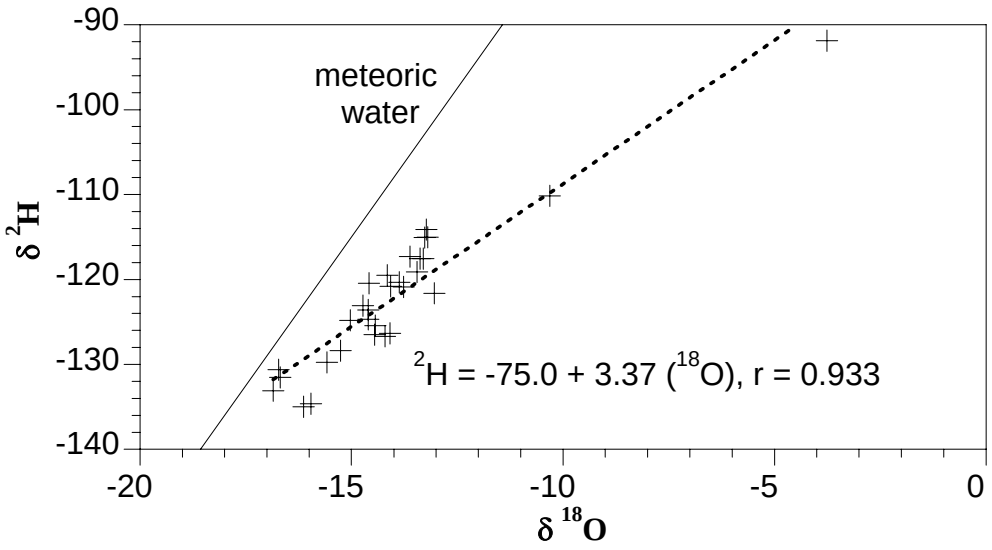

Figure B.6. Water Stable Isotope Data Extracted from Pore Water in Sediment from the C3826 Borehole and Auger Holes Relative to Meteoric Water

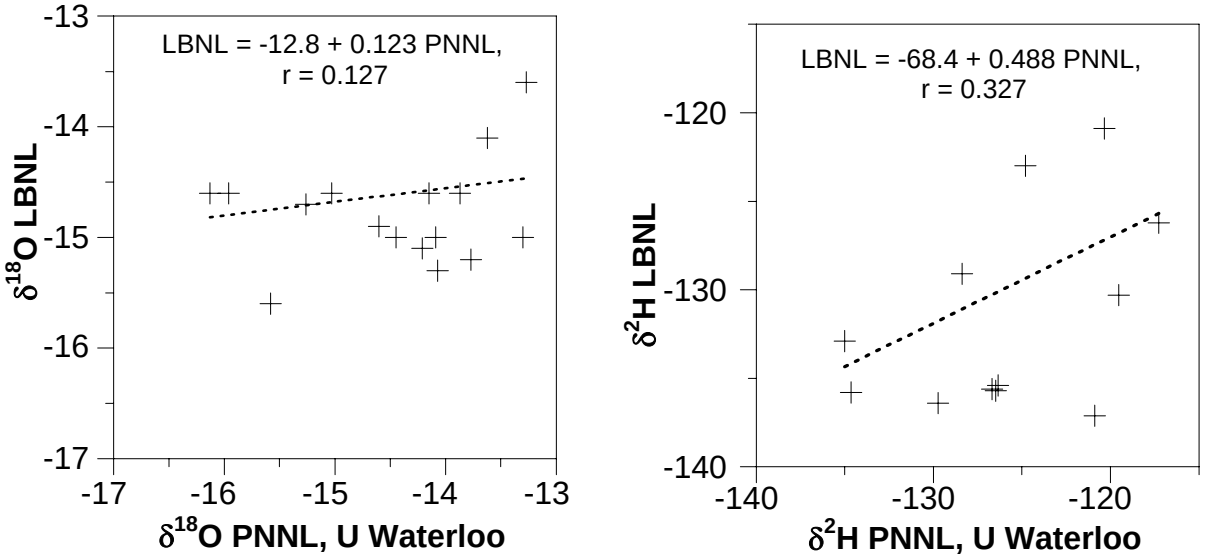

Figure B.7. Water Stable Isotope Data Extracted from Pore Water in Sediment from the C3826 Borehole and Auger Holes Relative to Meteoric Water

B.7 Conclusions

Vadose zone profiles of selected tracers were evaluated at two locations at the IDF site to estimate recharge rates and improve the understanding of recharge processes. Chloride profiles below 10 m show fairly low concentrations through much of the vadose zone. Average concentrations in the upper part of

the vadose zone suggested recharges rates of 0.35 mm/yr for C3177 and 0.47 mm/yr for C3826. Both values are in the range of values estimated previously and both are below the value of 0.9 mm/yr that was used to represent Rupert sand in the ILAW 2001 PA.

Deuterium and oxygen-18 profiles from C3826 suggested that the depth of evapotranspirative enrichment was 3.7 to 5.2 m. Numerical models of this site should use these depths as the minimum to represent the site accurately. The modeling studies conducted by Fayer et al. (1999) for the 2001 PA used a common soil depth of 4 m. While this depth of soil is certainly within the range of evapotranspiration depths estimated with tracers, simulations with deeper profiles ought to be evaluated to confirm the sensitivity.

B.8 References

Allison GB, GW Gee, and SW Tyler. 1994. "Vadose-Zone Techniques for Estimating Groundwater Recharge in Arid and Semiarid Regions." *Soil Sci. Soc. Am. J.* 58:6-14.

Barnes CJ and GB Allison. 1988. "Tracing of Water Movement in the Unsaturated Zone Using Stable Isotopes of Hydrogen and Oxygen." *J. Hydrol.* 100:143-176.

Barnes CJ, GB Allison, and MW Hughes. 1989. "Temperature Gradient Effects on Stable Isotope and Chloride Profiles in Dry Soils." *J. Hydrol*. 112:69-87.

DePaolo DJ, ME Conrad, K Maher, and GW Gee. 2004. "Evaporation Effects on Oxygen and Hydrogen Isotopes in Deep Vadose Zone Pore Fluids at Hanford, Washington." *Vadose Zone Journal* 3:220-232.

Fayer MJ, EM Murphy, JL Downs, FO Khan, CW Lindenmeier, and BN Bjornstad. 1999. *Recharge Data Package for the Immobilized Low-Activity Waste 2001 Performance Assessment.* PNNL-13033, Pacific Northwest National Laboratory, Richland, Washington.

Gaylord DR and LD Stetler. 1994. "Aeolian-Climatic Thresholds and Sand Dunes at the Hanford Site, South-Central Washington." *J. Arid Environ*. 28:95-116.

Ginn TR and EM Murphy. 1997. "A Transient Flux Model for Convective Infiltration: Forward and Inverse Solutions for Chloride Mass Balance Studies." *Water Resources Research* 33(9):2065-2079.

Graham DL. 1983. "Stable Isotopic Composition of Precipitation from the Rattlesnake Hills Area of South-Central Washington State." RHO-BW-ST-44P, Rockwell Hanford Operations, Richland, Washington.

Hajek BF. 1966. *Soil Survey Hanford Project in Benton County, Washington.* BNWL-243, Pacific Northwest Laboratory, Richland, Washington.

Horton DG, HT Schaef, RJ Serne, CF Brown, MM Valenta, TS Vickerman, IV Kutnyakov, SR Baum, KN Geiszler, and KE Parker. 2003. *Geochemistry of Samples from Borehole C3177 (299-E24-21).* PNNL-14289, Pacific Northwest National Laboratory, Richland, Washington.

Mann FM, KC Burgard, WR Root, RJ Puigh, SH Finfrock, R Khaleel, DH Bacon, EJ Freeman, BP McGrail, SK Wurstner, and PE Lamont. 2001. *Hanford Immobilized Low-Activity Waste Performance Assessment: 2001 Version*. DOE/ORP-2000-24, Rev. 0, U.S. Department of Energy, Office of River Protection, Richland, Washington.

Murphy EM, JE Szecsody, and SJ Phillips. 1991. *A Study Plan for Determining Recharge Rates at the Hanford Site Using Environmental Tracers*. PNL-7626, Pacific Northwest Laboratory, Richland, Washington.

Murphy EM, TR Ginn, and JL Phillips. 1996. "Geochemical Estimates of Paleorecharge in the Pasco Basin: Evaluation of the Chloride Mass-Balance Technique." *Water Resources Research* 32(9):2853-2868.

Prudic DE, DA Stonestrom, and RG Striegl. 1997. *Tritium, Deuterium, and Oxygen-18 in Water Collected from Unsaturated Sediments Near a Low-Level Radioactive-Waste Burial Site South of Beatty, Nevada*. Water Resources Investigation Report 97-4062, U.S. Geological Survey, Carson City, Nevada.

Puigh RJ and RM Mann. 2002. *Statement of Work for FY 2003 to 2008 for the Hanford Low-Activity Tank Waste Performance Assessment Program.* RPP-6702, Rev. 2, CH2M HILL Hanford Group, Inc., Richland, Washington.

Reidel SP. 2004. *Geologic Data Package for 2005 Integrated Disposal Facility Waste Performance Assessment*. PNNL-14586, Pacific Northwest National Laboratory, Richland, Washington.

Appendix C

Simulation Estimates of Recharge Rates for the Integrated Disposal Facility

Appendix C

Simulation Estimates of Recharge Rates for the Integrated Disposal Facility

MJ Fayer

C.1 Introduction

CH2M HILL Hanford Group, Inc. (CH2M HILL) is designing and assessing the performance of a near-surface disposal facility at Hanford for radioactive and hazardous waste. The CH2M HILL effort to assess the performance of this disposal facility is known as the Integrated Disposal Facility (IDF) Performance Assessment (PA), hereafter called the IDF PA activity. One of the requirements of the IDF PA activity is to estimate the fluxes of water moving through the sediment within the vadose zone around and beneath the disposal facility. These fluxes, loosely called recharge rates, are the primary mechanism for transporting contaminants to the groundwater (Mann et al. 2001).

Pacific Northwest National Laboratory (PNNL) assists CH2M HILL in their performance assessment activities. One of the PNNL tasks is to provide estimates of recharge rates for current conditions and long-term scenarios involving disposal at the IDF location. To support a previous PA analysis (the 2001 immobilized low-activity waste [ILAW] PA; Mann et al. 2001), Fayer et al. (1999) estimated recharge rates using a combination of lysimeter measurements, modeling, and tracer analyses.

The goal of the modeling analysis is to use a numerical recharge model to estimate recharge fluxes for scenarios pertinent to the PA for which data do not currently exist. Because of the long time periods involved, data do not exist for many of the scenarios. Therefore, the model is used to extend the observations and to estimate recharge rates for potential future scenarios.

Table C.1 shows the simulation results that supported the 2001 ILAW PA (Mann et al. 2001); those results are relevant to the 2005 IDF PA. This appendix summarizes the numerical modeling activities conducted to augment the results in Table C.1 for the 2005 IDF PA (Puigh and Mann 2002). First, some of the analyses in Table C.1 were updated using the six additional years of meteorological data that have been collected. Second, the model domain was deepened (per knowledge gained in Appendix B) to demonstrate the sensitivity to recharge. Third, the impact of variability on the silt loam hydraulic properties was evaluated. Finally, simulations were conducted to demonstrate the impact of hysteresis and heat flow.

Table C.1. Simulated Long-Term Drainage Rates Using the Isothermal, Non-Hysteretic Mode of UNSAT-H and a Shrub-Steppe Plant Community (unless noted otherwise) (adapted from Fayer et al. 1999)

Variable	Condition	Simulated Long-Term Drainage Rates (mm/yr)				
		Modified RCRA Subtitle C Barrier	Rupert Sand	Burbank Loamy Sand	Dune Sand on Barrier	Eroded Surface Barrier
Climate[a]	Current (1957 to 1997)	<0.1	2.2	5.2	<0.1	<0.1
	P↓	NA[b]	<0.1	NA	NA	NA
	P↑	NA	13.2	NA	NA	NA
	P↓T↑	NA	<0.1	NA	NA	NA
	P↓T↓	NA	<0.1	NA	NA	NA
	T↓	NA	7.5	NA	NA	NA
	T↑	NA	0.6	NA	NA	NA
	P↑T↑	NA	5.2	NA	NA	NA
	P↑T↓	<0.1	27.0	36.8	16.9	<0.1
Vegetation	Cheatgrass	NA	33.2	NA	18.4	NA
	No plants	<0.1	44.3	52.5	32.7	<0.1
	No plants, future climate (P↑T↓)	NA	88.6	98.0	NA	NA
Shrub Leaf Area Index	High (0.4 vs 0.25)	NA	1.6	NA	NA	NA
	Low (0.1 vs 0.25)	NA	5.6	15.2	4.1	NA
Rupert Sand Properties	Higher $K(h)$ vs Rupert sand	NA	2.7	NA	NA	NA
	Lower $K(h)$ vs Rupert sand	NA	3.3	NA	NA	NA
Complete Areal Plant Coverage	Cheatgrass	NA	26.6	NA	NA	NA
	Shrub	NA	<0.1	NA	NA	NA
Irrigation Efficiency	75%	26.4	58	NA	NA	NA
	100%	<0.1	30	NA	NA	NA

(a) Climate change was represented using changes in precipitation (P) and temperature (T). An increase is represented by ↑ and a decrease by ↓. The ranges were 50 to 128% of modern P and -2.5 to 2.8°C of modern T.
(b) NA = Not analyzed.

C.2 Methods

PNNL used the one-dimensional numerical model UNSAT-H to estimate recharge rates for the IDF. Two soil types (Rupert sand and Burbank loamy sand) and a relatively undisturbed shrub-steppe plant community cover the IDF. The elevation of most of the IDF ranges from 219 to 222 m. A surface barrier will cover the disposal site; the barrier will have a nominal 2% slope.

Based on this information, three scenarios were identified for simulation: the surface barrier, Rupert sand, and Burbank loamy sand. The purpose of the surface barrier is to store water and promote evapotranspiration rather than promote lateral flow. In addition, the side slope component of the barrier was

not evaluated here. Thus, the one-dimensional UNSAT-H model is appropriate. Two additional scenarios were included to address two types of surface barrier degradation. The simulation cases and associated model parameters are described in the following sections.

C.2.1 Simulation Cases

The same five scenarios used by Fayer et al. (1999) were used to demonstrate the response of recharge rates to a longer weather sequence and a deeper profile. The first three scenarios addressed functional disposal facility features: the proposed surface barrier and the two soil types found in the surrounding terrain. The fourth scenario addressed the impact of dune sand deposition on the surface barrier. The fifth scenario addressed the impact of erosion of a portion of the surface barrier. All five scenarios were evaluated for current climate conditions.

C.2.2 Model Description

Simulations were conducted using the UNSAT-H computer code (Fayer 2000). UNSAT-H was accepted for use at Hanford via the Tri-Party Agreement process (DOE 1991). The IDF (formerly ILAW) project has used this code since 1995 specifically to calculate recharge rates.

The UNSAT-H code has been tested with lysimeter data. Fayer et al. (1992) and Martian (1994) compared predicted and measured water storage values for lysimeters at Hanford. Both found that calibration of several parameters improved the match of predicted to measured values as determined by the root-mean-square (RMS) error. For a 1.5-year test of a lysimeter receiving an enhanced precipitation treatment, Fayer et al. (1992) calculated a RMS error of 0.8 cm after calibration (versus 2.2 cm without calibration). Martian (1994) looked at a much longer time period (5.5 versus 1.5 years) and found the RMS error was higher—about 1.8 cm for the calibrated model. The analysis was not done for the uncalibrated model. Martian determined the correlation coefficient for the comparison of measured and simulated soil water storage was 0.94, which is quite good. Fayer and Gee (1997) extended the comparison to 6 years. The data were collected from a non-vegetated weighing lysimeter containing 150 cm of silt loam over sand and gravel. They found that the RMS error for water storage predictions was about 2.3 cm regardless of whether the model was calibrated or whether it included heat flow or hysteresis. Fayer and Gee (1997) extended the comparison to matric potential and drainage. They found that the simulation with hysteresis was far better at predicting matric potentials throughout the 6-year period, and it was the only simulation to predict drainage (52% of the measured amount, with timing that matched the observations).

Khire et al. (1997) tested UNSAT-H for simulating water movement in surface barrier test plots in a semiarid setting in Washington and a humid setting in Georgia. They tested the model using a 3-year record of data that included overland flow, soil water storage, evapotranspiration, and percolation. Time series plots of the data and predictions showed that UNSAT-H generally mimicked the seasonal trends.

Khire et al. (2000) used UNSAT-H to assess the performance of capillary barriers relative to layer thickness, unsaturated hydraulic properties, and climate at four sites in the United States. They concluded that barrier performance was sensitive to all three variables.

Scanlon et al. (2002) compared the ability of seven codes to simulate the performance of engineered barriers in Texas and Idaho. They reported that most of the codes, including UNSAT-H, reasonably reproduced the measured water balance components. They also reported that the weakest comparison was of runoff. As Section 3.0 of this report attests, surface runoff is a very minor element of the water balance at Hanford and, thus, should not preclude the use of UNSAT-H.

The UNSAT-H code has been used at the Hanford Site to estimate the areal distribution of recharge rates (Fayer et al. 1996). The code has also been used elsewhere to evaluate infiltration through surface barriers (Magnuson 1993) and surficial sediments (Martian and Magnuson 1994).

C.2.3 Model Domain and Discretization

The model domains used by Fayer et al. (1999) were used again for most simulations in this report. The exception was a set of simulations in which the domain sizes were increased. The results in Appendix B suggested that the evapotranspiration process affected water behavior at the IDF to a depth somewhere between 3.7 and 5.2 m. The model domains used by Fayer et al. (1999) were 1.3 m for the barrier and 4.0 m for the soils. Experience had suggested that these depths were sufficient to minimize any impact on the predicted recharge rate. To demonstrate the sensitivity to domain depth, the domains were deepened by 2 m. For the surface barrier, the depth was increased from 1.3 to 3.3 m. For the soils, the depth was increased from 4 to 6 m.

The node spacing in all simulations started at 0.2 cm at the soil surface and gradually increased with depth. At material interfaces, the node spacing was decreased to 2 cm. Changes in node spacing from node to node were limited to less than 50%. Time step sizes were allowed to range from 10^{-10} to 1 hour, depending on the mass balance error.

C.2.4 Soil Information

Soil hydraulic properties consist of the soil water retention function and the hydraulic conductivity model. Soil water retention was described with the van Genuchten function and hydraulic conductivity was described with the Mualem conductivity model. Three soil models were considered: modified RCRA Subtitle C Barrier, Rupert sand, and Burbank loamy sand. Table C.2 lists the parameters for the materials making up each soil model; these parameters are identical to those used by Fayer et al. (1999). Possible changes in soil hydraulic properties in response to soil development were not addressed.

The variability of silt loam hydraulic properties was represented using the sixteen parameter sets assembled by Gee et al. (1989). The parameter sets were developed using lab-measured water retention and hydraulic conductivity data using samples packed to a bulk density of 1.37 Mg/m^3. Table C.3 shows the parameter sets that were used for the simulations. The original θ_s, θ_r, and K_s parameters from Gee et al. (1989) were adjusted to account for the gravel that will be added (15% by wt.) to create the silt loam admix layer. The adjustment method was that of Bower and Rice (1983), which is the same method used by Fayer et al. (1999). Variability in the hydraulic properties of the other materials was assumed to have minimal impact on barrier performance and was not addressed.

Table C.2. Parameters Used to Describe Soil Hydraulic Properties in the Simulations. The van Genuchten parameter *m* was set equal 1-1/*n*. The pore interaction term was specified using the standard value of 0.5. (adapted from Fayer et al. 1999)

Soil Type (depth interval, cm)	θ_s cm^3/m^3	θ_r cm^3/m^3	α 1/cm	n --	K_s cm/h
Modified RCRA Subtitle C Surface Barrier					
Silt Loam Admix (0 to 50)	0.422	0.0042	0.0163	1.37	2.64
Compacted Silt Loam (50 to 100)	0.353	0.111	0.0077	1.78	0.0049
Filter Sand (100 to 115)	0.445	0.01	0.0726	2.8	392
Filter Gravel (115 to 130)	0.419	0.005	4.93	2.19	1,260
Drainage Gravel (130 to 145)	0.4	0.005	10.0	3.0	3,600
Rupert Sand					
BWTF Sand (0 to 400)	0.433	0.0381	0.106	1.78	35.3
Sensitivity Case 1[(a)] (0 to 400)	0.357	0.007	0.155	1.72	21.6
Sensitivity Case 2[(a)] (0 to 400)	0.408	0.035	0.0355	2.04	21.6
Burbank Loamy Sand					
BWTF Sand (0 to 41)	0.433	0.0381	0.106	1.78	35.3
Loamy Sand, 45% gravel (41 to 76)	0.279	0.0160	0.0292	1.35	2.44
Loamy Sand, 85% gravel (76 to 89)	0.0760	0.0040	0.0292	1.35	0.519
Sandy Gravel (89 to 400)	0.0833	0.0084	0.0061	1.52	0.572
(a) Used by Fayer et al. (1999); not used for this report.					

The hysteresis phenomenon was evaluated for each of the five soil scenarios in Table C.1. There are four required hysteresis parameters: the number of hysteretic paths, the maximum amount of entrapped air, the factor that relates the sorption α to the desorption α (the one in Table C.2), and the minimum matric potential below which hysteresis is negligible. Hysteresis is not typically measured in the laboratory, so very little data exist. Instead, nominal values were used for this analysis to demonstrate the possible impact of hysteresis. The number of paths indicates how many times wetting and drying cycles can proceed along different scanning paths, which occur within main wetting and drying paths, before being constrained to the most recent path. The number of paths was set to 7. The maximum amount of entrapped air is the maximum fraction of pore space that can fill with air (not water) when the soil wets from its driest state to a matric potential of zero. This value was fixed at 0.25. The factor that determines the sorption α was set to 2.0, meaning that the sorption α was double the desorption α. Finally, hysteresis was limited to matric potentials above -1000 cm. These four parameter values were used for all soil types in all scenarios.

The soil properties required to simulate heat flow include heat capacity, thermal conductivity, and vapor enhancement. Parameters to describe these properties were obtained from Cass et al. (1984). The heat capacity for all materials was assumed to be 2.13 J cm^{-3} K^{-1}. Table C.4 shows the five parameters used to describe thermal conductivity and enhancement. For this report, the enhancement factors were chosen to yield a factor of 1.0 (i.e., no vapor enhancement).

Table C.3. Hydraulic Property Parameter Sets for Examining the Impact of Variability in the Silt Loam Admix Layer. The van Genuchten parameter *m* was set equal 1-1/*n*. The pore interaction term was specified using the standard value of 0.5. (adapted from original parameters in Gee et al. 1989)

Sample	θ_s cm^3/m^3	θ_r cm^3/m^3	α 1/cm	n --	K_s cm/h
D02-5-10	0.422	0.0142	0.0118	1.45	1.54
D02-5-16	0.422	0.0252	0.0064	1.66	1.13
D04-1-04	0.422	0.0000	0.0201	1.32	3.84
D04-1-10	0.422	0.0000	0.0214	1.32	1.82
D05-5-03	0.422	0.0000	0.0241	1.31	2.36
D07-1-04	0.422	0.0040	0.0167	1.36	1.87
D08-2-15	0.422	0.0083	0.0142	1.39	2.77
D09-7-01	0.422	0.0053	0.0165	1.36	2.83
D09-7-02	0.422	0.0118	0.0159	1.40	3.12
D09-7-05	0.422	0.0000	0.0255	1.32	1.17
D10-4-04	0.422	0.0000	0.0188	1.34	5.25
D11-7-06	0.422	0.0000	0.0272	1.31	43.5
D11-7-08	0.422	0.0000	0.0279	1.30	80.5
D12-4-14	0.422	0.0073	0.0113	1.39	0.55
D13-3-08	0.422	0.0060	0.0179	1.37	0.52
D14-3-04	0.422	0.0116	0.0145	1.41	1.17

Table C.4. Soil Heat Flow Parameters

Thermal Property Function	Parameter Values				
	a	*b*	*c*	*d*	*e*
Thermal Conductivity	0.5	0.7	6.0	0.26	5.0
Enhancement Factor	1.0	0.0	0.0	1.0	3.0

C.2.5 Initial Conditions

All simulations were started using the weather data for 1957. Initial matric potential values were not available for any of the scenarios, so the initial conditions were specified as -10^3 cm. This value is wetter than some measured vadose zone potentials (e.g., Prych 1998), so early drainage could reflect this initial water if recharge rates are lower for the given scenario. However, this limitation was overcome by repeating the 47-year sequence until the beginning and ending water storage values were within 0.1 mm of each other. This procedure uncoupled the results from the impact of initial conditions. The implicit assumption is that the 47-year weather record, when repeated, is representative of much longer periods.

C.2.6 Boundary Conditions

Boundary conditions describe the water inputs and outputs at the top and bottom of the model domain. For this report, these conditions are the weather data that affect the calculation of evapotranspiration, precipitation, and the drainage rate from the bottom of the profile. The weather data were derived from the meteorological data collected at the Hanford Meteorological Station (HMS) for the years 1957 to 2003. The HMS is located about 6 km west-northwest of the IDF at an elevation of 223 m (Hoitink et al. 2003). This elevation differs by less than 10 m from the elevations of the two disposal sites so that topographic differences in weather between the HMS and the IDF should be negligible.

The current climate conditions were represented using the daily weather data. Measured hourly precipitation rates were used to describe the water inputs. Snowfall was treated as an equivalent rainfall at the time it occurred. Weather data such as wind speed, cloud cover, relative humidity, solar radiation, and maximum and minimum air temperature were used to calculate potential evaporation using the Penman Method (Doorenbos and Pruitt 1977).

For heat flow, the upper boundary parameters are the roughness lengths for heat and momentum transfer and the zero plane displacement. Both roughness lengths were set to 0.00049 m based on measurements at Hanford (Ligotke 1993). The displacement height is an offset used to account for plants; this parameter was set to zero because the heat flow simulations were conducted without plants.

The bottom boundary was represented with a unit-gradient condition. This condition is generally acceptable when the boundary is well below the deepest plant roots, which were at 1 m in the silt loam layer of the surface barrier and 2 m in the soils in this report, and the drainage rate exceeds 1 mm/yr. For lower drainage rates, temperature cycling can have a significant effect on overall water movement via the temperature effect on vapor flow. In these cases, heat flow modeling can be used to examine total flux rates. The bottom boundary for heat flow was specified with a fixed temperature gradient of 0.047 K/m, which is an upward gradient similar to what has been observed in the vadose zone at Hanford (Hsieh et al. 1973).

C.2.7 Plant Information

The plant community is an important component of the IDF. The two major functions performed by the plants are the efficient removal of water stored in the near-surface soil (thus minimizing recharge) and protection of the soil surface from wind and water erosion (thus protecting the integrity of the surface barrier). By minimizing recharge and protecting the integrity of the surface barrier, plants help to ensure the successful long-term protection of the IDF.

For those simulations performed for this report that included plants, a shrub community was assumed. Table C.5 and Figure C.1 show the parameters used to represent the shrub community; the parameters are identical to those used by Fayer et al. (1999).

Table C.5. Plant Parameters for UNSAT-H Simulations (after Fayer et al. 1999)

Parameter Description	Parameter Value		
	Shrub	Cheatgrass[(a)]	Potatoes[(a)]
PET Partition Function	LAI	Cheatgrass	LAI
Active Days of the Year	Mar 1 to Nov 30	Mar 1 to May 31	April 9 to Sep 16
Bare Fraction	0.69	0.577	0.0
Maximum Rooting Depth (m)	2.0	0.6	0.6, Surface barrier 0.9, Rupert sand
Root Density Coefficients			
a =	0.217	1.17	1.17
b =	0.0267	0.131	0.131
c =	0.0109	0.0206	0.0206
Plant Uptake Potentials (-MPa)			
h_n =	0.003	0.003	0.003
h_d =	0.1	0.1	0.04
h_w =	7.0	2.0	1.6

(a) Used by Fayer et al. (1999); not used for this report.
LAI = Leaf area index.
PET = Potential evapotranspiration.

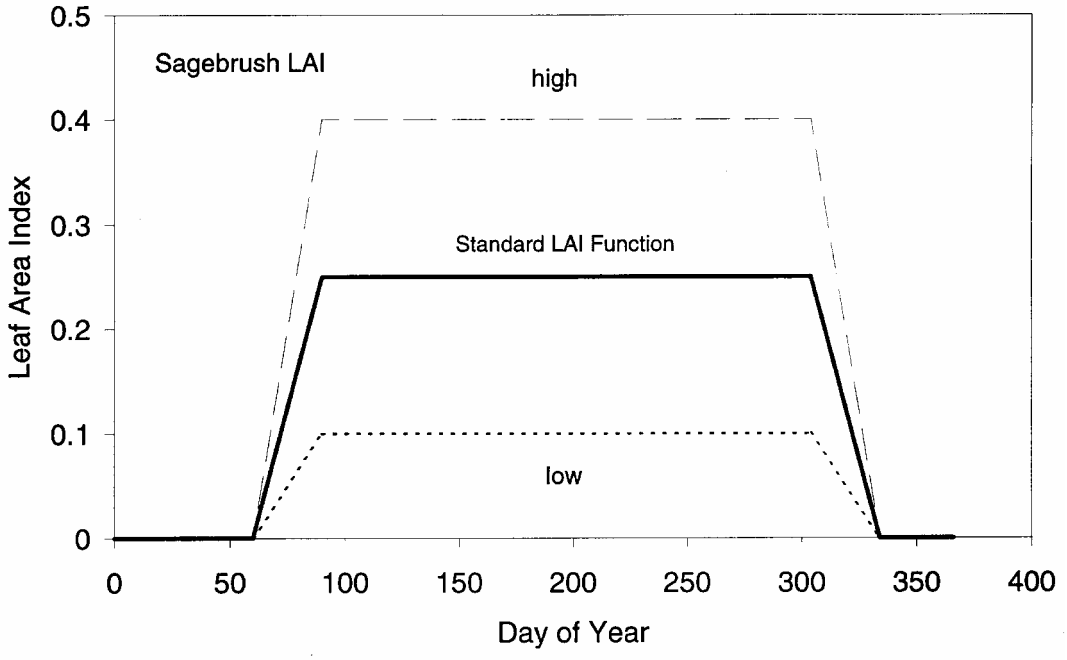

Figure C.1. Leaf Area Index for Sagebrush (after Fayer et al. 1999; only the Standard Leaf Area Index Function was used for this report)

C.3 Results

Each 47-year simulation took approximately 0.5 hours of dedicated time to run on a personal computer. In most cases, repeating the weather sequence just once was enough to establish a condition indicative of the long-term average. In several cases, three to four repetitions of the weather sequence were required for the profile to achieve a condition indicative of the long-term average. In some cases, one sequence was enough to establish that the soil profile was drying and that further repetition of the weather sequence would dry out the profile even more.

Table C.6 shows the average long-term deep drainage rate for all simulations conducted. The average rate was calculated for all 47 years of the last simulation sequence. For those simulations that indicated drying, the rate was assigned a value of <0.1 mm/yr. The symbol "<" was used to indicate the uncertainty of specifying such a small rate.

Table C.6. Simulated Long-Term Drainage Rates Using UNSAT-H, Weather Data from 1957 to 2003, and a Shrub Community (unless noted)

Variable	Condition	Simulated Long-Term Drainage Rates (mm/yr)				
		Modified RCRA Subtitle C Barrier	Rupert Sand	Burbank Loamy Sand	Dune Sand on Barrier	Eroded Surface Barrier
Climate	Current	<0.1 (0.0)	1.8 (-18%)	4.8 (-7.7%)	<0.1 (0.0)	<0.1 (0.0)
Vegetation	No plants	<0.1 (0.0)	43.9 (-0.9%)	52.1 (-0.8)	32.3 (-1.2%)	<0.1 (0.0)
Domain Size, Vegetation	2 m deeper profile; no plants	<0.1	43.9	52.1	32.3	<0.1
Hysteresis		<0.1	5.7	3.9	0.7	<0.1
Hysteresis, Vegetation	No plants	<0.1	67.6	59.4	62.5	<0.1
Heat Flow, Vegetation	No plants	NA	37.0	NA	NA	NA
Heat Flow, Vegetation, Domain Size	No plants; 10 m deeper profile	NA	37.0	NA	NA	NA

(a) NA = Not analyzed.
Note: Values in parentheses indicate percent change relative to the estimated rate provided by Fayer et al. (1999).

Two sets of simulations from Fayer et al. (1999) were repeated for this report using an additional six years (1998 to 2003) of data. The results in Table C.6 show that all three surface barrier scenarios showed <0.1 mm/yr drainage, with or without vegetation. These results are identical to those from Fayer et al. (1999) and demonstrate the robustness of the surface barrier. Noteworthy is that the simulation period includes some extreme events, including the 24-hr record precipitation of 48.5 mm. This amount is nearly equivalent to the predicted 1,000-yr 24-hr amount of 51.6 mm (Hoitink et al. 2003). The two soil scenarios showed some sensitivity to the additional six years of weather data. Under shrub-steppe

covers, the predicted recharge rates are 7.7 to 18% less. Without plants, the rates are only 1% less. In both cases, the rates dropped about 0.4 mm/yr. Because the rates under shrub-steppe were already low, the percentage was higher.

The set of simulations without plants was repeated with a 2 m deeper profile to demonstrate model sensitivity to domain size. The results are essentially identical, indicating that the current domain size is adequate for these particular simulations.

A set of sixteen simulations was conducted to demonstrate the sensitivity of the surface barrier to variations in the hydraulic properties of the upper 0.5 m silt loam layer. The results showed that all sixteen manifestations of hydraulic properties yielded the same zero-drainage outcome, once again highlighting the robustness of the surface barrier design. Six of the simulations generated runoff, but the amounts were small. Five averaged less than 0.1 mm/yr of runoff; the sixth averaged 0.3 mm/yr.

Two sets of simulations were conducted to show the effect hysteresis. Table C.6 shows that, with a shrub cover, hysteresis did not affect the performance of the surface barrier or the eroded barrier, but it did lead to some drainage, 0.7 mm/yr, for the surface barrier with dune sand. For the soils with a shrub cover, the results were mixed. Recharge for Rupert sand increased 1.8 to 5.7 mm/yr whereas the rate for Burbank loamy sand decreased from 4.8 to 3.9 mm/yr. These results indicate that the effect of hysteresis on recharge is sensitive to soil type.

When hysteresis was modeled in the absence of shrubs, the surface barrier and eroded barrier still limited recharge to less than 0.1 mm/yr. However, the recharge rate beneath the surface barrier with dune sand nearly doubled from 32.3 to 62.6 mm/yr. Hysteresis increased recharge in the two soil scenarios as well, but not by as much. For all the hysteresis simulations, a single set of parameters was used. The sensitivity of the results to those parameters was not determined.

A simulation was conducted to determine the influence of heat flow on recharge beneath Rupert sand without plants. The predicted rate was 37 mm/yr, which is about 16% less than the rate predicted using the isothermal model. The expectation is including heat flow in the other scenarios would result in similar reductions in predicted recharge.

As for water flow, there is a concern that the lower boundary for heat flow may not be sufficiently deep below the soil surface. Therefore, the heat flow simulation was repeated for a domain that was 10 m deeper. The result was a recharge rate that was identical to the rate with the shallower domain, thus providing confidence that the shallower domain could be used.

C.4 Conclusion

A set of simulations was used to estimate recharge rates for scenarios pertinent to the 2005 IDF PA. The scenarios included the surface barrier and two surrounding soil types, as well as two types of surface

barrier degradation. The simulations were conducted using a 47-year sequence of weather collected at the Hanford Site from 1957 to 2003. This sequence was repeated until the results remained unchanged to uncouple results from assumed initial conditions.

All of the simulation results indicated that the surface barrier limits drainage to <0.1 mm/yr, which is much better than the design goal of 0.5 mm/yr. The barrier maintained this performance level when plants were removed, when silt loam variability was considered, when 20 cm of the silt loam layer was eroded, and when hysteresis was included. The surface barrier was not able to maintain this performance when windblown sand was deposited to a depth of 20 cm and hysteresis was included. In this case, the predicted rate was 0.7 mm/yr, which is slightly above the design goal of 0.5 mm/yr.

Drainage rates in the two surrounding soils were 1.8 to 4.8 mm/yr under shrub-steppe vegetation. Removing plants from the simulations dramatically increased recharge by a factor of 10 or more. Including hysteresis in the simulation generally increased the predicted recharge rate, but for Burbank loamy sand the rate actually decreased. This result indicates that the effect that hysteresis has on recharge will depend on the specific soil and plant conditions.

Several simulations were conducted to demonstrate the impact of domain size. The results all indicated that the domain sizes used by Fayer et al. (1999) were adequate and did not need to be enlarged.

C.5 References

Bouwer H and RC Rice. 1983. "Effect of Stones on Hydraulic Properties of Vadose Zones." In *Proceedings of the Characterization and Monitoring of the Vadose (unsaturated) Zone*." National Water Well Association, Worthington, Ohio.

Cass A, GS Campbell, and TL Jones. 1984. "Enhancement of Thermal Water Vapor Diffusion in Soil." *Soil Sci. Am. Journal* 48:25-32.

DOE. 1991. *Descriptions of Codes and Models to be Used on Risk Assessment.* DOE/RL-91-44, U.S. Department of Energy, Richland, Washington.

Doorenbos J and WO Pruitt. 1977. *Guidelines for Predicting Crop Water Requirements*. FAO Irrigation Paper No. 24, Food and Agriculture Organization of the United Nations, Rome, Italy, pp. 1-107.

Fayer MJ. 2000. *UNSAT-H Version 3.0: Unsaturated Soil Water and Heat Flow Model, Theory, User Manual, and Examples*. PNNL-13249, Pacific Northwest National Laboratory, Richland, Washington.

Fayer MJ and GW Gee. 1997. "Hydrologic Model Tests for Landfill Covers Using Field Data." In *Landfill Capping in the Semi-Arid West: Problems, Perspectives, and Solutions.* TD Reynolds and RC Morris (eds.). May 21-22, 1997, Jackson, Wyoming, ESRF-019, Environmental Science Research Foundation, Idaho Falls, Idaho.

Fayer MJ, ML Rockhold, and MD Campbell. 1992. "Hydrologic Modeling of Protective Barriers: Comparison of Field Data and Simulation Results." *Soil Sci. Soc. Am. J.* 56:690-700.

Fayer MJ, GW Gee, ML Rockhold, MD Freshley, and TB Walters. 1996. "Estimating Recharge Rates for a Groundwater Model Using a GIS." *J. Environ. Qual*. 25:510-518.

Fayer MJ, EM Murphy, JL Downs, FO Khan, CW Lindenmeier, and BN Bjornstad. 1999. *Recharge Data Package for the Immobilized Low-Activity Waste 2001 Performance Assessment*. PNNL-13033, Pacific Northwest National Laboratory, Richland, Washington.

Gee GW, RR Kirkham, JL Downs, and MD Campbell. 1989. *The Field Lysimeter Test Facility (FLTF) at the Hanford Site: Installation and Initial Tests*. PNL-6810, Pacific Northwest Laboratory, Richland, Washington.

Hoitink DJ, KW Burk, JV Ramsdell, and WJ Shaw. 2003. *Hanford Site Climatological Data Summary 2002 with Historical Data.* PNNL-14242, Pacific Northwest National Laboratory, Richland, Washington.

Hsieh JJC, AE Reisenauer, and LE Brownell. 1973. *A Study of Soil Water Potential and Temperature in Hanford Soils*. BNWL-1712, Battelle Pacific Northwest Laboratories, Richland, Washington.

Khire MV, CH Benson, and PJ Bosscher. 1997. "Water Balance Modeling of Earthen Final Covers." *J. Geotech. Geoenviron. Engr*. 123(8):744-754.

Khire MV, CH Benson, and PJ Bosscher. 2000. "Capillary Barriers: Design Variables and Water Balance." *J. Geotech. Geoenviron. Engr*. 126(8):695-708.

Ligotke MW. 1993. *Soil Erosion Rates Caused by Wind and Saltating Sand Stresses in a Wind Tunnel*. PNL-8478, Pacific Northwest Laboratory, Richland, Washington.

Magnuson SO. 1993. *A Simulation Study of Moisture Movement in Proposed Barriers for the Subsurface Disposal Area, INEL*. EGG-WM-10974, EG&G Idaho, Inc., Idaho Falls, Idaho.

Mann FM. 1999. *Scenarios for the Hanford Immobilized Low-Activity Waste (ILAW) Performance Assessment*. HNF-EP-0828, Rev. 2, Fluor Daniel Northwest, Richland, Washington.

Mann FM, KC Burgard, WR Root, RJ Puigh, SH Finfrock, R Khaleel, DH Bacon, EJ Freeman, BP McGrail, SK Wurstner, and PE Lamont. 2001. *Hanford Immobilized Low-Activity Waste Performance Assessment: 2001 Version.* DOE/ORP-2000-24, Rev. 0, U.S. Department of Energy, Richland, Washington.

Martian P. 1994. *Calibration of HELP Version 2.0 and Performance Assessment of Three Infiltration Barrier Designs for Hanford Site Remediation*. EGG-EES-11455, EG&G Idaho, Inc., Idaho Falls, Idaho.

Martian P and SO Magnuson. 1994. *A Simulation Study of Infiltration into Surficial Sediments at the Subsurface Disposal Area, Idaho National Engineering Laboratory*." EGG-WM-11250, EG&G Idaho, Inc., Idaho Falls, Idaho.

Prych EA. 1998. *Using Chloride and Chlorine-36 as Soil-Water Tracers to Estimate Deep-Percolation at Selected Locations on the U.S. Department of Energy Hanford Site, Washington*. Open File Report 94-514, U.S. Geological Survey, Tacoma, Washington.

Puigh RJ and RM Mann. 2002. *Statement of Work for FY 2003 to 2008 for the Hanford Low-Activity Tank Waste Performance Assessment Program*. RPP-6702, Rev. 2, CH2M HILL Hanford Group, Inc., Richland, Washington.

Scanlon BR, M Christman, RC Reedy, I Porro, J Simunek, and GN Flerchinger. 2002. "Intercode Comparisons for Simulating Water Balance of Surficial Sediments in Semiarid Regions." *Water Resour. Res.* 38(12):1323-1339.

Distribution

No. of Copies

OFFSITE

B. R. Scanlon
Bureau of Economic Geology
University of Texas at Austin
J.J. Pickle Research Campus, Building 130
10100 Burnet Road
Austin, TX 78758-4445

J. Selker
Professor, Bioengineering
Room 210, Gilmore Hall
Oregon State University
Corvallis, OR 97331-3906

ONSITE

8 **CH2M HILL Group**

FA Anderson	E6-35
DC Comstock	H6-19
JG Field	H6-62
AJ Knepp	E6-35
FM Mann	E6-35
DA Myers	H0-22
G Parsons	H6-19
C Wittreich	H6-62

2 **U.S. Department of Energy/RL**

JG Morse	A6-38
RD Hildebrand	A6-38

No. of Copies

4 **U.S. Department of Energy/ORP**

CA Babel	H6-60
RW Lober	H6-60
PE LaMont	H6-60
RM Yasek	H6-60

8 **Fluor Daniel Hanford, Inc.**

MW Benecke	E6-35
JD Davis	E6-35
BH Ford	E6-35
TW Fogwell	E6-35
R Jackson	E6-35
LC Swanson	E6-35
ME Todd-Robertson	E6-35
MI Wood	H8-44

2 **Fluor Daniel Northwest, Inc.**

R Khaleel	B4-43
RJ Puigh	B4-43

32 **Pacific Northwest National Laboratory**

DH Bacon	K9-33
MP Bergeron	K9-33
RW Bryce	K6-75
JL Downs	K6-85
MJ Fayer (10)	K9-33
MD Freshley	K9-33
GW Gee	K9-33
CT Kincaid	K9-33

No. of Copies		No. of Copies	
KM Krupka	K6-81	SP Reidel	K6-81
GV Last	K6-81	ML Rockhold	K9-33
CW Lindenmeier	K6-81	RJ Serne	K6-81
BP McGrail	K6-81	JE Szecsody	K3-61
PD Meyer	BPO	AL Ward	K9-33
LF Morasch	K6-86	F Zhang	K9-33
WE Nichols	K9-33	Hanford Technical Library (2)	